FORWARD DYNAMIC MODELING OF HUMAN LOCOMOTION

By

James Lanphier Patton

A THESIS

Submitted to
Michigan State University
in partial fulfillment of the requirements
for the degree of

MASTER OF SCIENCE

Department of Material Science and Mechanics

1993

ABSTRACT

FORWARD DYNAMIC MODELING OF HUMAN LOCOMOTION

By

James Lanphier Patton

The purpose of this thesis was to investigate the prospects of predictive modeling of human motion. Using measured motions with measured ground reaction forces and moments, an inverse dynamic model can determine time histories of the internal (joint) forces and moments. These forces and moments can be used to drive a dynamic synthesis of motion. If the original measured motions are obtained, the model can be used in a predictive manner to study parametric changes.

Initial investigations found full-body three-dimensional models too complex and problematic. Therefore, two simple models were developed in two-dimensions, the first a single rigid body, and the second a three segment model of the leg. It was found that stabilizing elements, such as joint torsional springs and torsional dampers, were necessary in order to achieve stable gait simulations. In order to obtain motions closer to measured, control strategies may be required.

To my bride Jill, who had the patience to
endure my many late nights at the lab.

ACKNOWLEDGMENTS

Special thanks go to my major advisor, Robert Soutas-Little, for his guidance and support. Thanks to Mechanical Dynamics Inc., for Choosing the Biomechanics Evaluation Laboratory as a beta test site for ADAMS/Android. Thanks to Brooks shoe company, for funding much of the research and equipment used. Thanks also to Dr. Gary Cloud, who instructed me in an independent study on advanced three dimensional dynamics. Additionally, the support of my peers should not go without thanks: Terry Bemis, Cheng Cao, Yasin Dhaher (whose knowledge and insight seem endless), Kathy Hillmer, Brock Horsley, Kimberly Lovasik, Dave Marchinda (who beat me in the great thesis race), and Tammy Reid-Bush. These people provided an environment where scientific principles, knowledge, and experience were constantly in exchange. Thanks also to Patricia Soutas-Little for providing a clinical context for my ideas to be used. I would also like to acknowledge the long-distance help of Tom Kepple at the National Institutes of Health, who also worked on the ADAMS/Android project. Many thanks for his efforts to share information.

TABLE OF CONTENTS

		PAGE
LIST OF TABLES		**vii**
LIST OF FIGURES		**viii**
INTRODUCTION		**1**
1.	**SURVEY OF LITERATURE**	**5**
	1.1 Introduction	5
	1.2 Indirect Dynamic Modeling of Human Motion	5
	1.3 Synthesis of Human Motion	8
	1.4 Computer Simulation of Surgery	20
2.	**PRELIMINARY STUDY: DYNAMIC MODELING OF HUMAN MOTION USING ADAMS/ANDROID**	**24**
	2.1 Introduction and Background	24
	2.2 Overview of ADAMS and ADAMS/Android	25
	2.3 Model Development	29
	2.3.1 Planar Model	29
	2.3.2 Three Dimensional Full Body Model	33
	2.4 Results and Discussion	36
3.	**METHODS**	**41**
	3.1 Introduction and Background	41
	3.2 Methods for Planar Dynamic Analysis of a Single Rigid Body	42
	3.2.1 Experimental Procedure	42
	3.2.2 Data Reduction	44

3.2.3 Inverse Dynamic Analysis 50
3.2.4 Forward Dynamic Synthesis 54
3.3 Methods for Planar Dynamic Analysis of Human Locomotion 57
3.3.1 Experimental Procedure 57
3.3.2 Data Reduction 60
The Foot 63
The Leg 65
The Thigh 66
3.3.3 Indirect Dynamics 67
3.3.4 Forward Dynamic Synthesis 70

4. RESULTS AND DISCUSSION 79
4.1 Results and Discussion for Dynamic Analysis of a Single Rigid Body 79
4.2 Results and Discussion for Planar Dynamic Analysis of Human Locomotion 93

4. SUMMARY AND CONCLUSIONS 114

APPENDIX A: A SYSTEM OF EQUATIONS FOR DYNAMIC SYNTHESIS 116

APPENDIX B: THE BEL DATA LINK PROGRAM (BLINK) 121

LIST OF REFERENCES 125

LIST OF TABLES

TABLE		PAGE
3.3.1	The target position descriptions.	59
3.3.2:	The anthropometric scaling scheme used.	62

LIST OF FIGURES

FIGURE		PAGE
2.1.1	A general schematic of the modules for ADAMS.	25
2.3.1	The ADAMS planar model.	30
2.3.2	The ADAMS/Android three dimensional full body model.	34
2.3.3	The ADAMS/Android default foot (right) and the NIH Foot (left).	35
2.4.1	Vertical ground reaction force results from a simulation of the planar model.	36
2.4.2	The results of gait driven by motions at the joints and constraint of the orientation of the pelvis relative to the inertial reference frame.	37
2.4.3	Simulation results showing the instant just before a fall. Joints were kinematically driven and the orientation and translation of the pelvis relative to the inertial reference was allowed to be free.	38
3.2.1	The dimensions of the slender rod.	43
3.2.2	The experimental procedure showing the lab (inertial) reference frame.	44

		PAGE
3.2.3	The coordinates of the inertial (lab) reference and the rod.	45
3.2.4	Model of the rod for dynamic analysis using forces expressed in the inertial coordinate system ("Inertial-based approach").	51
3.2.5	Model of the rod for dynamic analysis using forces expressed in the coordinate system embedded in the rod ("Body-based approach").	53
3.3.1	The environment used showing the lab (inertial) reference frame.	58
3.3.2	The targeting protocol used.	59
3.3.3	The convention used for link-segment analysis.	61
3.3.4	Foot analysis from targeting. a) bottom view. b) side (in-plane) view.	64
3.3.5	Leg and thigh analysis from targeting. Lateral aspects. a) Leg b) Thigh.	66
3.3.6	Free body diagrams for the mechanical system and the convention used for the direction of the forces.	71
3.3.7	The integration process for the system of equations.	74
3.3.8	The equivalent force system used to reduce the resulting moment and force results from the forward dynamics problem to a force at distance COP from the heel.	76
4.1.1	Target trajectory motion for a typical trial. a) Motion in the plane, b) Motion in a perpendicular plane.	78

		PAGE
4.1.2	Marker distances throughout a 4 second trial. a) distance vs. time, b) distance vs. rod's angle with vertical.	79
4.1.3	Smoothed and un-smoothed rod kinematics for a typical trial. A 2-pass, 7 point rectangular signal processing window was used. a) Center of mass (CM) x-distance vs. time, b) (CM) z-distance vs. time. c) Rod's orientation with vertical (Θ) vs. time.	81
4.1.4	The effects of smoothing on the angular acceleration.	82
4.1.5	Angular displacement, angular velocity, and angular acceleration for a typical trial. a) Rod's angle with vertical. b) Angular velocity calculated using equation 3.2.6 and using equation 3.2.7. c) Angular acceleration calculated using equation 3.2.9 and using equation 3.2.10	83
4.1.6	Angular derivatives corrected and un-corrected for target motion along the axis of the rod. a) Angular velocity (see equations 3.2.11 to 3.2.13), b) Angular acceleration (see equations 3.2.14 to 3.2.17).	85
4.1.7	Indirect dynamic results. a) X-directed forces. b) Z-directed forces. c) Moments See Figure 3.2.3 for the definition of forces.	86
4.1.8	The contribution of several different effects to the net acceleration of the rod in the Z direction for a typical trial.	87

		PAGE
4.1.9	Forward dynamics-synthesized trajectories compared to the original measured motion for two mechanical approaches: Forces specified in the inertial reference frame and forces specified in the body-coordinate system embedded in the rod.	89
4.1.10	Dynamic synthesis results comparing two integration approaches with the original measured values: Single step (Euler) integration and Two step (Modified Euler) integration.	90
4.1.11	Dynamic synthesis results from a trial in which the forces were manually increased. The peak vertical applied force was higher than the trial seen in Figure 4.1.10 by a factor of 2.6.	91
4.2.1	Indirect dynamics results for a female adult subject walking normally. a) ankle b) knee c) hip.	93
4.2.2	A stick figure representation (0.05 second intervals, end time .3 seconds, using the Modified Euler Method (2 iterations)) of a model being allowed to collapse under its own weight from a standing configuration, for two integration step sizes (h): a) h=.001 sec, b) h=.05sec.	94
4.2.3	Simple pendulum to demonstrate the constraint violation problem: a) time=0 b) time=h.	95
4.2.4	Example of the iterative process of integration and re-evaluation of acceleration. This is the angular position of the thigh for one integration time step, for time=.006 in a) below.	97

4.2.5 A stick figure representation (0.05 second intervals, end time .3 seconds, h=.05) of a model being allowed to collapse under its own weight from a standing configuration, for two integration strategies: a) 10 iterations, b) 1 iteration. 97

4.2.6 Synthesized accelerations of the leg for an adult walking subject. a) x coordinate b) z coordinate c) theta coordinate. 100

4.2.7 Synthesized accelerations of the thigh for an adult walking subject. a) x coordinate b) z coordinate c) theta coordinate. 101

4.2.8 Comparison of initial synthesis results with the measured motions. a) Measured b) Synthesis results, (h=.0005, 15 iterations). 102

4.2.9 Comparison of synthesis results for varying torsional passive joint elements. a) Measured b) Synthesis results, no passive elements c) Synthesis results, k=10, c=20 d) Synthesis results, k=100, c=100. (h=.0005, 15 iterations). 103

4.2.10 Original Motion and simulation results for when the hinge constraints are imposed on the system before the indirect problem. a) motion used for the indirect problem. b) simulation results. 104

4.2.11 Ground Applied Force (GAF) parameters in the inertial coordinate system for a simulation compared to original measured values from the force plate. a) Forces b) center of pressure (COP). 106

4.2.12 The contribution of each factor to the moments on the segments. a) foot b) shank c) thigh. 109

4.2.13 An inverted pendulum driven by a manipulating moment M(t). 110

PAGE

A.1 The matrix form of the 21 Equations for the forward dynamics problem 115

INTRODUCTION

Engineers have utilized modeling to gain a broad understanding of many systems. Modeling provides an ability to analyze and experiment, with little cost or risk. One can attempt parametric changes that may not be feasible to test on the actual system. Cause-and-effect relationships can be understood, and complexities examined.

Dynamic modeling is useful in the analysis of human movement. Human motion is a result of the central nervous system controlling the release of metabolic energy in muscles for the purpose of generating forces on a system of interconnected, rigid and deformable links. Human motions are effected by the skeleton, muscles, tendons, ligaments, the articular surfaces, surrounding tissue, external forces, the nervous system, and other factors on the physiological level. Modeling of this nature requires knowledge of the task, knowledge of the body's structure and function, and knowledge of the body's interface with its environment.

A large part of the complexity of human motion stems from the dynamics of musculoskeletal articulation, and will thus be the focus of this thesis. The dynamics of motions such as walking involve many factors:

- Inertial forces of each body segment contribute to the system's motion. These forces depend on the position, velocity, and acceleration of each segment.

- The musculoskeletal system is redundant in its application of active forces: multiple muscles are capable of causing similar motions.

- Gravity contributes to the system's motion.

- Dynamic coupling is a large factor in the motion because the system has many joints. A muscle spanning one joint can have a greater effect on the motion of another joint if conditions are correct [Zajac and Gordon 1990].

- Muscles can span multiple joints, and the function of two-joint muscles may not be to produce motion, but instead to restrict motion, to transfer power, or to stabilize motion.

- In a dynamic system, the lack of motion of a joint can mean that energy is being transferred somewhere else in the system, not simply that there is no energy.

- Motion occurs in three dimensions for almost all tasks. Gyroscopic and Coreolis effects change the forces generated in a system during motion.

Dynamic modeling provides an excellent addition to gait biomechanics. In the inverse or indirect dynamic problem, the forces and moments of each joint are determined from measured motions using a model and the corresponding equations of motion. Link-segment models that reduce the kinematic and kinetic gait laboratory data to joint motions, forces, and torques have been used for years by many researchers [Elftman 1939; Bresler and Frankel 1950; Capozzo 1984; Winter 1984; Verstraete 1988]. These models provide a concise and reliable set of time histories of joint loads and moments. Some researchers have attempted to relate the system loads to muscle tension using static optimization [Crownenshield and Brand 1981; Seirig and Arvikar 1975]. These extensions may be

unreliable due to a lack of the understanding of the dynamics over the entire duration of the task, the somewhat arbitrary choice of the cost function, and the inherent need for co-contraction to provide stability to the system [Zajac 1989]. In any case, motion is caused by the imbalances of the internal and external forces and moments at joints. This thesis was limited to forces and concentrated moments. Once the forces and concentrated joint moments are determined, the contribution of each individual muscle can be approximated using optimization techniques.

Modeling also permits the study of motions in response to applied forces, and this will be the central focus of this thesis. This approach is termed the forward dynamics problem, the direct dynamics problem, or the dynamic synthesis problem. The possibility of modifying the mechanical system is usually simple with a model, and the effects of the modification can be determined.

Direct dynamic modeling is a difficult task, however. The process involves imposing forces on the system and integrating a non-linear system of coupled, differential equations. Problems occur when the values obtained in the indirect problem are put back through the system in a forward dynamics approach. The synthesized motions may become unstable due to the coupled and non-linear nature of the system, which is extremely sensitive to inaccuracies. Researchers have attempted to avoid this problem by placing controls on the system in order to stabilize the dynamics [Townsend and Seirig 1972; Chow and Jacobson 1971]. Others have modified the joint moment-time histories in order to achieve stable gait [Pandy and Berme 1989; Ishac and Winter 1990]. Some have approached the task from a purely analytical standpoint using dynamic optimization [Koopman and Grootenboer 1989; Yamaguchi and Zajac 1990,

Hurmuzlu 1988; Pandy, Zajac et al. 1988]. Considerable research has been conducted in dynamic synthesis of motion, but an effective way to approach predictive motion studies has not been developed.

The goal of this work was to investigate the prospects of dynamic simulation as a tool for understanding and treating pathological musculoskeletal motion. Specifically, this work was a movement toward the final goal: to establish a subject-specific predictive model of human locomotion. The first part examined feasibility and methods of using common measurement techniques to develop a predictive model within ADAMS/Android software. Due to the complexity and inherent instability of multibody dynamic modeling, later sections focused on the details of dynamics and numerical methods in order to build a substantial foundation for more complex work. This was done by calculating the indirect dynamics problem on simplified models, and then using the results (forces and moments) in the forward dynamics problem.

1. SURVEY OF LITERATURE

1.1 Introduction

The survey of literature encompasses three main areas: indirect dynamic modeling of human motion, direct dynamic synthesis of human motion, and the simulation of surgery. The purpose is to provide a general overview of some key studies to provide a context in the area of dynamic modeling.

1.2 Indirect Dynamic Modeling of Human Motion

Many researchers confine themselves to the indirect problem in much of their work. Bresler and Frankel pioneered the method of determination of forces and moments at each joint by simple repetition of the free body model of each segment [Bresler and Frankel 1950]. This was a continuation of Elftman's work [Elftman 1939]. Bresler and Frankel measured ground reaction forces and moments using a force plate; motion patterns were determined using photogrammetric techniques; and the human body was idealized as a system of interconnected rigid body links. The dynamic equations of motion were used to calculate the proximal end forces and moments from the distal end forces and moments for each body segment. The method started at the foot and continued up the limb. No computers

were used in this work. 14,000 calculations and 72 graphs were all hand-generated, requiring a total of approximately 500 man-hours.

Hardt and Mann published a brief note demonstrating the technique of determining the dynamic joint forces and moments during gait without the use of a force plate [Hardt and Mann 1980]. A model of the lower extremities and a head and trunk (HAT) segment were used to determine the forces and the moments. It was suggested that a Newtonian instead of Lagrangian (or some other) formulation of the dynamic equations should be used, because of the inverse dynamics nature of the problem, and because the analysis could be easily performed by the simple repetition of the free body model of each individual segment.

Hof used a floor reaction force vector (FRFV) method for determining joint moments [Hof 1992]. The link-segment equations of motion were solved for each joint to be analyzed. This technique has been questioned as incorrect, however, because it does not take into account the dynamic forces and moments of all segments distal to the joint in question, and it does not work for the swing phase of gait [Winter 1990]. The FRFV technique has been shown to be only accurate for the ankle, with a small error at the knee and a large error at the hip [Wells 1981].

Kadaba and Ramacrishnan have published several works that discuss the importance of accuracy and sensitivity in indirect dynamics methodology. In 1989, the repeatability of gait analysis measures (kinematic-Euler angle, kinetic, and EMG) were compared for trials within the same day as well as from day-to-day [Kadaba, Ramacrishnan, et al. 1989]. It was found that sagittal plane kinematics and kinetics were very consistent for both same-day and day-to-day, but out-of-sagittal were less repeatable for day-to-day. This was attributed to errors in marker placement. In general, the

results demonstrated that gait variables were repeatable for subjects walking at their natural speed. In another study [Ramacrishnan, Kadaba et al. 1991a], a sensitivity analysis was performed on joint center estimation based on variations in kinematic target placement. The estimated joint center and 3D axes of rotation were perturbed (20 or 10 mm and ±15° respectively in each direction) in order to study the effects of the calculated joint moment in gait. The peak moments were studied as measure of change, and it was shown that moments can vary up to 114% in magnitude (ankle abduction moment), and up to 36% in timing (knee abduction moment). In a similar work [Ramacrishnan and Kadaba 1991b], kinetics were investigated in more detail, and the helical axis approach to joint kinetics calculations was found to be even more sensitive to perturbations than the Euler angle approach.

The characterization of normal kinetic patterns of gait is important for the understanding of the mechanics of motion. Many researchers have presented investigations concerning the presentation and understanding of these patterns. Some are reviewed in this thesis; this passage, however, is only a list of some examples, and is not intended to be a comprehensive review. David Winter has conducted a large number of investigations of sagittal plane motion [Winter 1984], where kinematic and kinetic patterns are examined to understand variations and their cause and effect relationships. Intra-subject kinetic pattern variability was shown to be high for the hip and knee joints. Variability between subjects was considerable with variations in cadence. Compensating patterns were discussed. Expected gait patterns of normal gait and two pathologies, myelomeningocele and cerebral palsy, were examined at Newington Children's Hospital [Ounpu 1990; Ounpu, Gage et al. 1991].

1.3 Synthesis of Human Motion

The goal of this thesis is to investigate dynamic simulation of gait as a tool to enhance gait analysis. The main areas of contribution are robotics, computer graphics, and biomechanics. Some of those who study dynamic synthesis limit their work to simpler tasks, such as kicking [Audu and Davy 1985], jumping [Green ,Yamaguchi 1992; Pandy, Zajac et al. 1988], or postural control [Zajac and Gordon 1989]. However, many researchers have attempted the simulation of gait by limiting their model with constriants [Bandera, Minnen et al. 1990; Amirouche, Ider et al. 1990; Chow and Jacobson 1971; Hurmuzlu 1988; Koopman and Grootenboer 1989; Onyshko and Winter 1980; Pandy and Berme 1989a; Townsend and Serieg 1972; Yamaguchi and Zajac 1990; Yamaguchi, Green et al. 1992]. Many of these take an analytical approach to the synthesis of motion, using trial and error, dynamic optimization, or other control schemes to develop the proper force time histories necessary to drive the motion. A few [Bandera, Minnen et al. 1990; Onyshko and Winter 1980; Yamaguchi, Green et al. 1992] have used the indirect dynamics results from gait lab data (usually with adjustments) to drive the motion.

Audu and Davy applied a planar, 2 DOF model to kicking motions [Audu and Davy 1985]. This model was used to investigate different muscle models. The trade-off between muscle model complexity and computation time was investigated for five different muscle models, including the most commonly used [Hill 1938; Hill 1953]. Comprehensive joint models that included the passive envelope of motion [Mansour and Audu 1986; Yoon and Mansour 1982] were used. The most efficient model proved to be that of Hill.

One of the first studies in synthesis of locomotion using modern computers and optimal programming was that of Chow and Jacobson [Chow and Jacobson 1971; Chow and Jacobson 1972]. The model incorporated the musculoskeletal system in detail, including the nature of neurophysiology and human control and stability strategies. The model was a 7 segment mechanism with planar joints, and the feet were considered massless. The torso was modeled as an inverted pendulum. Kinematic relations were discussed and applied to the model to reduce the degrees of freedom to 2. Hip trajectory was specified. The model was separated into two legs and the torso, and a control criterion of minimal mechanical energy with respect to muscle was used in the optimization. Despite the simplifications, the results compared very well to accepted norms for ground reaction forces, joint moments, and overall kinematics. The second paper [Chow and Jacobson 1972] focused on the motion of the trunk. In this work, the trunk was again considered as an inverted pendulum and its unstable equilibrium was controlled by linear feedback and on-off perturbations. A Liaponov function for the control of the motion was developed and shown to be effective for a variety of initial configurations.

Hatze and coworkers have been instrumental in the area of dynamic synthesis of human motion. A model of a single leg was presented, in which five muscle groups were used in a time-optimal problem [Hatze 1976]. A dynamic muscle model was developed based on the work of Hill [Hill 1938]. Dynamic programming techniques were used to find optimal muscle coordination strategies for moving the leg to hit a specified target. Results were compared to experimental data and were shown to correlate well. In a later study, these methods were expanded to the entire human body [Hatze 1977]. The modeling was divided into the development of the link-segment

dynamic equations and the musculo-mechanical equations of motion. The control parameters considered both motor unit recruitment and stimulation rate of the muscle models. This approach was specifically applied to the take-off phase of the long jump [Hatze 1981]. This model contained 17 segments and 46 muscles. Constraint relations for impact situations were developed (such as those that occur at heel strike in locomotion). The objective function that includes the task (the performance criterion) of the long jump was determined and discussed. An overview of this methodology was presented in 1984 [Hatze 1984]. Two approaches to modeling the foot-floor interface in forward dynamics simulations of locomotion were discussed by Hatze and Venter [Hatze and Venter 1981]. In this study, the numerical methods for using viscoelastic contact points and for using kinematic constraints (to freeze foot motion) were examined in detail. A computationally efficient method was presented that produced superior results using kinematic constraints.

Hemami and Stokes presented an overview of the types of control systems that might be used for the simulation of human locomotion [Hemami and Stokes 1983]. Each system was founded on neurophysiological principles. Some of these principles were applied to the control of a 9 link model [Hemami Zheng et al. 1982], in which the initiation of gait was considered. Deformable joints connected by ligaments were described but not used, and stabilization strategies were discussed.

Hurmuzlu has worked in the areas of control and nonlinear stability for successive long-term locomotion cycles. The modeling was initiated based on an inverted pendulum and a simple three element rigid body mechanism in 2D and 3D consisting of a head and trunk (HAT) segment and two rigid legs [Hurmuzlu and Moskowitz 1987a]. The 2D model was 3 DOF, while the

3D model was 6 DOF (the HAT segment and each joint had 2 DOF). However, the system was then further constrained using kinematic "functional relations," which reduced the model to 1 DOF (the flexion of the ankle during stance), and control was applied to the system at that point. It was therefore restricted to single stance simulations, and an abrupt switch between the two feet occurred during the each gait cycle. Stability was analyzed for resistance to perturbations, and Poincare' maps in the phase plane were generated to understand the cycle patterns of stable gait. Several initial conditions were investigated to illustrate the mapping. The effect of perturbations on this model was small and the system proved to be stable. This approach was refined [Hurmuzlu and Moskowitz 1987b], when the model was expanded to a 4 body, 7 DOF model in which functional relations were again applied to reduce the system to 1 DOF, and stability was again evaluated using Poincare' maps. The original 3 DOF model was then examined again [Hurmuzlu 1988], and the system was reduced via functional relations to a 2 DOF. This enabled the system to perform more complex tasks, such as climbing stairs and avoiding obstacles. Again, a stable repeating pattern was obtained and variations in stability were investigated in response to structural and kinetic parameter perturbations. An interesting result was that the system may be destabilized by increased ankle stiffness.

An analytical, 3D, 7 DOF model was developed by Koopman and co-workers [Koopman , Grootenboer, et al. 1989], and consisted of HAT, 2 thighs, 2 shanks and 2 feet. Controls were interactively added to the system to minimize imbalance and energy consumption. The system was evaluated at different walking velocities, and energy was found to rise with velocity in a quadratic relationship.

Meglan presented a global approach to the analysis of human motion in his Ph.D. dissertation [Meglan 1991]. A central issue was the modeling of the foot and its compliance properties. This stressed the importance of a legitimate model of the foot-floor interface for predictive models. The foot model contained three spherical sphere-shaped passive elements that exhibited non-linear spring damper and frictional (shear) characteristics when in contact with the floor. The foot also contained simple toes that contributed to the force the foot generated late in stance. The foot model was integrated with a full body, 3D, 13 segment, 34 DOF model. The equations of motion were formulated using a Newton-Euler Algorithm [Orin, McGhee et al. 1979] as used in other gait simulations [Pandy and Berme 1989a]. Passive elements were placed at the joints to stabilize the model. Several tasks were driven by experimentally measured gait data (indirect dynamics), and then motion was synthesized using the joint torques. None of the synthesis attempts were capable of motion for an indefinite length of time. Additionally, Meglan developed a comprehensive method for the understanding of dynamic coupling effects in human movement.

One of the few dynamic models of the knee joint was presented in 1988 [Moeinzadeh and Engin 1988]. The approach involved the development of a 3D model that was later reduced to a 2D model for analysis and simulation of motion. The skeletal model and the origins and insertions were taken from the work of Crownenshield and co-workers [Crownenshield, Pope et al. 1976], while the ligaments were modeled using the results from a later study by Wismans [Wismans, Veldpaus et al. 1980]. The synthesis of motion was described as a reduction of a second order non-linear system of ordinary differential equations to an algebraic system and then linearized. The tibia was subjected to several dynamic loading situations as different

mathematical function shapes, and the resulting dynamic forces were computed. The contact points, joint orientation, and joint and ligament loads were reported, and showed that knee extension caused elongation of the medial and lateral collateral and anterior cruciate (ACL) ligaments, but not the posterior cruciate ligament (PCL). It was also shown that the ACL carried the highest load. This study did not consider the effects of muscles or parametric changes such as the loss of a ligament or the manipulation of the geometry.

Onyshko and Winter presented an important model of locomotion in 1980 [Onyshko and Winter 1980]. In this work, the issue of responsible modeling was stressed in regard to pure synthesis (forward dynamics). It was proposed that many locomotion models were simplified in order to reduce the computational burden, and by constraining the model, the range of possible muscle moments is restricted. The model used in this study was fully moment and force driven, formulated using Lagrange's equations of motion. It contained 7 segments including a HAT segment and triangular feet, and was confined to sagittal plane motion. It was stated that at least this level of complexity was needed for an accurate predictive model. "Soft constraints" were employed at the hip of the stance leg in order to obtain less complex constraint equations. To some extent, this de-couples the motion of the lower limbs. The gait cycle was divided into four phases of dynamic representations, and the foot was locked to the floor during the "flat-foot" stage of gait. The motion was driven by forces and moments obtained from gait analysis laboratory data through the indirect dynamics problem. It was necessary that these drivers be altered to obtain the original motion due to differences between the model and reality. Euler's integration technique was used to solve the forward dynamics problem. It was shown that this

technique worked fairly well, although it was suggested that more sophisticated approaches could be used for a more accurate solution. An increase in ankle moment was shown to shorten stride length. The results were presented using graphical stick-figure representations to reflect the simulations.

A later study presented a 3D, 7 segment model with revolute joints [Ishac and Winter 1990]. This model was driven by inverse dynamic forces and moments obtained from a gait analysis laboratory, and a forward solution was obtained using ADAMS[1] dynamic modeling software. Ground contact was modeled as spring-damper forces on an ellipsoid foot to reflect the progression of the center of pressure. Torsional spring-dampers were placed at each joint to regulate the motion. The model was applied to the swing phase of gait, and joint moments were altered in order to obtain kinematic patterns similar to the original measured motion. It was suggested that an invalid model (one that does not accurately model the actual object it represents) can only be made to walk by altering the moment patterns, or as it was put, "two wrongs can make it right." [Ishac and Winter 1990].

Markus Pandy's Ph.D. dissertation research involved the modeling of 2D and 3D models to simulate gait patterns, and was published in several journals. The original model [Pandy and Berme 1988a] was planar, and was numerically formulated using the Newton-Euler Algorithm [Orin, McGhee et al. 1979]. In the second phase of the study [Pandy and Berme 1988b], it was shown that stable planar gait can be achieved by driving it with joint moments, and that there were 6 major "determinants of gait," which dominate the performance and stability of the model. This research was then

[1] ADAMS: "Automatic Dynamic Modeling of Mechanical Systems" by Mechanical Dynamics Inc., Ann Arbor, Michaigan.

extended to 3D, where the modeling algorithm was improved for the more complex motion. This algorithm also possessed the capability of including muscles and their time-varying moment arms in the model, as well as the previous joint torques [Pandy and Berme 1989a]. The 3D model included a foot, shank, and thigh for the stance leg, a HAT segment, and a thigh and shank for the swing leg. The model was driven by joint moments established by the hip abductor and ankle plantar flexor muscles, and 3D moments at each joint. A linear damped spring was placed between the ankle and hip joints to manage the fine control of the knee in early stance. This model was only capable of the simulation of open-chain dynamics and thus excluded double support. An important feature of this 3D model is that it included pelvic list which proved to be an important determinant of gait. The model exhibited five critical determinants of gait: stance knee flexion, foot and knee interaction, pelvic list, and transverse pelvic rotation. The system was used to investigate the dynamic determinants of pathological gait [Pandy and Berme 1989b], and several elements were removed to study the resulting effects on the dynamics. Another work involved the modeling of double stance using closed-chain dynamic formulations of the planar model [Pandy and Berme 1988c]. This paper pointed out the importance of knee flexion for weight acceptance of the forward limb, and the importance of the trailing limb's plantar flexor muscles for unloading (the ankle appeared to dominate the overall response of the unloading limb). This was easily illustrated by the model's sensitivity to ankle planar flexor and hip abductor muscle forces, and the resulting patterns compared well with the literature. The pre-swing and early swing knee was found to undergo almost passive flexion due to the ankle and hip moments.

Models of gait based on a single concentrated mass were presented by Siegler and Seliktar [Siegler and Seliktar et al. 1982]. This work involved the study of stance phase by imposing initial conditions just before stance and letting the model move through stance without any driving forces. The leg was not modeled as a thigh, shank and foot, but instead a massless linear spring damper was used, the coefficients of which were determined empirically using force plate and motion data on real subjects. Separate formulations of the dynamical equations of motion were used for single and double stance. Three variations of the model were evaluated: a 2D application, a 2D application with a rigid foot element attached to the bottom of the spring damper, and a 3D model without a foot. The results showed good correlation to gait laboratory data, and the ground reaction force was more sensitive to kinematics than to variations in the spring damper parameters. The addition of the foot to the model caused the forces in late stance to increase to a normal range. The best correlation to real data was in the 2D model. One conclusion was that the shear forces in late stance were a result of the body dynamics, and not active muscle activity, since the pattern appeared normal without the need for driving forces. The muscles appeared to play more of a stabilizing than an active role in gait.

Townsend and Seireg conducted early investigations into dynamic simulation of gait using optimal control [Townsend and Seireg 1972]. A 3D dynamic model was developed for the study of energy and foot trajectory optimization control strategies. It consisted of a single rigid body with two rigid, massless, extendable legs. This produced a simple 6 degree of freedom model upon which optimal analysis was performed. The system was originally driven by functions from measured kinematic data on gait, and then compared to the optimization results. Two different optimization

problems were investigated, each with different weight given to the two cost function criterion: mechanical work efficiency and foot placement. Neither result yielded energy comparable to that reported in the literature. A later study [Townsend and Seireg 1973] with a more complicated model (a two part head and trunk with different DOF) and a third optimization criterion (minimize the maximum excursion of the joints), showed that several classes of motion result. These different motions all resembled specialized versions of gait, such as prosthetic gait. Energy results best matched reported values when the simple model was used.

Tsai and Mansour applied dynamic synthesis to the design of a prosthetic [Tsai and Mansour 1986] . The model was two dimensional with two degrees of freedom, and a parametric study was conducted to find the optimal weighing and constraints for normal knee and hip motion in gait. The results showed that normal motion could be obtained, and superior results were obtained with a more heavily weighted prosthetic than was currently accepted as best.

Van Den Bogert developed a 20 segment, 2 dimensional model of a horse [Van Den Bogert, Schamhardt et al. 1989] that successfully simulated trotting. A systematic method for formulating the equations of motion was developed. 8 of the 19 joints were kinematically driven by measured data, while 11 joints were torque driven using linear feedback. Thus the simulation was a mixed forward and inverse dynamics simulation. Numerical methods were stressed as an important factor in the quality of the results, and it was suggested that stiff differential equation solvers be used on such non-linear systems. Ground contacts were modeled using linear spring dampers for the vertical component, and a modified Coulomb

frictional relation for the horizontal (shear) component. Both motion and ground reaction forces correlated well with measured data.

Yamaguchi has contributed to the area of muscle modeling and dynamic synthesis of gait in several works. His dissertation research investigated the prospects of restoring natural gait to paraplegics using functional neuromuscular stimulation (FNS) [Yamaguchi and Zajac 1989a, Yamaguchi and Zajac 1990]. The modeling scheme used for this study was analytical with experimental verification, and was formulated for 8 DOF using Kane's equations of motion [Kane and Levinson 1983]. The goal was to determine the minimum number of muscles necessary for stable gait, and model control strategies using FNS to achieve stable gait. The motion was driven by Hill muscle models whose force functions were dependent on the tendon material characteristics, the muscle and tendon slack lengths, the contraction velocity, and an activation function. The kinematics of the knee were reduced to one degree of freedom based on a previous study [Yamaguchi and Zajac 1989b]. A dynamic programming technique was employed for optimal control of the system, and 48% of gait was modeled with an assumption of symmetry. Although the study showed that closed loop control is impractical for FNS of the paraplegic, the model produced analytical results not previously known, such as the energy storage role of tendon during gait. Induced accelerations were briefly discussed with respect to each muscle stimulated.

Many of Yamaguchi 's later studies involved more empirical approaches. He increased the complexity of a human model to address many of the unanswered questions in the study of locomotion, particularly with respect to the analysis and treatment of pathological gait. The affect of asymmetry of a model was investigated, and it was shown that small side-

to-side variations in geometric and muscle parameters greatly effect the performance of a model [Green and Yamaguchi 1992].

Yeadon presented an application of dynamic synthesis to the motion of the human body in athletic aerial maneuvers. A comprehensive methodology was developed for the determination of kinematics [Yeadon 1990a], the modeling a specific subject using body measurements [Yeadon 1990b], determination of the angular momentum of the entire body in flight [Yeadon 1990c], and the simulation of the motion using dynamic modeling [Yeadon, Atha et al. 1990].

Zajac and Gordon presented a comprehensive paper on the dynamics of human motion, in which the focus was the complexity of dynamic coupling effects [Zajac and Gordon 1989]. The practices of indirect dynamics, dynamic synthesis, static optimization for the determination of muscle forces, and the importance of dynamic optimization were discussed. It was suggested that dynamic optimization is the most useful approach to understanding musculoskeletal motion because it not only models the dynamics of the system, but it also models the task based on a performance criterion. The major point of this paper was the principles of "motion-induced accelerations" and "synergistics", in which the motion of one body part can greatly affect the motion of another, even in relatively slow activity. The soleus muscle was presented as an example, in which it was shown that the soleus can accelerate the knee into extension more effectively than it can accelerate the ankle into plantar flexion. The unique capability of the two-joint muscles to transfer power without accelerating a joint was demonstrated, as well as how single joint muscles perform "joint stiffening" tasks.

1.4 Computer Simulation of Surgery

Mann was one of the first to discuss the prospects of computer aided surgery [Mann 1985]. The discussion outlined the potential of computers to assist in the kinematic and kinetic analysis of movement, and in mechanical modeling of the musculoskeletal system. A computer tomographic method for determining mass distribution and musculotendonous origin and insertion sites was presented. However, the discussion was mostly an outline of future work. A hypothetical example (femoral osteotomy) was presented, and suggested that a surgeon could evaluate its outcome through dynamic modeling.

Delp has contributed several studies in the area of simulated surgery through computer graphics models of muscle and tendon. In his Ph.D. dissertation [Delp, Loan, et al. 1990], he expanded the research of Mansour [Mansour and Periera 1987], where the lower extremity musculature was investigated in detail for a typical subject. The joint kinematics could be specified by functional relations, and a one degree of freedom knee based on a study by Yamaguchi's [Yamaguchi and Zajac 1989b] was used. The system investigated instantaneous configurations under static and dynamic loading, and allowed for changes to the system to simulate surgical procedures. It accommodated changes in direction of the lines of action of each musculotendinous element and considered muscle and tendon slack lengths and pennation angles. Muscle moment arms (MA) were calculated using the technique developed by Hoy and co-workers [Hoy, Zajac, et al. 1990], in which the moment generating capability of each muscle at each flexion angle is defined by its instantaneous length-angle relation:

$$MA = dl / d\Theta$$

where l is the length of the muscle and Θ is the corresponding joint angle. A three dimensional interactive graphics system was employed to investigate force-length relations of muscle under alterations. Three dimensional shaded color graphics made it possible to view the system from any angle, and allowed for modification of any of the parameters, and several examples were presented (posterior tendon transfer and heel cord lengthening). The system was used to investigate locomotion and gait analysis [Delp 1991]. This was specifically applied to crouch gait with focus on the hip musculature [Speers and Delp 1993]. In this study, the hip flexors were shown to remain short through gait, while the hamstrings were found to have a normal excursion, indicating that the iliopsoas tendon may be a more important consideration for surgical intervention in crouch gait patients. The tendon transfer sight of the rectus femoris transfer was examined and optimized in a later publication [Ringwelski and Delp 1992].

Other works by Delp's group concentrate on the hip joint and musculature. An investigation that concentrated on the Chiari Pelvic Osteotomy and the related biomechanics determined optimal strategies for intervention [Delp, Bleck et al. 1990]. This surgical technique involves surgical reconstruction of the pelvis to produce a more advantageous geometry for the acetabulum of the hip joint, and is known for its variable outcome (limping, Trendelenburg gait). The surgery was simulated in varying degrees and it was discovered that certain procedures reduce the hip abductor muscles' torque-generating capacity. A later work discussed the sensitivity of the lower limb musculoskeletal system to hip joint center position [Delp and Maloney 1993]. In this study, the force generating capacity of the muscle groups crossing the hip are shown to be greatly

affected by a change in hip joint center position. Superior-inferior displacement had the greatest effect, while an inferior and medial positioning of the hip was shown to be optimal with respect to the moment generating capacity of the muscles.

Lewis' group at the University of Minnesota has presented several empirically determined 3D models of the knee joint contact and ligament forces, including the anterior cruciate ligament (ACL) [Lew and Lewis 1978; Loch, Lou, et al. 1992]. In the latest study, the knee stiffness matrices were shown to compare well with experimental data. The model was then used to evaluate the knee in a predictive manner, looking at graft cartilage forces and quasi-static motion before and after ACL removal. ACL reconstructions were also investigated, and changes load sharing of the different elements of the knee were used to simulate the results of trauma and surgery. This research is similar to the work of the University of Cincinnati group [Grood and Hefzy 1986], and an earlier study [Wismans, Veldpaus 1980].

2. PRELIMINARY STUDY: DYNAMIC MODELING OF HUMAN MOTION USING ADAMS/ANDROID

2.1 Introduction and Background

Models that would enable testing of surgical or rehabilitative procedures must be sophisticated enough to truly reflect the human musculoskeletal system. Consequently, the mathematical and computational costs are high. The formulation of the equations alone, particularly in complex, three dimensional systems, is a long, error-prone process. Therefore, a tool for automatically generating and analyzing subject-specific models is desired.

Several software packages exist that perform such modeling. These enable quick, accurate solutions of forward and inverse dynamic problems for mechanical systems. Some programs explicitly formulate the equations of motion. For these, the equations can be fed to a symbolic manipulation program such as MACSYMA or Mathematica for simplification before the numeric integration process is begun. Examples of this are Autolev [Schaechter and Levinson 1988], and SD/Fast [Rosenthal and Sherman 1986], which possesses its own symbolic simplification module. Other programs numerically formulate the equations of motion [Pandy and Berme' 1988b]. Commercial packages of this type are available, such as DADS [Haug 1989]

and ADAMS [Chace 1985; Orlandea 1973]. This thesis focused on one software package: ADAMS.

2.2 Overview of ADAMS and ADAMS/Android

ADAMS (Automatic Dynamic Analysis of Mechanical Systems) was developed by Mechanical Dynamics Inc., Ann Arbor, Michigan. It is a 3-dimensional modeling package for simulation of dynamic mechanisms, whose features have evolved since its beginning in the early 1970's. Components are divided into parts, and the most general structures of ADAMS are: the pre-processor, simulation routine , and post-processor. These modules can be seen in Figure 2.1.1.

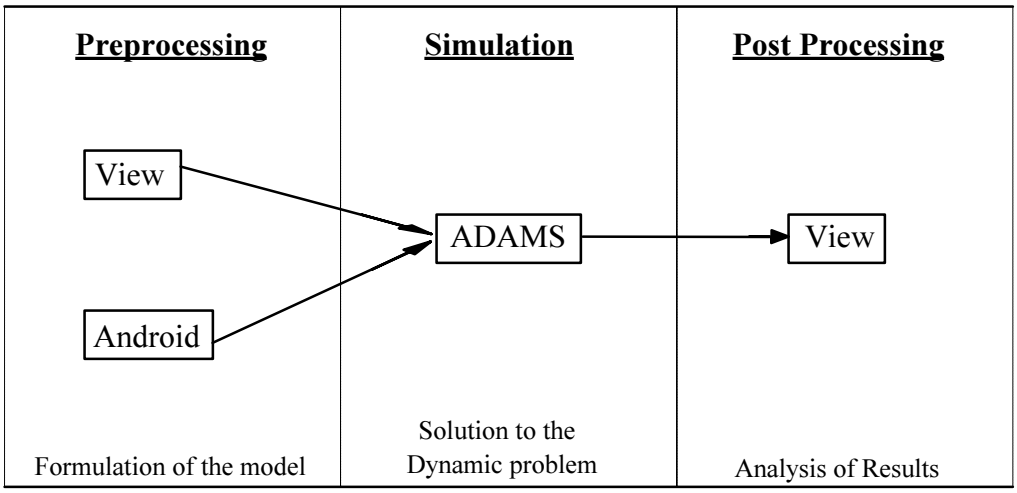

Figure 2.1.1 *A general schematic of the modules for ADAMS.*

ADAMS uses a Lagrangian approach to formulate the equations of motion. In order to accomplish this task, the user is required to idealize the mechanism to a system of rigid bodies and constraints. Each part is initially considered free, possessing six degrees of freedom (three rotational and three translational), and is later subjected to constraints. This approach allows the constraint forces to be calculated using Lagrange multipliers. A library of relations for establishing constraints is available (i.e. revolute joint, translational joint, etc.). Constraint relations can also be customized using FORTRAN subroutines. ADAMS is equipped with provisions to avoid singular configurations and simulations of closed-loop dynamic systems.

An interactive graphics module can be used for model definition (ADAMS/View), or the user may describe the model using English commands and values. The model is formulated into a system of equations for solution of forward or inverse dynamics problems.

The user specifies the simulation time, and other integration parameters to begin the simulation. The first step in this phase is to determine if the system is an indirect dynamics problem (kinematic analysis) or a direct dynamics problem (dynamic analysis). The decision is based on the Gruebler method for determination of dynamic degrees of freedom:

$$N = 6S - C$$

Where N is the total number of dynamic degrees of freedom of the system, S is the number of rigid body segments, and C is the number of active constraints specified. A dynamic analysis is required if the system exhibits at least one degree of freedom. In the case of the kinematic analysis, a set of algebraic equations is obtained, and the system is solved simultaneously for each instant of time.

If the system is determined to be a dynamic analysis problem, a system of nonlinear differential equations is obtained. A Jacobian matrix (a matrix of partial derivatives) is found for each instant of time, and the equations are integrated. The default method for solution of stiff systems (systems with widely varying time constants) is Gear's method [Gear 1971]. Data files are written that chronicle the simulation.

The final stage is the analysis of results. ADAMS/View provides graphic animation, charting, and processing of results (frequency domain analyses, etc.). Data can also be restructured into different forms (spreadsheet files, bitmaps, etc.).

Several modules also exist to quickly generate specialized models for simulation. Among these is ADAMS/Android, a specialized model generating package that creates idealizations of the human body as a mechanism. It generates a full-body, 3-dimensional, subject-specific model of a human, with surface contacts for human-environment interfaces. Body parts are linked by rotational joints. Full-body, subject specific models can be obtained by any of the following options:

1.) Entering each body part's parameters by hand: mass, inertia tensor, geometric surface; position and orientation of the center of mass; principle axes, joint axes; and the location of each joint relative to the center of mass.

2.) Entering 32 specific body measurements. Segments are then created from the measurements and published segmental density characteristics.

3.) Entering only height, weight, sex and age. The model is generated automatically using regression equations from the research of several investigators [Jensen 1986; Young, Chandler et al. 1983; Chandler , Clauser et al. 1975] to obtain

an estimate of the segmental geometric and mass distribution parameters.

A three dimensional interactive graphics window displays the model's initial configuration. The android can be placed in a modeling "environment," which is another model such as an automobile or a flat rigid floor. Motions, forces and torques can be specified using several approaches (cubic spline, Fourier expansion, etc.) Additionally, other features offered by ADAMS libraries can be employed.

A valuable feature of ADAMS/Android is the division of the model into parts for data storage. The independent files are assembled by ADAMS/Android and described below:

___**.and** file — The "android" file governs the geometry of the model. All joints, segments, surfaces, geometry for graphics, positions, and masses are defined here.

___**.prp** file — The "property" file governs the specification of motions, forces, and other inputs to the system during the simulation. It the specification of all functions that relate motion to time, force to time, etc. (The cubic splines necessary for gait lab-acquired motion drivers are found here.)

___**.pst** file — The "posture" file specifies a three dimensional positioning of the android in space. These values are used for the initial configuration.

___**.mdl** file — The "model" file specifies how all the elements come together, and the environment in which the android should be placed.

Because these files exist independently, several models can be driven by the same motion or force data, or a model can be placed in different environments. The functions that drive the model (the ___**.pst** and __**.prp** files) can be determined by measured data on a subject in a gait analysis laboratory.

2.3 Model Development

Several steps were taken to investigate ADAMS as tool for analysis and simulation of human locomotion. A planar model and a three dimensional, full-body model were developed.

2.3.1 Planar Model

Initially, a planar model was created without using the Android preprocessor, in order to gain a fundamental understanding of the modeling process. The model, shown in Figure 2.3.1, was a 7 link, 8 degree of freedom system consisting of two feet, two legs, two thighs, and a head and trunk (HAT) segment were connected by revolute joints. Joint motions and the position of the pelvis along the direction of motion were specified by standard gait lab data. A computer program was written to convert Biomechanics Evaluation Laboratory (BEL) angle data files to an ADAMS Spline (natural cubic spline) statement. The foot was initially modeled using the IMPACT command provided by ADAMS, in which the user can specify a relationship that activates force in a continuous fashion dependent on any user-specified system variable (vertical penetration into the floor was used). Each foot consisted initially of two impact elements, one at the heel and one at the ball

of the foot. Later this model of the foot was enhanced to a two element model consisting of a rearfoot and toe, each with two impact elements on each end. Shear or frictional forces were not considered because the HAT segment was driven forward by a cubic spline function (measured data), and braking and propulsion were therefore not necessary for forward progression.

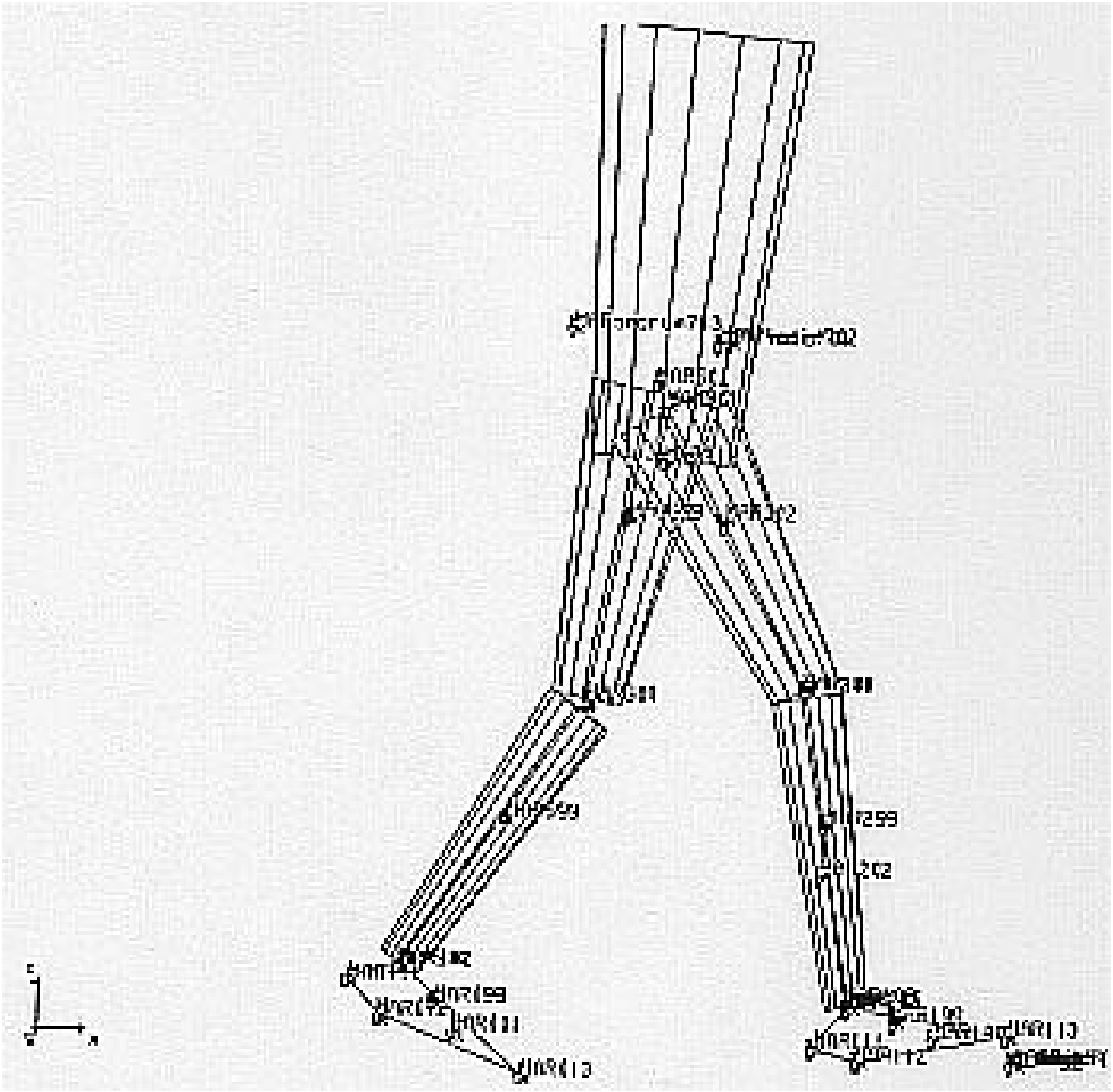

Figure 2.3.1 *The ADAMS planar model.*

The final degree of freedom, HAT vertical translation, was left free to move in response to the reaction of the model to the floor. This became an obvious necessity due to the sensitivity of the impacts at the foot. This approach allowed the foot to find its own vertical penetration in response to body weight and dynamic forces. Initially it was believed that the HAT could be forced to follow a vertical displacement spline, however the sensitivity of the impacts to small changes in kinematics of the foot result in large discrepancies in the ground reaction force (GRF) due to an over- or under-penetration of the foot into the floor.

Literature shows several studies on the importance of the foot-floor interface (FFI). Valiant [Valiant 1990] published investigations on the dynamic characteristics of the plantar surface of the foot. His work was followed up by Meglan [Meglan 1991; Meglan 1992], who investigated the load-deformation characteristics of the FFI for the purpose of dynamic synthesis of locomotion. Meglan developed general equations for vertical force using optimization techniques to fit Valiant's data to a simple polynomial. His resulting vertical force-deformation equation was:

$$F(x,v) = (4.658E10)x^4 + (9.719E10)x^4v$$

where F is the resulting force, x is the penetration depth and v is the velocity of penetration. The ADAMS modeling tools do not allow for such a polynomial to be specified without writing superfluous code, but offer instead the following cubic function (IMPACT statement):

$$F(x,v) = kx + \{c(x/d)^2 * [3 - 2(x/d)]\}v$$

where k is some linear spring constant, c is some damping coefficient, and d is the depth of penetration at which the damping value (c) must reach its effective value. This type of cubic function is advantageous because it is a smooth function for any impact velocity and the damping effects do not cause an instantaneous jump in force at impact. An approximation of Meglan's function for the normal range of penetration (1 cm) was found by minimizing the square of the difference of the two curves. The estimates of the ADAMS impact coefficients that represent Meglan's relations were:

k = 465.8 N/cm
c = 971.9 N/cm/sec
d = 1.685 cm

Similar to Meglan, the foot model included a toe element as a separate part, connected by a revolute joint to the foot (metatarsalphalangeal joint). A linear torsional spring damper governed the motion-force relationship, using coefficients from Meglan's work:

$(K_{rot})_{toe} = 1$ N/rad
$(C_{rot})_{toe} = 0.1$ N*cm/rad

The final step of the planar model study was to determine joint moments that result from the motion of the system (indirect dynamics) and use them to drive the system (direct dynamics). The best model was used to generate a knee moment time history for one gait cycle (right foot strike to right foot strike). The left knee, striking the floor about half way through the gait cycle, was used. The model was then driven by its previous motion splines except

for the knee, which was driven by a moment-spline. A parametric study was conducted in which the system was evaluated (inverse or kinematic problem) and synthesized (forward or direct problem) with varying values of torsional spring constant and torsional damping coefficient and an optimal range was determined that resulted in stable, realistic gait.

2.3.2 Three Dimensional Full Body Model

One hypothesis was that stable gait for a predictive model would only be possible if the entire body was considered, so that all body segments and their dynamic contributions were considered. A three dimensional model was created using ADAMS/Android preprocessor, using the standard regression equations based on height and weight. A typical model rendering is shown in Figure 2.3.2. The model was developed to possess 35 degrees of freedom: three rotational degrees of freedom each at the ankles, knees, hips, lumbar spine, shoulders; one degree of freedom at each elbow; and three translational and three rotational degrees of freedom of the pelvis segment relative to the inertial reference.

The ADAMS/Android convention used to describe angular displacements from one body segment to another is the Cardan Angles method (also called Bryant Angles method), which is a variation of Eulerian angles [Greenwood 1988]. This convention can be described as the three finite rotations which transform the proximal segment coordinate system to the distal segment coordinate system: first about the X axis, then the Y axis, then the Z axis. A computer program was developed for the management of laboratory data and calculation of the necessary splines for motions (see Appendix B). Ground reaction force and moment splines were also generated for indirect dynamic analyses.

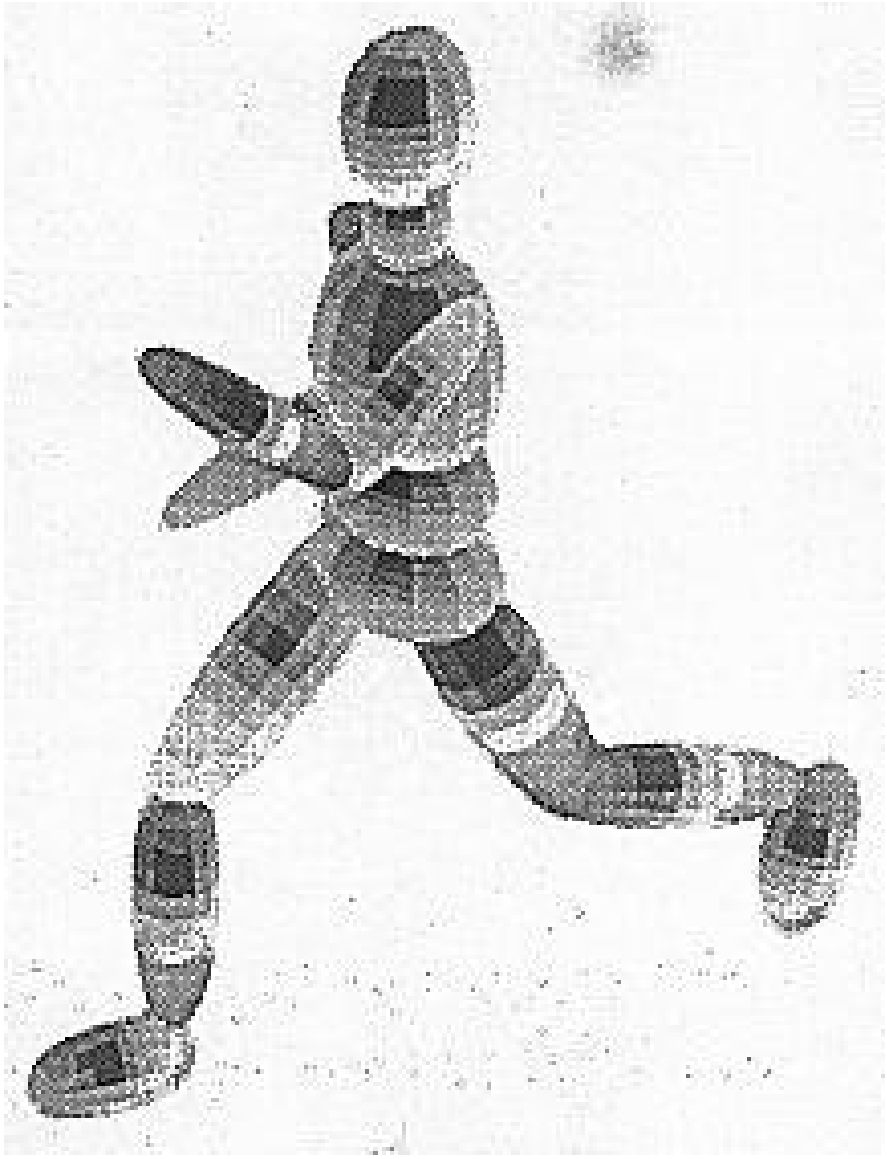

***Figure* 2.3.2** *The ADAMS/Android three dimensional full body model.*

Initially all joint motions were kinematically constrained using splines for determination of joint moments. Several combinations of joint moment values mixed with the original motion splines were used for forward dynamic simulations.

An enhancement to the default model of the foot was also investigated. A foot model was especially developed for ADAMS/android at the National Institutes of Health (NIH), shown in Figure 2.3.3, and consisted of three ellipsoidal surfaces [Kepple 1992]. The dynamic values were taken from Meglan's and Valiant's work, and were modified in order to allow smooth transition from rearfoot to forefoot:

k = 460 N/cm

c = 970 E3 N/cm/sec

e = 4

d = 1.00 cm

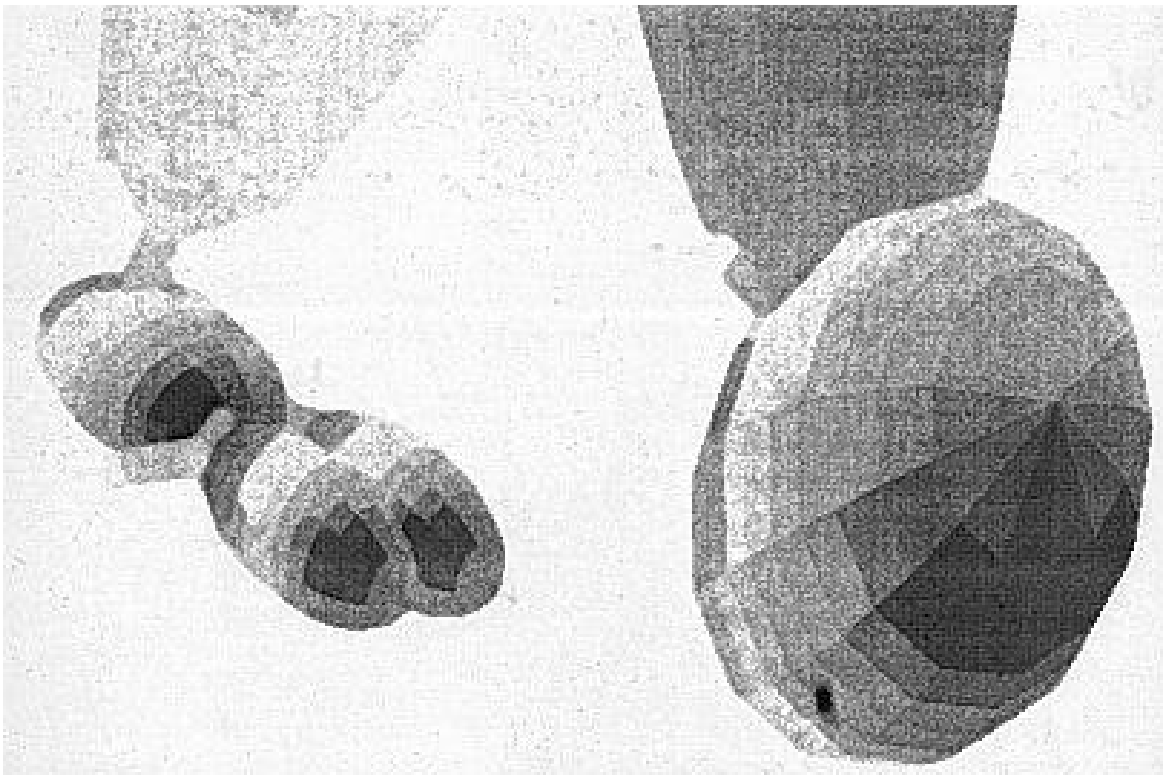

Figure 2.3.3 *The ADAMS/Android default foot (right) and the NIH Foot (left).*

2.4 Results and Discussion

For the planar model, the ground reaction force values proved to be similar to Meglan [Meglan 1990]. GRF curves were a noisy facsimile of the values measured with the force plate. The system was the most sensitive to model geometry and to kinematics. A slight modification to either of these would cause toe-drag or excessively long stride lengths. These results are also found in the literature for similar studies [Meglan 1991; Yamaguchi and Zajac 1990]. Trial and error adjustments to the geometry, initial conditions, and foot parameters yielded very different results. The best simulation exhibited some discrepancies in the foot coming in contact with the floor too early, but the model exhibited a good transition from one foot to the other. The vertical forces for this trial are shown in Figure 2.4.1.

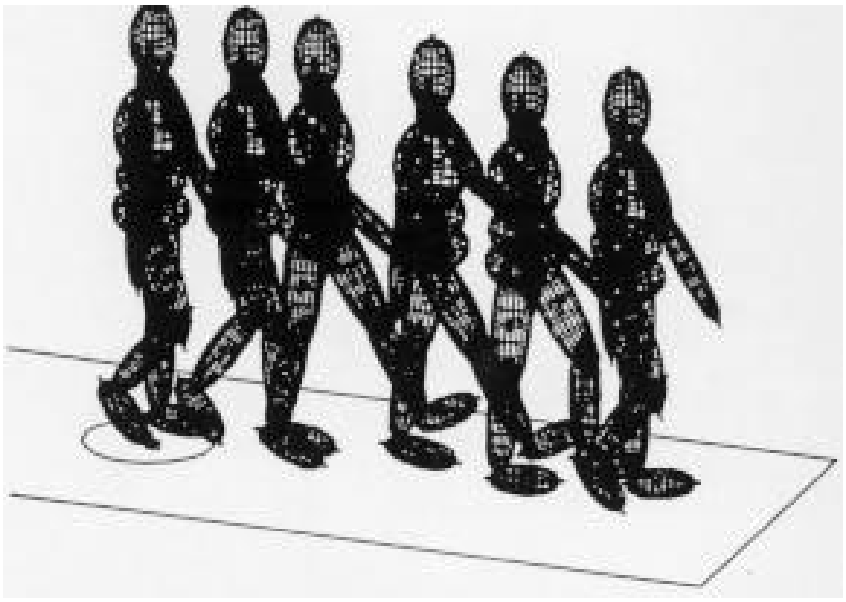

Figure 2.4.1 *Vertical ground reaction force results from a simulation of the planar model.*

In the forward dynamics solution, the response was unstable. Catastrophic falls occurred if the passive torsional spring at the knee was not stiff enough. Best values for the torsional spring and damper were:

$$(k_{rot})_{knee} = 100 \ \text{N*cm/rad}$$
$$(c_{rot})_{knee} = 10 \ \text{N*cm/rad/sec}$$

For the three dimensional model, stable gait was only possible when certain constraints were imposed on the system. Figure 2.4.2 shows the results of a simulation in which the pelvis orientation and all joint rotations were kinematically constrained by splines, and the entire body was allowed to move in two translational degrees of freedom (in the line of progression and in the vertical direction).

Figure 2.4.2 *The results of gait driven by motions at the joints and constraint of the orientation of the pelvis relative to the inertial reference frame.*

Other simulations resulted in stable gait only for short periods, followed by some catastrophe such as collapse, tripping, falling backwards, or falling sideways. Figure 2.4.3 shows the model just before a fall; the result of full kinematically-driven motions at the joints, but allowing the orientation of the body relative to the inertial reference to be free. The undesired motions that precipitated this fall gradually built up over the simulation time (the instant in the figure is t= 0.55 seconds, where foot contact occurred at time zero), and could be caused by errors in the motion detection, leg length discrepancies in the subject modeled, improper modeling of the plantar surface of the foot, inaccurate initial conditions, or joints whose neutral positions (all Cardan angles are zero) are inconsistent with those assumed in the calculations from motion data.

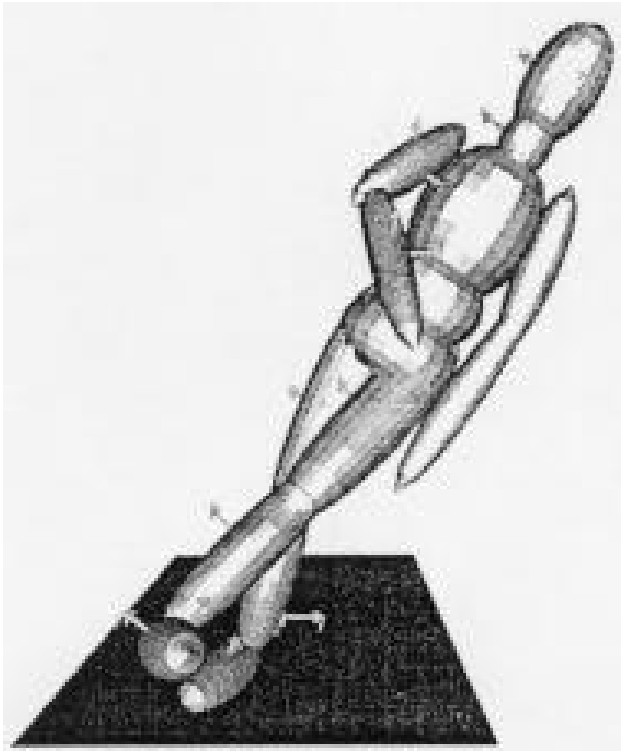

Figure 2.4.3 *Simulation results showing the instant just before a fall. Joints were kinematically driven and the orientation and translation of the pelvis relative to the inertial reference was allowed to be free.*

A problem occurred when a foot impacted the ground a split-second too early. The cause of this may be improper modeling of the surface geometry of the foot, or an overestimation of the length of some body segment. When such an early (or late) impact occurs, the sequencing of the moment time histories obtained in the indirect problem do not match the actual impact, and a large load is rapidly placed on the system at the wrong time. The joint motions deviate slightly from their intended trajectories, and a subsequent catastrophe usually occurs (due to the non-linear nature of the system).

The only way to understand the causes of such problems was to successively test the model after a change in a parameter; there were no straightforward approaches. It was often found that an attempt to correct one problem only led to another. An example is an attempt to avoid tripping by shortening a limb. The result was that the toe did not catch during swing, but the subsequent gait pattern exhibited an excessively long stride length. This type of problem has been documented in similar studies [Yamaguchi and Zajac 1990]. The use of unnatural constraints, such as locking the pelvis' orientation only lead to violent motions when events such as a toe catch occur (i.e. the model flies off vertically). Additionally, it can be argued that a realistic predictive model cannot have such unrealistic constraints. Full kinetically driven models with no unrealistic constraints, however, were unsuccessful in completing even the stance phase of a gait cycle. This difficulty with kinetically driven models has been documented [Meglan 1991].

Unfortunately, the causes of the problems mentioned above are hidden in the complexity of the model. Such modeling processes are so involved that gaining an understanding is virtually impossible. No feeling for the parametric sensitivity of the system is possible in a system so complex and hidden in the software. Clearly, methods must be investigated before full

body three-dimensional models can be used. The numerical analysis techniques, the dynamic stability, the non-linear effects, and the coupling effects need to be investigated. Control strategies may be necessary, and muscle co-contraction must be considered [Zajac and Gordon 1989]. However, this modeling protocol stands ready to be used, and can be enhanced once a there is a better knowledge of the process.

The necessity for such understanding is the impetus for the remainder of the research of this thesis, in which the focus was on the systematic inaccuracies of forward dynamic simulations using simpler models.

3. METHODS

3.1 Introduction and Background

The goal of this research was to investigate in detail the factors contributing to difficulty of forward dynamic modeling of human locomotion. A wide variety of literature exists on human gait patterns for comparison of results. Gait studies limited to the saggital plane have been successful due to the dominance of motion in that plane [Winter 1984], thus the model developed was planar.

The goals were to develop a model that is both sufficiently complex to use in predictive analyses and sufficiently simple to allow the underlying process to be understood and manipulated. The initial phase of the experiment was not conducted on human motion, but on the planar motion of a single rigid body (a slender rod) coming in contact with the floor. The intention was to isolate unknown causes of error so they can be reduced or eliminated. This second phase of work carried strategies developed in the analysis of the single rigid body to the application of human motion, particularly walking. For this reason, the model will be planar and focus on three body segments: the foot, the leg, and the thigh.

3.2 Methods for Planar Dynamic Analysis of a Single Rigid Body

The methods involved in developing a predictive model can be divided into four steps: experimental procedure, data reduction, inverse dynamics analysis, and forward dynamic synthesis.

3.2.1 Experimental Procedure

A uniform hardwood rod of known length was chosen so that the moment of inertia and mass could be accurately determined. The assumption that the rod is slender requires the length to be much greater than the diameter, and the rod used met these specifications, with a length to diameter ratio of 37.2. The dimensions of the rod are shown in Figure 3.2.1. The rod was targeted with two retro reflective markers created by wrapping a rectangular strip of retro-reflective tape around the outer diameter of the rod.

The center of mass was measured by finding a balance point, and was almost exactly at the midpoint of its length. The rod was cylindrical in shape with a diameter of 3.5 centimeters.

A Motion Analysis Corporation system was used to collect motion data using four 60 Hertz cameras and a three dimensional tracking system (*EV3D* by Motion Analysis Corporation). The environment used was calibrated using 16 targets defining a volume 2 meters long by 1 meter wide by 1.38 meters high, with origin at the center of the force plate. The three dimensional coordinates were calculated using a direct linear transformation algorithm [Walton 1981].

Forces were measured at 1000 Hertz with an Advanced Mechanical Technology, Inc. six channel force plate. The device measures three forces and three moments about the instrument center, located beneath the surface.

Figure 3.2.2. illustrates the actions of the rod. The rod was placed with one tip on the force plate and held tightly by hand at the other end. The rod was then manually maneuvered in an inverted pendulum-like fashion for 4 seconds. Several trials were collected at slow and fast speeds with varying degrees of force application. Care was taken to constrain the motion to one plane by placing strands of string as guides.

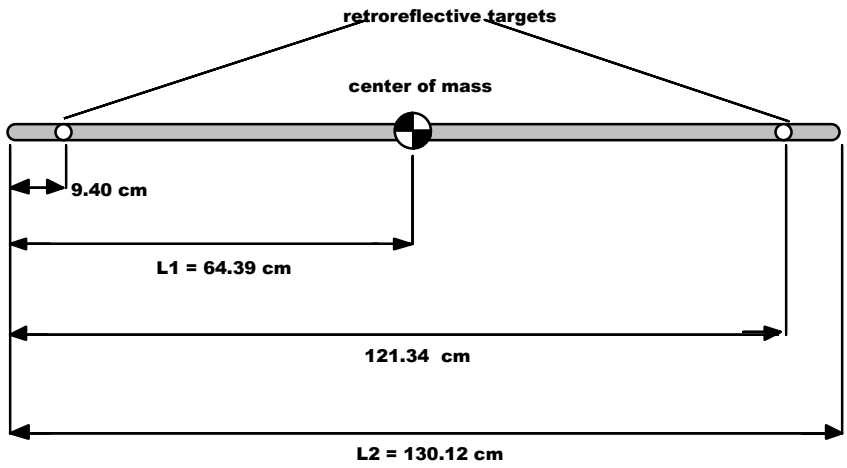

Figure 3.2.1: *The dimensions of the slender rod.*

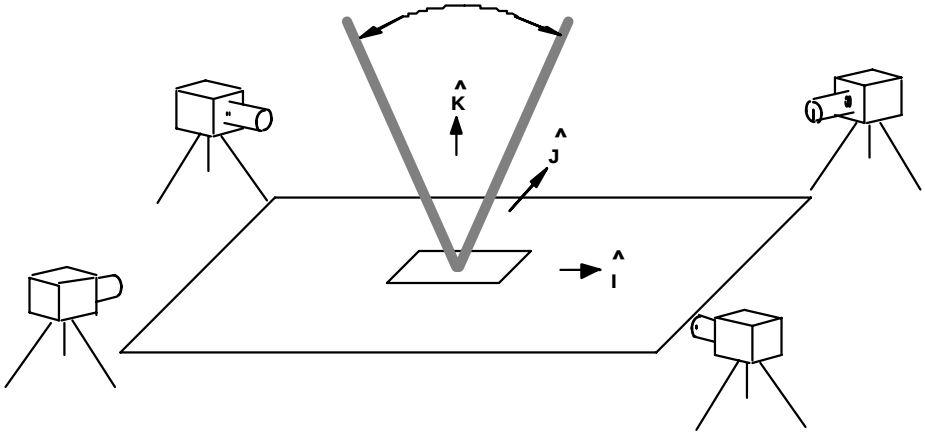

Figure 3.2.2: *The experimental procedure showing the lab (inertial) reference frame.*

3.2.2 Data Reduction

A software program was developed to reduce the force data to a mechanical wrench whose intercept with the force plate's surface is the center of pressure (COP), [Soutas-Little 1987]. Motion and force data were synchronized in time.

A dynamics software program was written to continue the analysis. The force time data and target trajectories were smoothed using a rectangular signal processing window (straight averaging). Several different degrees of smoothing were attempted to investigate the sensitivity in subsequent calculations.

Each coordinate was differentiated using a central difference technique, with the forward and reverse differences used at the endpoints [Wylie and Barrett 1982]. The effects of three-point and five-point methods of differentiation were investigated. The velocities were differentiated again to determine the accelerations. It is well known that photogrammetric data is noisy, and that this noise is greatly magnified in the process of

differentiation, [Winter 1990, Zajac and Gordon 1989]. Thus the result of smoothing before each derivative was evaluated.

The distance between the markers was calculated for each trial. Because the rod is rigid and the targets are rigidly placed on the rod, a change in inter-marker distance during the motion is a measure of the errors in the experimental motion detection.

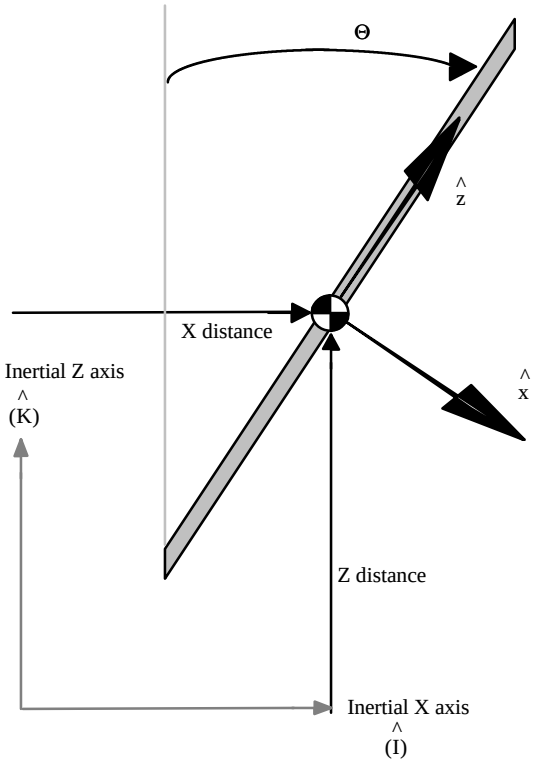

Figure 3.2.3: *The coordinates of the inertial (lab) reference and the rod.*

The smoothed target trajectories were used to calculate the angle from the laboratory vertical z-axis ($\hat{K}$) to the long axis of the rod ($\vec{R}$) from bottom to top target, and its unit vector $\hat{x}$. To eliminate out of plane effects, a vector in the plane of motion and perpendicular to the rod ($\hat{x}$) was formed and used for the detection of angles:

$$\hat{x} = \frac{\vec{R} \times \hat{J}}{\left|\vec{R} \times \hat{J}\right|} \qquad (3.2.1)$$

where $\hat{J}$ is the laboratory unit vector in the inertial **Y** direction of a right-handed coordinate system. The angle, Θ, was defined as:

$$\Theta = \sin^{-1}(\hat{x} \bullet \hat{K}) \qquad (3.2.2)$$

The complement of the angle between $\hat{K}$ and $\hat{x}$ is Θ, and using the inverse sine function makes it possible to calculate Θ using $\hat{x}$ instead of $\vec{R}$ which may be out of the *xz* plane. This method also allows the determination of the sense of Θ as well as its magnitude.

Although the experimental procedure was such that $\vec{R}$ did not deviate outside a small region near vertical, a mathematical correction was placed in the algorithm for excursions of Θ which were greater than ±90°, with the intentions of using this algorithm later on human motion. This correction involved modification of the angle calculation when Θ is within 20° of ±90°. At this point it is necessary to shift to new calculations:

$$\Theta = 90° - \sin^{-1}(\hat{z} \bullet \hat{K}) \text{ if } \hat{z} \text{ in the positive } \hat{I} \text{ direction when } \Theta \text{ is within } 45° \text{ of } 90° \qquad (3.2.3)$$

$$\Theta = -90° + \sin^{-1}(\hat{z} \bullet \hat{K}) \text{ if } \hat{z} \text{ in the negative } \hat{I} \text{ direction when } \Theta \text{ is within } 45° \text{ of } -90° \qquad (3.2.4)$$

It may appear that angular velocity, $\vec{\omega}$, should be determined by differentiating the angle, Θ. However, this approach is problematic because errors associated with the calculation of Θ have the potential of being magnified in further calculations. It was determined that the use of the

smoothed target trajectories and their derivatives produced the best results for angular velocity and angular acceleration, [Verstraete and Soutas Little 1990]. The well known kinematic relation between angular velocity and positions of a rigid body is:

$$\vec{V}_{a/b} = \vec{\omega} \times \hat{R} \qquad (3.2.5)$$

The velocity of point *a* relative to point *b* is the cross product of angular velocity with the relative postion vector, $\vec{R}$. Each target trajectory was resolved into the *xz* plane, and for a planar rigid body situation this equation was expanded into components resulting in two possibilities:

$$\omega 1 = (Va/b)x \,/\, Rz \qquad (3.2.6)$$

$$\omega 2 = -(Va/b)z \,/\, Rx \qquad (3.2.7)$$

The choice of which equation to use is theoretically arbitrary, but has important bearings on the quality of the data in measured motion applications. Thus, the two options were investigated for their effects on the system.

Angular acceleration, $\vec{\alpha}$, was calculated next. This calculation again uses a well known kinematic relation:

$$\vec{A}_{a/b} = \vec{\alpha} \times \vec{R} + \vec{\omega} \times (\vec{\omega} \times \vec{R}) \qquad (3.2.8)$$

The acceleration of point *a* relative to point *b* is equal to two separate terms, the tangential and normal acceleration components, respectively. Note that the determination of $\vec{\omega}$ is necessary before this can be calculated. Similar to

the angular velocity, this equation can be expanded into components and shown that for a planar rigid body, two possibilities exist for the solution:

$$\alpha 1 = [\ (Aa/b)x\ + w^2Rx]/\ Rz \qquad (3.2.9)$$

$$\alpha 2 = [-(Aa/b)z\ + w^2Rz]/\ Rx \qquad (3.2.10)$$

Again, the choice is important and thus was investigated for effect on the outcome.

It is important to emphasize that these kinematic relationships are for the assumption of a rigid body. With rigidly attached targets the absolute distance between two targets does not vary, but in actuality, errors due to pixel resolution, target obstruction, imperfect calibration, and tracking all cause error. Particularly in human motion, the errors are increased due to skin motion and targets near non-ideal joints.

A planar, rigid body assumption implies that relative velocity between two targets is perpendicular to the line connecting them (equation 3.2.5). To make the data more closely resemble the motion of a true rigid body, the erroneous component of the relative velocity that is parallel to the line between the two targets was subtracted away:

$$(\vec{V}_{a/b})_{parallel} = (\vec{V}_{a/b} \bullet \hat{z})\hat{z} \qquad (3.2.11)$$

$$\vec{V}_{a/b}' = \vec{V}_{a/b} - (\vec{V}_{a/b})_{parallel} \qquad (3.2.12)$$

Equation 3.2.5 becomes:

$$\vec{V}_{a/b}' = \vec{\omega} \times \hat{R} \qquad (3.2.13)$$

The value obtained in equation 3.2.13 is thus a more accurate representation of the relative velocity, and can be used in equations 3.2.6. and 3.2.7 for the determination of angular velocity.

Similarly, the angular acceleration can be corrected for inter-target motion. In the case of acceleration, however, a planar, rigid body assumption suggests that only the first term on the right hand side of equation 3.2.8 ("tangential" acceleration) is perpendicular to the line connecting the targets. Equation 3.2.8 can be expressed as a vector expression in which both the left and right sides are perpendicular to the line connecting the targets:

$$\vec{A}_{a/b} - \vec{\omega} \times (\vec{\omega} \times \vec{R}) = \vec{\alpha} \times \vec{R} \qquad (3.2.14)$$

The left hand side can then be evaluated, and the parallel component can be subtracted away:

$$(\vec{A}_{a/b})_{parallel} = \{[\vec{A}_{a/b} - \vec{\omega} \times (\vec{\omega} \times \vec{R})] \bullet \hat{z}\}\hat{z} \qquad (3.2.15)$$

$$\vec{A}_{a/b}' = \vec{A}_{a/b} - (\vec{A}_{a/b})_{parallel} \qquad (3.2.16)$$

Equation 3.2.8 becomes:

$$\vec{A}_{a/b}' = \vec{\alpha} \times \vec{R} + \vec{\omega} \times (\vec{\omega} \times \vec{R}) \qquad (3.2.17)$$

The value obtained in equation 3.2.17 is thus a more accurate representation of the relative acceleration, and can be used in equations 3.2.9. and 3.2.10 for the determination of angular acceleration.

Once the values for angular velocity and acceleration are known, the values for the linear velocity and acceleration of the center of mass can be found using:

$$\vec{V}_{CM} = \vec{V}_b + \vec{\omega} \times \vec{r}_{CM/b} \tag{3.2.18}$$

$$\vec{A}_{CM} = \vec{A}_b + \vec{\alpha} \times \vec{r}_{CM/b} + \vec{\omega} \times (\vec{\omega} \times \vec{r}_{CM/b}) \tag{3.2.19}$$

where $\mathbf{r}_{CM/b}$ is the vector from target b to the center of mass expressed in the inertial coordinate system.

3.2.3 Inverse Dynamic Analysis

The rod was modeled as shown in Figure 3.2.4. A slender rod with concentrated moments and forces at the bottom and top was used.

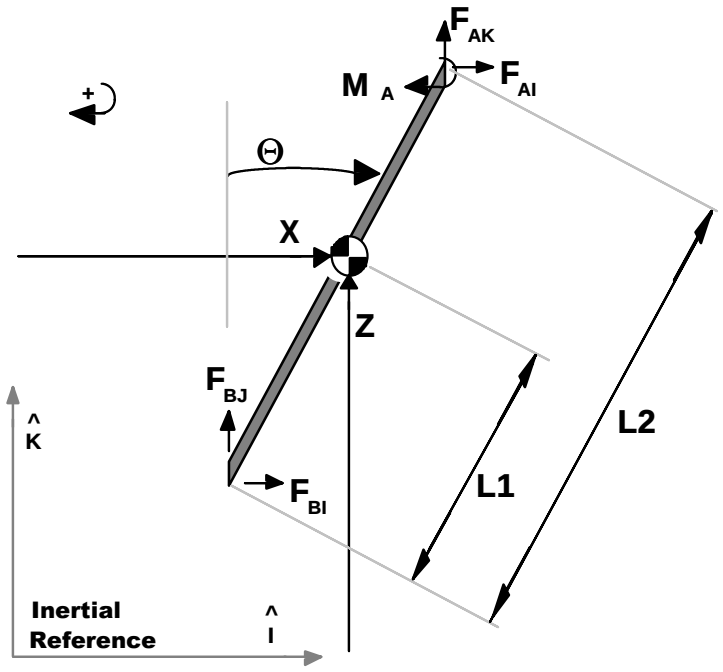

Figure 3.2.4: *Model of the rod for dynamic analysis using forces expressed in the inertial coordinate system ("Inertial-based approach").*

The equations of motion involve the motion of the rod in three degrees of freedom (DOF): rotation in the plane (Θ), and motion of the center of mass in two planar directions (*x* and *z*). The inertia used for the moment equation was that of a slender rod rotating about its center of mass:

$$I = \frac{1}{12}(\text{mass})(\text{length})^2$$

Using a Newtonian approach, the inertial forces and moments due to accelerations are equal the net applied forces and moments:

$$m\ddot{X} = F_{AI} + F_{BI} \qquad (3.2.20)$$

$$m\ddot{Z} = F_{AK} + F_{BK} - mg \qquad (3.2.21)$$

$$I\ddot{\Theta} = M_A - F_{AI}(L2 - L1)\cos\Theta + F_{BI}(L1)\cos\Theta + F_{AK}(L2 - L1)\sin\Theta - F_{BK}(L1)\sin\Theta \quad (3.2.22)$$

These coordinates are also displayed in Figure 3.2.4.

In the situation where forces at one end are known (measured by the force plate), the equations can be reformulated for the indirect dynamics analysis by moving the unknown values to the left hand side:

$$F_{AI} = m\ddot{X} - F_{BI} \quad 3.2.23)$$

$$F_{AK} = m\ddot{Z} - F_{BK} + mg \quad 3.2.24)$$

$$M_A = I\ddot{\Theta} + F_{AI}(L2 - L1)\cos\Theta - F_{BI}(L1)\cos\Theta - F_{AK}(L2 - L1)\sin\Theta + F_{BK}(L1)\sin\Theta \quad 3.2.25)$$

These values can then be evaluated for each frame of data by solving in the order presented above. The result of this analysis is a time history of forces and moments at the top of the rod.

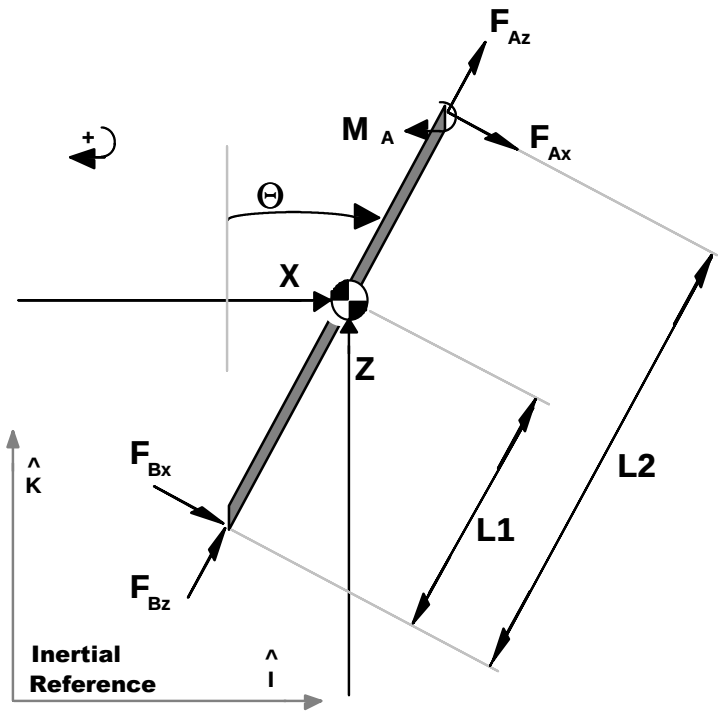

Figure 3.2.5: *Model of the rod for dynamic analysis using forces expressed in the coordinate system embedded in the rod ("Body-based approach").*

The equations of motion can also be written for forces and moments specified in the coordinate system of the rod, as defined in Figure 3.2.5. These equations include the 2 dimensional coordinate transformation factors in order to relate forces to motion in the inertial reference frame:

$$m\ddot{X} = (F_{Ax} + F_{Bx})\cos\Theta + (F_{Az} + F_{Bz})\sin\Theta \qquad (3.2.26)$$

$$m\ddot{Z} = -(F_{Ax} + F_{Bx})\sin\Theta + (F_{Az} + F_{Bz})\cos\Theta - mg \qquad (3.2.27)$$

$$I\ddot{\Theta} = M_A - F_{Bx}(L2 - L1) + F_{Bx}(L1) \qquad (3.2.28)$$

Where the subscripts z and x denote the orthogonal directions along the rod and perpendicular to the rod, respectively. In this situation, the direction of

the forces move with the rod. The advantages of this are twofold. First, the forces are now known in the coordinate system of the rod instead of an arbitrarily chosen reference frame. This method lends itself well to biomechanical analysis, in which the joint and muscle forces are much more meaningful if they are known in the reference frame of a body segment. Second, the removal of any ties to an inertial reference frame reduces non-linear effects on the system. In Equation 3.2.28, $\ddot{\Theta}$ is not dependent on Θ, and this changes the rod's dynamic behavior in the forward dynamics problem. This will be further discussed in the next section. Results were obtained for both the inertial-based approach and body-based approaches.

3.2.4 Forward Dynamic Synthesis

Using the rod as modeled above and shown in Figure 3.2.4, the equations of motion were driven by the forces and moments calculated in the indirect dynamics analysis. In this phase, the forces that drive the system are regarded as known, while the motion is derived by solving the equations of motion. Therefore, the equations 3.2.22 to 3.2.24 can be reformulated by moving the unknown values to the left hand side:

$$\ddot{X} = \frac{1}{m}(F_{AI} + F_{BI}) \tag{3.2.29}$$

$$\ddot{Z} = \frac{1}{m}(F_{AK} + F_{BK} - mg) \tag{3.2.30}$$

$$\ddot{\Theta} = \frac{1}{I}(M_A - F_{AI}(L2 - L1)\cos\Theta + F_{BI}(L1)\cos\Theta + F_{AK}(L2 - L1)\sin\Theta - F_{BK}(L1)\sin\Theta) \tag{3.2.31}$$

If the forces and moments are specified in the coordinate system of the rod, the equations can be reformulated similarly. Again, these equations possess the 2 dimensional coordinate transformation factors in order to relate forces to motion in the inertial reference frame:

$$\ddot{X} = \frac{1}{m}[(F_{Ax} + F_{Bx})\cos\Theta + (F_{Az} + F_{Bz})\sin\Theta] \qquad (3.2.32)$$

$$\ddot{Z} = \frac{1}{m}[-(F_{Ax} + F_{Bx})\sin\Theta + (F_{Az} + F_{Bz})\cos\Theta - mg] \qquad (3.2.33)$$

$$\ddot{\Theta} = \frac{1}{I}[M_A - F_{Bx}(L2 - L1) + F_{Bx}(L1)] \qquad (3.2.34)$$

These equations are coupled, and some equations are nonlinear due to the trigonometric terms. Many solutions are possible, depending on the initial conditions imposed. A straightforward symbolic integration is therefore extremely difficult, and a numerical solution is the only option.

The method of integration used was the Modified Euler Method [Wylie and Barrett 1982]. This technique involves two predictive iterations of integration. The current acceleration is calculated from the forces (and current position, if necessary) using the equations of motion shown above. The current acceleration and velocity are used to predict the velocity and position for the next instant of time. Some of the above equations (3.2.31 for example) are coupled and nonlinear and must use the integrated position to calculate acceleration for the next instant of time. Once the estimate of the velocity and acceleration for the next instant of time is obtained, the process is repeated using the average of the newly estimated velocity and acceleration for the next instant and the velocity and acceleration from the current instant. Upon completion of the second iteration, the system

advances to the next time step and the process continues until a specified ending time. Note that further repetition of estimating and averaging would improve the quality, and many techniques actually involve an indefinite number of iterations until the resulting values converge (or diverge, in which case other alternatives must be implemented, such as reduction of the time increment) [Gear 1971]. Other methods that implement the contribution of previous time steps (Runge-Kutta methods), or use predictors and error correctors (Adams and Gear methods) are simply more sophisticated variations, and can be implemented in the future if a higher accuracy is desired. However, the Euler Method was shown to be a successful approach in human motion synthesis [Onyshko and Winter 1980].

3.3 Methods for Planar Dynamic Analysis of Human Locomotion

Similar to the rod simulation, the methods involved in developing a predictive model of human locomotion can be divided into four sections: experimental procedure, data reduction, inverse dynamics analysis, and forward dynamic synthesis.

3.3.1 Experimental Procedure

The environment calibration and data collection procedure was performed using the same equipment described in section 3.2.1. Again, motion was collected at 60 Hz and force was collected at 1000 Hz. The calibration space used was again established by 16 stationary targets, but varied in size for each subject, and the procedure for establishing dimensions for the space were as follows: The length of the space (x direction) was estimated as 20% longer than the stride length of the subject, the space centered about the gait cycle beginning near foot strike and ending near the second foot strike of the same leg. The width of the space was one meter wide, and the height was estimated as 20% higher than the subject's superior iliac spine, to assure sufficient assessment of pelvic motion. The environment was positioned so that the force plate was centered in the width of the space and near one end of the length (approximately 10% of the length) so that the first foot strike fell on the force plate. This is illustrated in Figure 3.3.1.

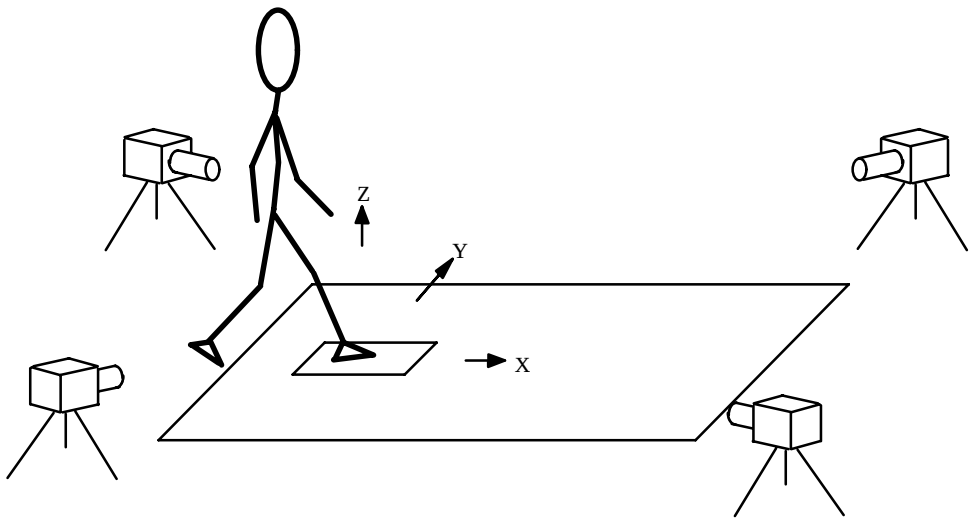

Figure 3.3.1: *The environment used showing the lab (inertial) reference frame.*

Prior to the experiment, the subject was informed of the nature of the research and the protocol of the experiment, and that the data would remain confidential. An informed consent form was signed and filed under the UCHRIS IRB#89-559.

Anthropometric data was obtained on each subject through measurements. The distances between targets and several bony landmarks were measured for purposes of calculating the mass distribution properties and joint positions. In addition, neutral target positions and normal posture were measured in a standing trial, in which the subject stands erect on the force plate.

The targeting protocol used is an extension of that described by Soutas-Little [Soutas-Little 1990], and is outlined in Table 3.3.1. Three targets were placed on bony landmarks of each body segment. Although this protocol was developed for three dimensional kinematic analysis, it was used to allow more accurate identification of the segmental joint and mass distribution positions. The protocol is also the standard clinical protocol of the Michigan

State University Biomechanics Evaluation Laboratory, where a large volume of data, both pathological and normal, is available.

Figure 3.3.2: *The targeting protocol used.*

Table 3.3.1: *The target position descriptions.*

Thigh	Leg	Foot
Greater Trochanter	Proximal Tibial Crest	Calcaneus
Lateral Condyle	Distal Tibial Crest	Medial Rearfoot
Medial Condyle	Posterior Distal Leg	Lateral Rearfoot

The experiment was conducted on several subjects that walked at a normal pace through the environment. Trials were discarded if the subject failed to remain in the space or strike the force plate cleanly with one foot. For consistency, all trials were collected with the subjects barefoot. The data for each trial was shortened to approximately 10% before and 10% after the gait cycle.

3.3.2 Data Reduction

The data reduction phase is similar to that of section 3.2.2. Each body segment's position, velocity, and acceleration were determined in the same way as the rod in section 3.2.2.

The management of large volumes of motion data and the conversion to a planar-modeled motion was done as part of a large computer software program developed for data reduction of standard gait laboratory data at the Michigan State University Biomechanics Evaluation Laboratory (BEL). The program, Blink, is outlined in detail in Appendix B. Segment targets were used to define two points in space for the same calculations for the determination of kineamtic quantities described in Section 3.2.2.

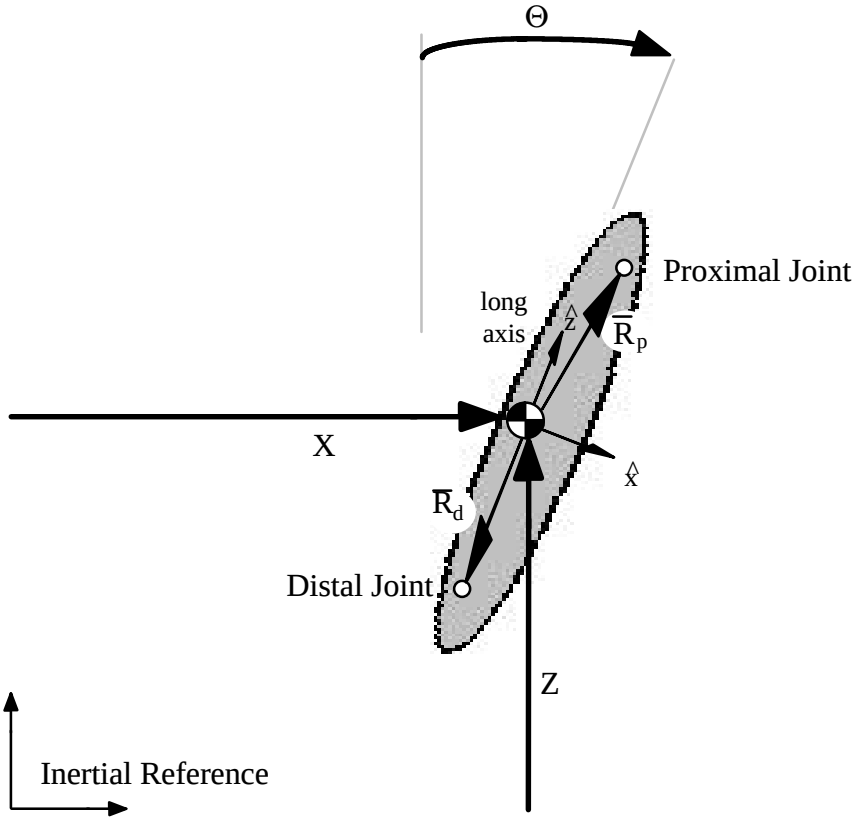

Figure 3.3.3: *The convention used for link-segment analysis.*

Each body segment possessed a distal and proximal joint vector. The convention used is shown in Figure 3.3.3, and the specific definitions are summarized in Table 3.3.2. The vectors were expressed in the principle coordinate system of the body segment, originating at the segment's center of mass. For the equations of motion, a 2 dimensional transformation of the joint vectors to the inertial reference frame was needed for each instant in time, based on the orientation of the segment. Each joint position vector was held constant, but researchers argue whether the joints should be mechanically analyzed as ideal hinges, [Yamaguchi and Zajac 1989; Scott and Winter 1991], thus provisions have been made for joint position vectors to be expressed as a functions instead of a constants.

Instead of choosing one anthropometric scaling scheme for mass distribution and center of mass position, the methods employed will reflect the work of Verstraete, [Verstraete 1988], in which the results of several investigators [Braune and Fisher 1889; Dempster 1955; Clauser, McConville et al. 1969; Chandler, Clauser et al 1975; McConville, Churchill et al. 1980; Young, Chandler et al. 1983] were averaged to obtain the most accurate value. The values used are summarized in Table 3.3.2. Mass distribution values were estimated based on the values presented in [Winter 1990].

Table 3.3.2: *The anthropometric scaling scheme used.*

Measure:	**Foot**	**Leg**	**Thigh**
Mass (m) †	.0145 * (bodyweight)	.0465 * (bodyweight)	.100 * (bodyweight)
Polar Moment of Inertia †	mass * $(.475*length)^2$	mass * $(.302*length)^2$	mass * $(.323*length)^2$
Direction of principle long axis (**z**) ††	2^{nd} toe to the calcaneus	line formed by the tibial crest	Lateral condyle of the knee to the greater trochanter †††
Center of Mass in the segment **X** direction ††	From the sole: .522 * (distal malleolus height when standing)	From the tibial crest: .4247 * (width)	From the anterior aspect: .5335* (width)
Center of Mass in the segment **Z** direction ††	From the toe: .564 * (length)	From the tibial crest: .384*(length)	From the greater trochanter: .4101 *(length)
Distal joint position ††	Center of Pressure (COP)	(measured) Midpoint between the medial and lateral malleolus	Midpoint between the medial and lateral condyles of the knee
Proximal joint position ††	(measured) Midpoint between the medial and lateral malleolus	Midpoint between the medial and lateral condyles of the knee	Greater trochanter

† From [Winter 1990] †† From [Verstrate 1988] ††† Estimated

The Foot

The foot motions were calculated by averaging the two rearfoot target positions, establishing a distal landmark, and using the calcaneal target as the

proximal landmark. The foot segment coordinate system was then established as a vector from the foot distal landmark to the proximal landmark (foot *z* axis) and a vector perpendicular to the z axis and the inertial y axis, directed according to the right hand rule. This convention is illustrated in Figure 3.3.4. Care was taken in placing the targets to align their positions about the principle axes of the foot, as described by several authors as the line from the calcaneus to the second toe, [McConville, Churchill et al. 1969; Young, Chandler et al. 1983]. The result was a special case where the targeting coordinate system was oriented with the principle coordinate system, and the need for coordinate transformations is eliminated.

Once the principle coordinate system was established, the center of mass was defined as 56.4% of the foot length and 47.8% of the foot distal medial malleolus height along the *z* and *x* axes, respectively. This was established from standing file data. A measurement of the position of the ankle joint relative to the target (both x and z components) was necessary to establish the position of the center of mass relative to the calcaneal target in the foot's coordinate system.

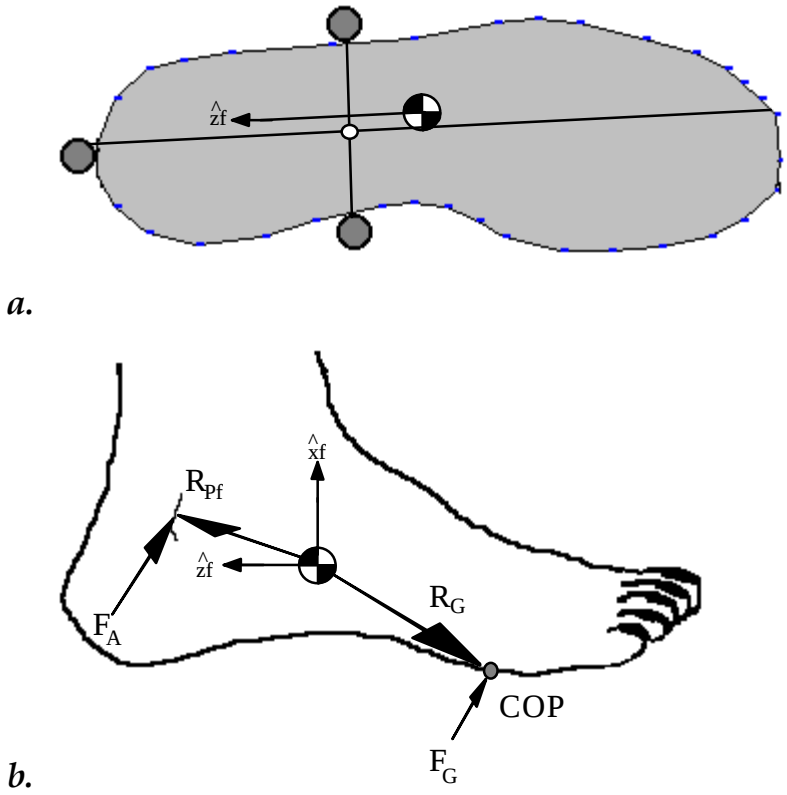

Figure 3.3.4: *Foot analysis from targeting. a) bottom view. b) side (in-plane) view.*

The ankle joint center was defined to lie on the contact surface of the talus and the tibia, at the midpoint of the line between the distal medial malleolus and point on the lateral malleolus at the same distance from the ground during normal standing, [Verstraete 1988]. This was established by the standing file data and body measurements taken prior to data acquisition. These measurements established the position in foot coordinates from the calcaneal target to the ankle joint center. The ankle joint center was then expressed as a position vector relative to the center of mass ($\vec{R}_{pf}$) using vector subtraction. This vector was considered constant throughout time.

The foot possesses no distal joint. Instead, a ground applied force GAF exists during stance phase. The GAF's point of application can be expressed

as a vector function of time, based on the instantaneous position of the foot and the position of the center of pressure (COP). Similar to the ankle joint position vector, the vector $\vec{R}_G$ was expressed as a position of the COP relative to the center of mass, and was calculated for each instant of time using vector subtraction.

The Leg

The leg analysis, summarized in Figure 3.3.5a, was performed by using the distal and proximal targets, mounted along the tibial crest. This was assumed in alignment with the principle coordinate system of the leg. A position vector was established to obtain the center of mass in the coordinate system of the leg from the proximal leg targets based on standing file data, body measurements, and the values presented in Table 3.3.4.

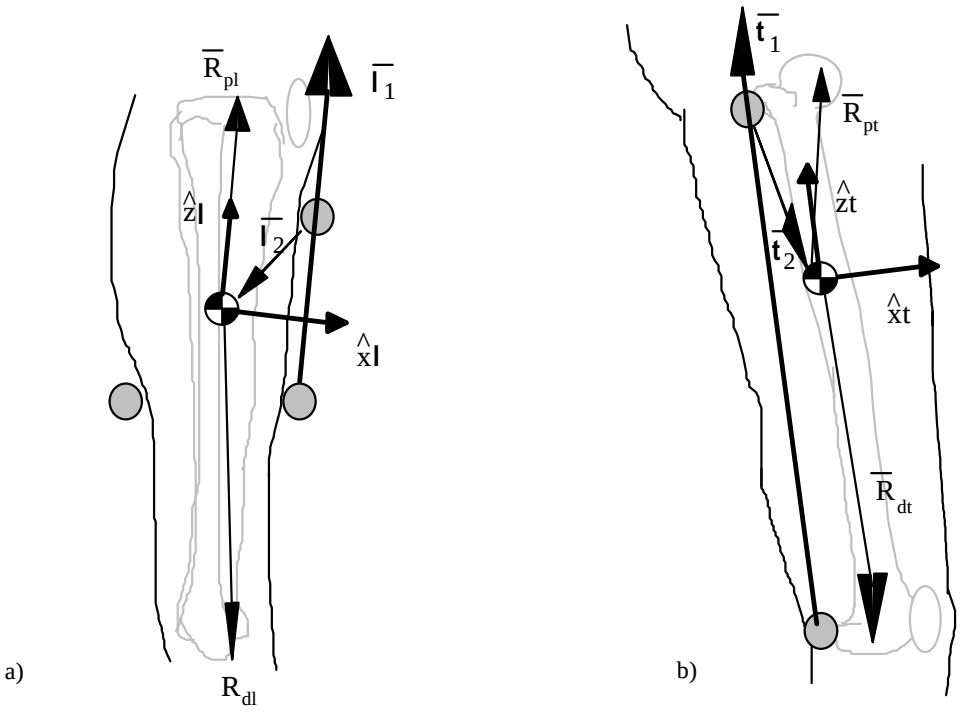

Figure 3.3.5: *Leg and thigh analysis from targeting. Lateral aspects. a) Leg b) Thigh.*

The distal joint for the leg (the ankle) was obtained by vector subtraction of the position of the ankle in the standing file and the center of mass. The proximal joint for the leg (the knee) was obtained by subtraction of the midpoint between the medial condyle targets and the center of mass.

The Thigh

The thigh analysis is illustrated in Figure 3.3.5b. The principle long axis (z) was established by a line between the lateral condyle and the greater trochanter targets. Again, a position vector was established to obtain the center of mass in the coordinate system of the leg from the proximal leg targets based on standing file data, body measurements, and the values presented in Table 3.3.4.

The distal joint position for the thigh (the knee) was established using vector subtraction of the center of mass of the thigh from the knee joint center based on standing file data (the center of the medial and lateral condyle targets). The proximal joint position (the hip) was defined at the standing file's greater trochanter position.

3.3.3 Indirect Dynamics

The increase in complexity from a single slender rod to a system of interconnected rigid bodies necessitated several changes to the equations of motion. The equations had to accommodate non-slender segments where the centers of mass and principle long axes did not necessarily lie on a line between the distal and proximal joints (see Figure 3.3.3). This affected the moment equations, requiring more general expressions for the cross products of joint forces and joint positions.

It was also necessary to explore the effects of passive torsional elements on the dynamics of the system. Therefore, a provision was made in the moment equations so that moments due to user-specified passive joint torsional springs and dampers ($M_{passive}$) were isolated from the active muscle moments (M_{active}). The torsional spring moment can be defined as:

$$M_k = -k(\Theta_d - \Theta_p - \Theta_\circ) \qquad (3.3.1)$$

where k is the torsional spring constant and the quantity in the parentheses represents the joint angle expressed as a relative angle of the distal to the proximal segment, offset by a neutral joint angle position $\Theta_\circ$. The torsional damping moment can be defined as:

$$M_C = -c(\dot{\Theta}_d - \dot{\Theta}_p) \qquad (3.3.2)$$

where c is the damping constant and the quantity in the parentheses represents the joint velocity expressed as a relative velocity of the distal to the proximal segment. A net effect of both of these parameters was calculated: $M_{passive}$. Setting the spring and damping coefficients to zero assumed no contribution of passive elements ($M_{passive} = 0$).

Forces were expressed in the body segment coordinate systems due to the success of such an approach using the slender rod. Therefore, each equation of motion contained 2 dimensional transformations of forces to the inertial coordinate system, so that motion was determined relative to the inertial reference. A convention was adopted where all forces acting on the proximal joint of a segment were expressed in the coordinate system of the

segment. The equations of motion for each planar body segment moving in the inertial reference frame are:

$$m\ddot{X} = (F_{Dx} + F_{Px})\cos\Theta + (F_{Dz} + F_{Pz})\sin\Theta \tag{3.3.3}$$

$$m\ddot{Z} = -(F_{Dx} + F_{Px})\sin\Theta + (F_{Dz} + F_{Pz})\cos\Theta - mg \tag{3.3.4}$$

$$\begin{aligned} I\ddot{\Theta} = \; & (M_D)_{active} + (M_P)_{active} + (M_D)_{passive} + (M_P)_{passive} \\ & + (R_{Dz}F_{Dx} - R_{Dx}F_{Dz}) + (R_{Pz}F_{Px} - R_{Px}F_{Pz}) \end{aligned} \tag{3.3.5}$$

where the subscript D denotes the force or moment at the joint distal to the segment, and P denotes the force or moment at the joint proximal to the segment. In the case of the foot, where there was no distal joint, the subscript G (ground applied force) was substituted for D in the above equations, and the COP position could be treated mechanically as a moving point where force is applied. The subscript $_{active}$ denotes the contribution of the active or muscle moment and the subscript $_{passive}$ denotes the passive torsional joint spring damper elements.

Analysis began with the foot segment, where the forces measured from the force plate were used with measured foot accelerations to solve for forces and a moment at the ankle. The ankle forces and moment were reversed in sign to be used with the measured leg motions to solve for forces and a moment at the knee joint. The knee forces and moment were reversed in sign to be used with the measured thigh motions to solve for forces and a moment at the hip joint. This process was continued for each $1/60^{th}$ of a second time increment until roughly one gait cycle was completed.

Note that this type of analysis assumes that the joint positions are aligned (i.e. the foot-defined ankle joint is in the same position in space as the leg-defined ankle joint). Because each body segment's motion is independently described, it is possible for the system to not stay together due to incorrect limb length measurements, principle axis directions, center of mass position estimates, and joint position estimates. This is commonly referred to as the internal validity problem [Winter 1990]. The result is force and moment time histories that are in error.

One approach to the problem was to correct the model's geometric values by re-measuring body parameters and adjusting anthropometric estimates. A simple interactive graphics presentation of the model as a stick figure was used to display the model in certain configurations to assure that the validity of the geometry.

An alternative approach was to impose hinge joint constraints on the knee and ankle motion before conducting the indirect dynamic analysis, forcing the x and z trajectories of the thigh and leg to follow directly from the angle measurements and the segmental dimensions. This method was mathematically consistent with the forward dynamics problem, but did not represent the true motion of the body segments. Both of these methods were investigated.

3.3.4 Forward Dynamic Synthesis

The addition of new segments to the model required the adoption of several conventions with respect to forces and motions. As mentioned above, joint force was expressed as applied to the segment immediately distal to it, in the coordinate system of that segment, as shown in Figure 3.3.6. Ground applied forces (GAF) and moment (GAM) are expressed in the

inertial coordinate system. Again, each equation of motion contained the necessary 2 dimensional transformations to directions in the inertial coordinate system for the calculation of motions. The result was nine equations of motion (three for each segment).

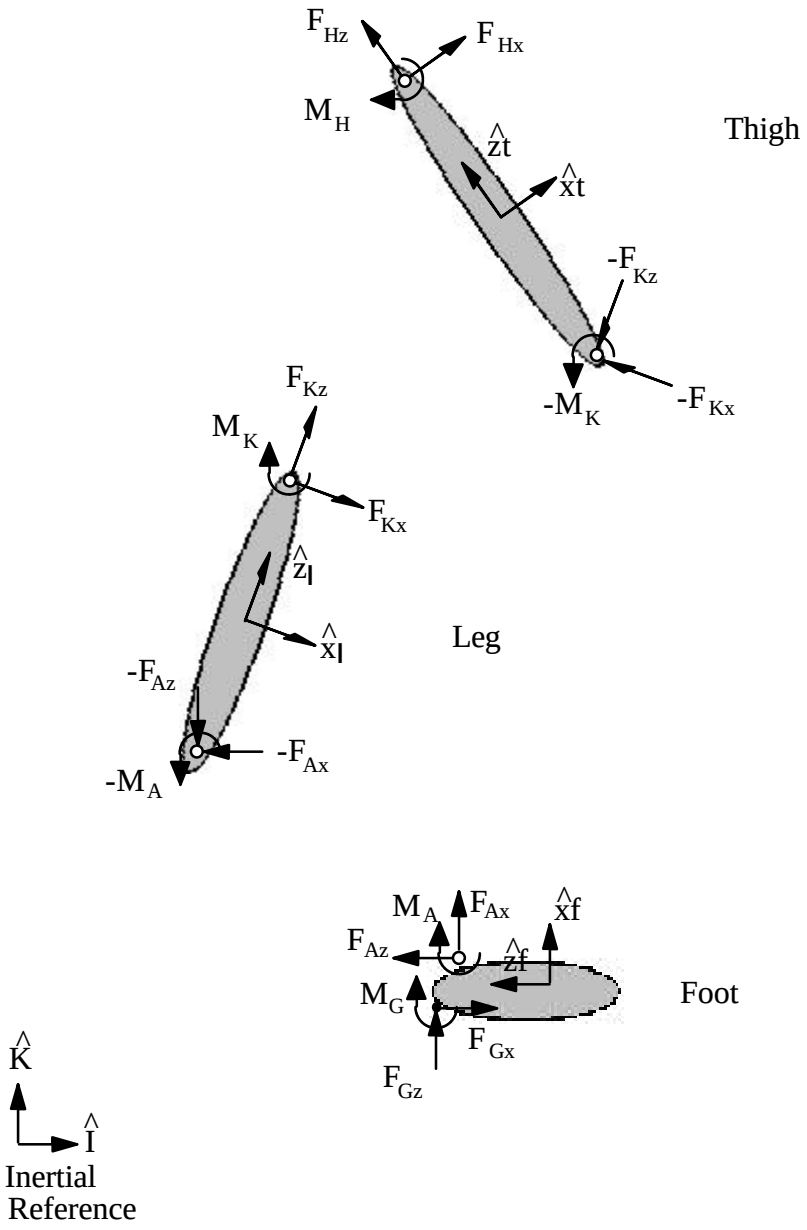

Figure 3.3.6 : *Free body diagrams for the mechanical system and the convention used for the direction of the forces.*

Unlike the indirect analysis, the assumption was made that each joint (the knee and ankle) was an ideal hinge. The addition of segments connected by hinge joint constraints required the simultaneous solution of the equations of motion subjected to additional equations of constraint. The acceleration of the joint was expressed in terms of the motions and the joint position vectors of the two segments which the joint connects:

$$\ddot{\vec{\rho}}_a + \vec{\alpha}_a \times \vec{R}_{pa} + \vec{\omega}_a \times (\vec{\omega}_a \times \vec{R}_{pa}) = \ddot{\vec{\rho}}_b + \vec{\alpha}_b \times \vec{R}_{db} + \vec{\omega}_b \times (\vec{\omega}_b \times \vec{R}_{db}) \qquad (3.3.6)$$

where $\ddot{\vec{\rho}}$ is the acceleration of the segment's center of mass, and subscript a refers to the segment distal to the joint and subscript b refers to the segment proximal to the joint. Note that this is in the inertial reference, so all $\vec{R}$ vectors must be transformed to the inertial reference frame. For the planar model, the expansion of this vector expression into scalar forms resulted in two equations of constraint for each joint. The two equations can be written in a general form as (including the 2 dimensional transformations of the $\vec{R}$ components):

$$\begin{aligned} &\ddot{X}_a + (-R_{apx}\ddot{\Theta}_a \sin\Theta_a + R_{apz}\ddot{\Theta}_a \cos\Theta_a) + (-R_{apx}\dot{\Theta}_a{}^2 \cos\Theta_a + R_{apz}\dot{\Theta}_a{}^2 \sin\Theta_a) = \\ &\ddot{X}_b + (-R_{bpx}\ddot{\Theta}_b \sin\Theta_b + R_{bpz}\ddot{\Theta}_b \cos\Theta_b) + (-R_{bpx}\dot{\Theta}_b{}^2 \cos\Theta_b + R_{bpz}\dot{\Theta}_b{}^2 \sin\Theta_b) \end{aligned} \qquad (3.3.7)$$

$$\begin{aligned} &\ddot{Z}_a + (-R_{apx}\ddot{\Theta}_a \cos\Theta_a - R_{apz}\ddot{\Theta}_a \sin\Theta_a) + (R_{apx}\dot{\Theta}_a{}^2 \sin\Theta_a - R_{apz}\dot{\Theta}_a{}^2 \cos\Theta_a) = \\ &\ddot{Z}_b + (-R_{bpx}\ddot{\Theta}_b \cos\Theta_b + R_{bpz}\ddot{\Theta}_b \sin\Theta_b) + (R_{bpx}\dot{\Theta}_b{}^2 \sin\Theta_b - R_{bpz}\dot{\Theta}_b{}^2 \cos\Theta_b) \end{aligned} \qquad (3.3.8)$$

The effects of passive element contributions (joint torsional spring and torsional dampers) on system motion were included in the equations. Each torsional spring and damper was consistent with those used in the indirect dynamics solution, and was included in the equations of motion. A calculation of the joint angle and joint angular velocity was required for every instant in order to calculate the passive moment values.

The resulting 13 equations (9 equations of motion and 4 equations of constraint) and 21 total unknowns (9 degrees of freedom and 12 forces) were used to calculate a forward dynamics problem in which the forces at the hip, the moments at the hip, knee, and ankle, and the motions of the foot were specified. The remaining motions (the shank and the thigh motions) the joint forces at the knee and ankle, and the ground applied forces at the foot were calculated in the forward dynamics solution. A coupled, non-linear system of ordinary differential and algebraic equations was obtained. The final system of 21 equations and 21 unknowns are shown in detail in Appendix A.

A simple application was first simulated in order to evaluate (and debug) the system. The model was posed initially in a typical standing configuration ($\Theta foot=0°$, $\Theta leg=5°$, $\Theta thigh=-5°$). All external moments and forces were set to zero, and the system was allowed to collapse under its own weight. This approch allowed the inherent problems associated with the integration process and equations of motion and constraint to be uncovered without being complicated by the effects of driving forces and moments.

The system was then used to simulate human locomotion. Hip forces and moments, knee moments, ankle moments and foot motion were obtained from the indirect dynamics results. Knee and ankle joint forces, ground

reaction forces, and shank and thigh motion were solved in the forward dynamics calculations.

The method for solution was chosen as a simple linearization and integration technique, outlined in Figure 3.3.7. The integration process began with initial conditions manually specified or determined from the original measurements of motion. Care was taken to assure that the initial conditions did not violate the constraints. Each position and orientation for a given instant was used to find the forces and accelerations for that instant. This was done by solving the 21 equations and 21 unknowns using a Gauss-Jordan elimination matrix routine [Phillips and Taylor 1973]. The accelerations were integrated in order to find positions and orientations for the next time instant. The values obtained were then averaged with the values of the original time step, and the accelerations were calculated and integrated again, and then the integrator advanced to the next time step.

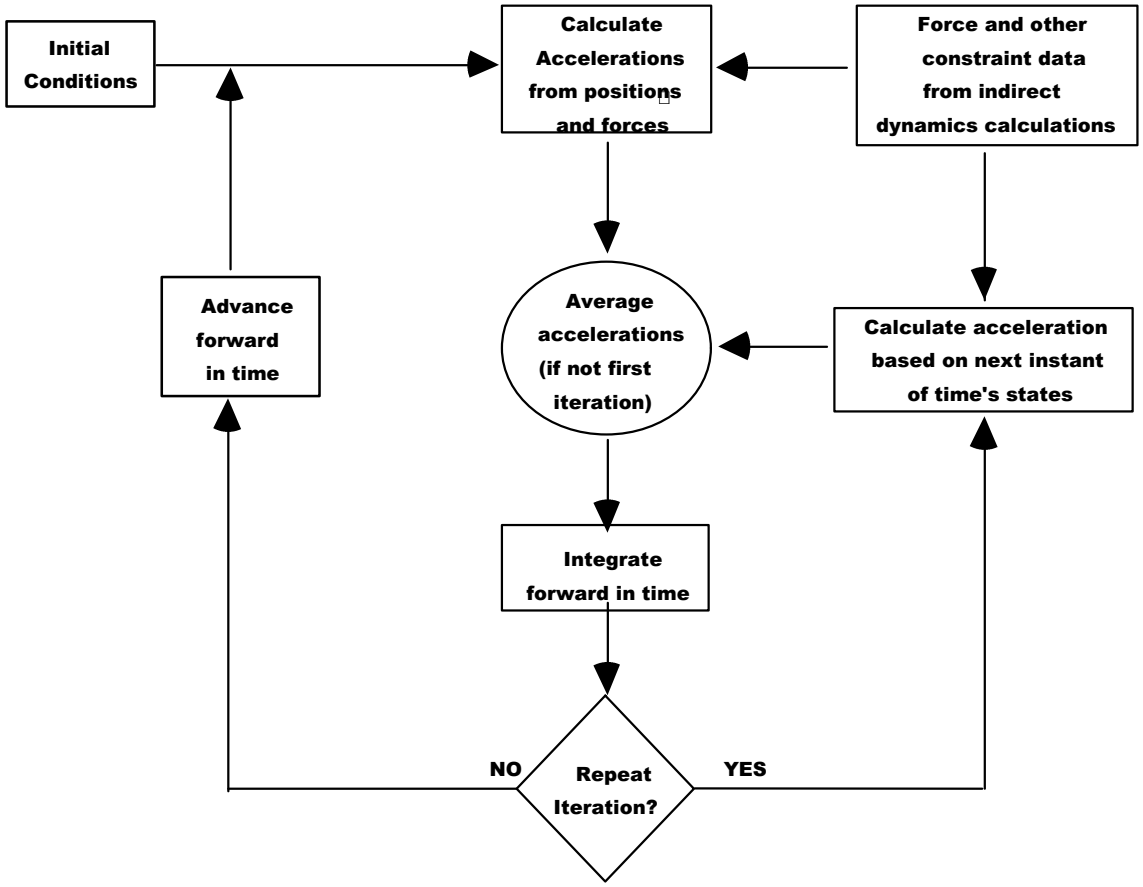

Figure 3.3.7 : *The integration process for the system of equations.*

To improve the integration results, the two step Modified Euler Method, discussed in section 3.2.4, was used so that the process could be iterated indefinitely [Wylie and Barrett 1982]. Several different solutions were obtained using different numbers of iterations for each time step. Another strategy used to improve the integration results was to vary the integration time step (h). This necessitated interpolation methods for the inputs to the simulation (ankle motion and applied forces). Newton's divided difference formula was chosen to perform this task [Wylie and Barrett 1982]. The effects of changing the step size were evaluated.

A graphics stick figure representation of the overall motion was developed to quickly evaluate the results of simulation. It has been

suggested by authors as a concise method to present results from such studies, due to the large amounts of data that result [Onyshko and Winter 1980; Pandy and Berme 1988a].

The ground applied forces (GAF) were believed to be a good measure of the predictive ability of a model. The foot's COP position vector was arbitrarily chosen as constant at the heel. The dynamic simulation yielded a force and a moment at the heel, and was reduced to a COP measure and an applied force after the simulation was complete.

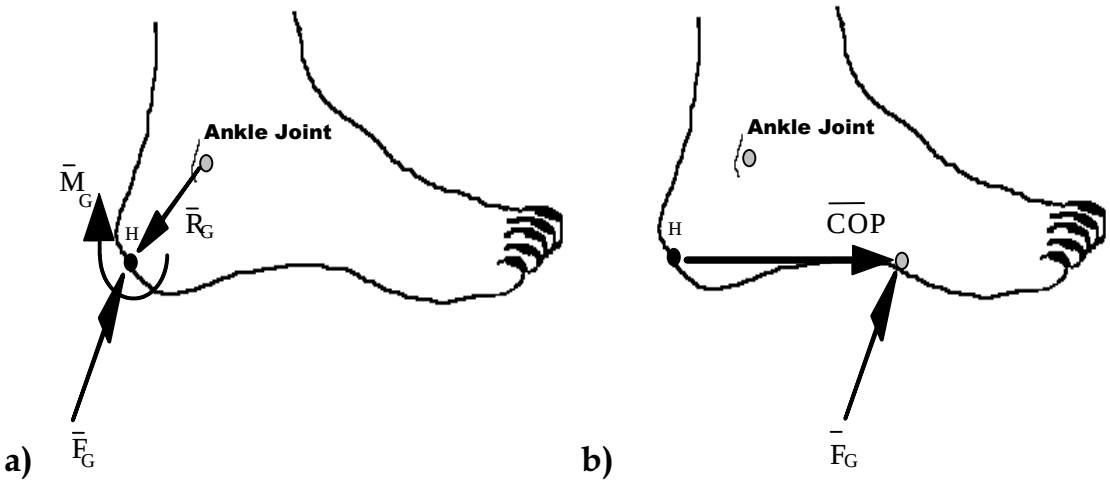

Figure 3.3.8 : *The equivalent force system used to reduce the resulting moment and force results from the forward dynamics problem to a force at distance COP from the heel.*

The calculation of these parameters requires the assumption that the entire planar surface of the foot is a smooth surface on which GAF can be applied. A realistic assumption is that the moment applied to the foot was zero. Thus the moment and force obtained in the solution of the forward dynamics

problem should be converted to only a force using an equivalent force system. A mechanical couple was used [Greenwood 1988]. The force and moment that exist at point H can be expressed as a force alone applied at some distance (COP) from point H:

$$\vec{\mathbf{M}}_{G/H} = \overline{\mathbf{COP}} \times \vec{\mathbf{F}}_G \tag{3.3.9}$$

Assuming that the vertical and out-of-plane ($\hat{\mathbf{J}}$) components of $\overline{\mathrm{COP}}$ are zero, equation 3.3.9 reduced and re-expressed in terms of the X-component of $\overline{\mathrm{COP}}$:

$$COP_x = \frac{M_{G/H}}{F_{GZ}} \tag{3.3.10}$$

The mechanical scheme is presented in Figure 3.3.8. GAF and COP results were compared to the original measured values.

4. RESULTS AND DISCUSSION

4.1 Results and Discussion for Dynamic Analysis of a Single Rigid Body

A graph of the target trajectories for a typical trial is shown in Figure 4.1.1, showing both in-plane and out-of-plane motion.

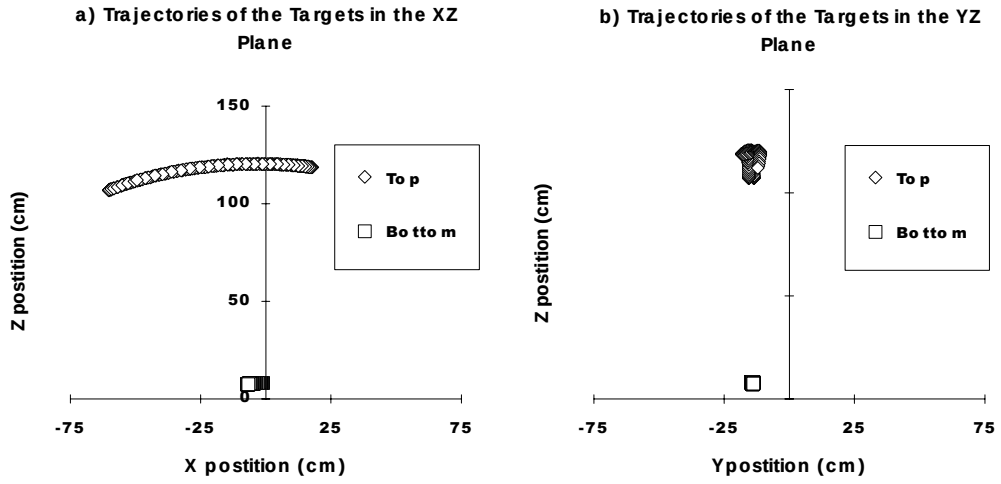

Figure 4.1.1: *Target trajectory motion for a typical trial. a) Motion in the plane, b) Motion in a perpendicular plane.*

A change in distance between the markers throughout the duration of the trial is an excellent measure of the errors due to marker visibility and three dimensional tracking. Distance for a typical trial is shown in Figure 4.1.2. The coupling effect of marker distance with the rod's angle with

vertical is shown in Figure 4.1.2b. This is attributable to the change in the shape of each target's image in the tracking software. The tagets are not spherical, thus the calculated centroid of the target image will not be constant due to changing angles of view. Mathematically, however, the resolution to the plane of motion depends heavily on the cosine function of rod's angle with the plane. A vector 15 ° out of plane maintains 97% of its magnitude when resolved to the plane. Therefore, due to the nature of the system and the motions given, the planar assumption in itself is not a major contributor to error.

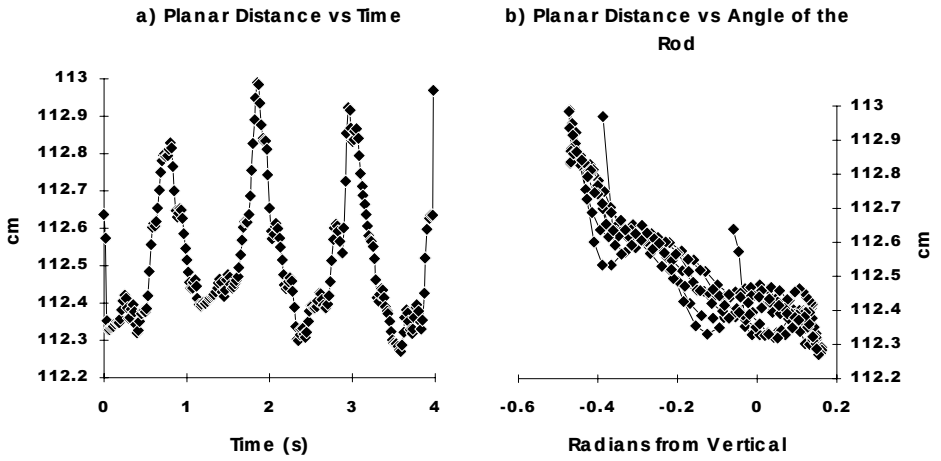

Figure 4.1.2: *Marker distances throughout a 4 second trial. a) distance vs. time, b) distance vs. rod's angle with vertical.*

The kinematic results of the rod for a typical trial are shown in Figure 4.1.3, illustrating the effects of signal conditioning on the target trajectories. Smoothing had a somewhat minimal effect on the position data, where only slight decreases in the peaks can be seen. Signal conditioning of the target trajectories is well known to have a critical effect on the quality of the time

derivatives of kinematics inverse dynamic calculations [Winter 1990], and smoothing had the most pronounced effect on angular acceleration, which is shown in Figure 4.1.4. The result of using 3 point or 5 point difference methods had little effect on the results if the target trajectories were smoothed.

The effects of smoothing at different times in the data reduction also affect the outcome of the forward dynamics problem. If smoothing is performed on the velocity before differentiating to find acceleration, a smoother acceleration is obtained, and this can be further smoothed before the indirect dynamic analysis to obtain smooth force and moment time histories. However, if a signal is differentiated then smoothed, integration can not yield the original signal due to the fact that the signal was altered (smoothed) during the process of differentiation. Therefore, all smoothing must be done before any numeric differentiation is begun.

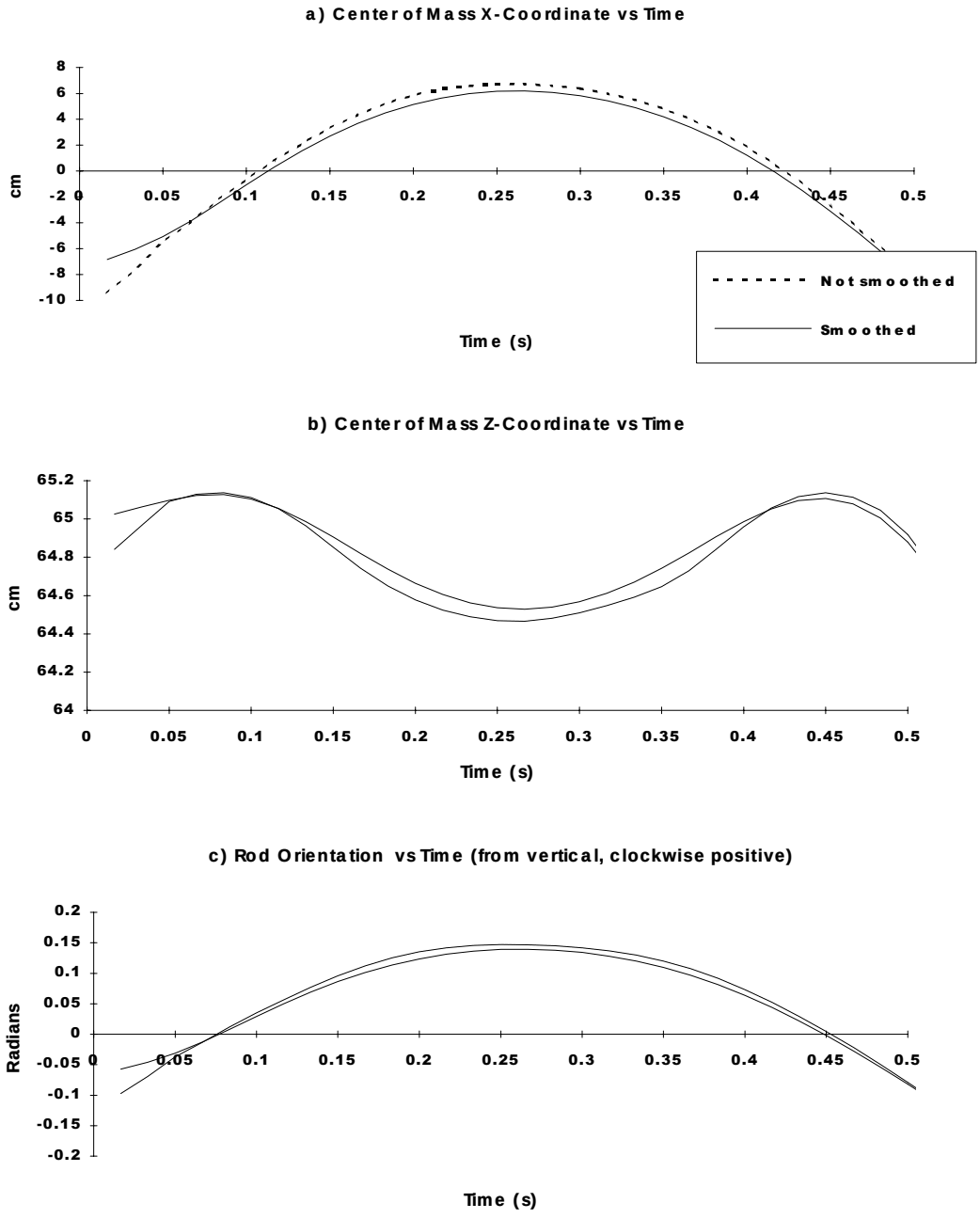

Figure 4.1.3: *Smoothed and Unsmoothed rod kinematics for a typical trial. A 2-pass, 7 point rectangular signal processing window was used. a) Center of mass (CM) x-distance vs. time, b) (CM) z-distance vs. time. c) Rod's orientation with vertical (Θ) vs. time.*

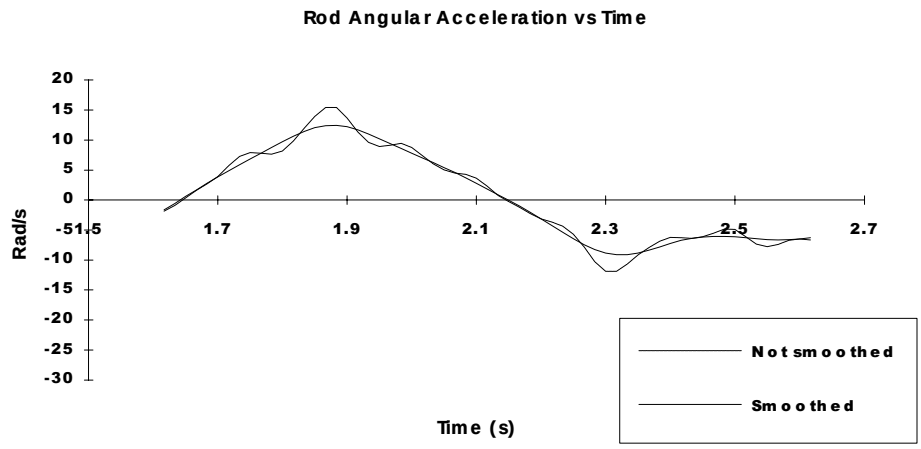

Figure 4.1.4: *The effects of smoothing on the angular acceleration.*

The choice of equations to use for the determination of angular velocity and acceleration proved important. A quick examination of these equations 3.2.6, 3.2.7, 3.2.9, and 3.2.10 will show that certain orientations of the rod lend themselves to mathematical discontinuity. Particularly, as the denominator of these equations become zero, the numerator should also become zero. A calculation which uses measured data may result in a singularity. The rod was manipulated near vertical for all trials, and therefore equations 3.2.7 and 3.2.10 are problematic. This problem is illustrated in Figure 4.1.5 for calculation of angular velocity and angular acceleration. Angular acceleration suffers extensively from this problem, due to its dependence on the result of the angular velocity calculation. Note that these values are also used to calculate the linear velocity and accelerations. This problem was avoided in further work by using only equations 3.2.6 and 3.2.9 when the rod was near vertical ($\Theta < \pm 45°$), and 3.2.7 and 3.2.10 when near horizontal ($\Theta > \pm 45°$).

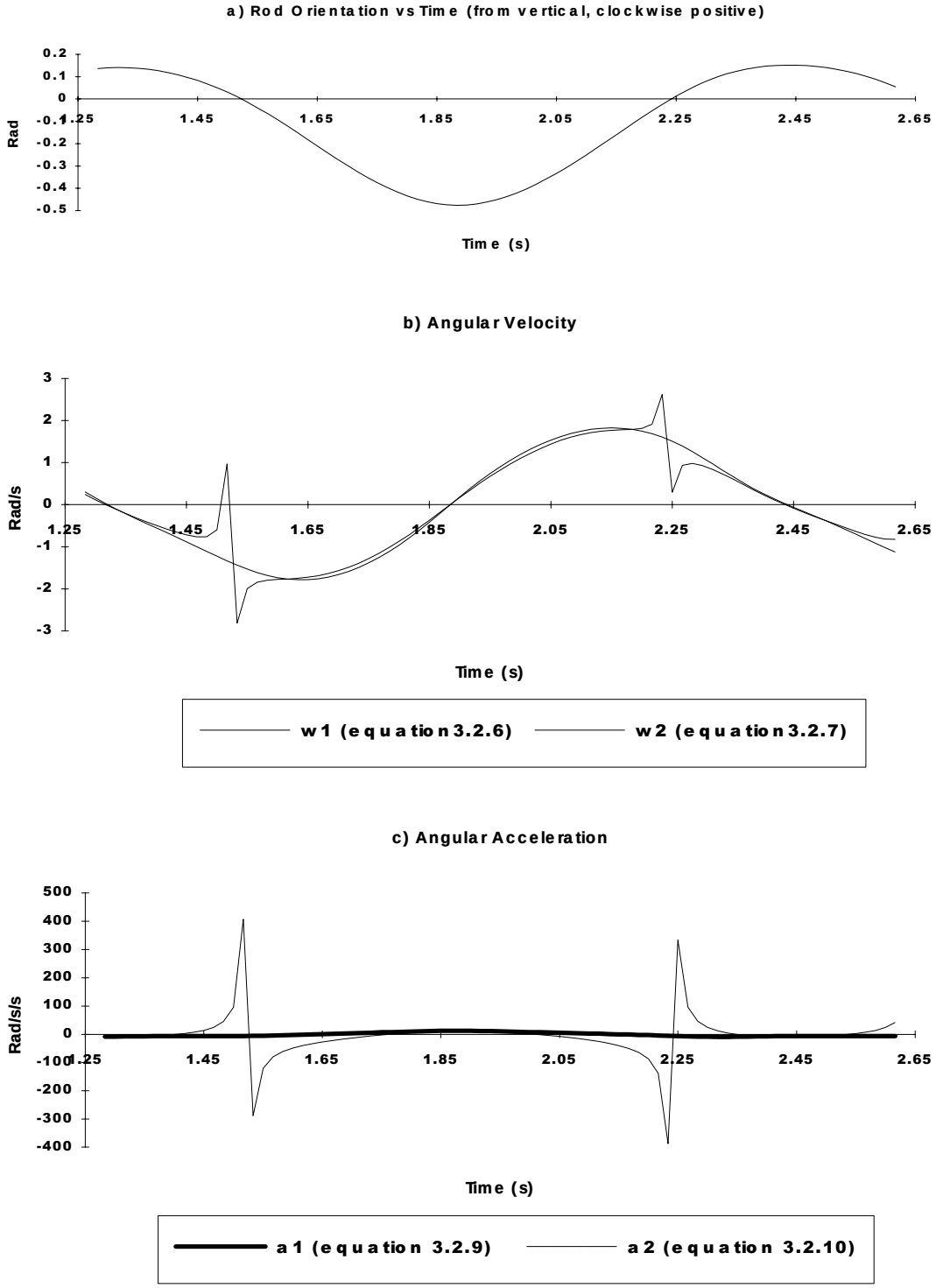

Figure 4.1.5: *Angular displacement, angular velocity, and angular acceleration for a typical trial. a) Rod's angle with vertical. b) Angular velocity calculated using equation 3.2.6 and using equation 3.2.7. c) Angular acceleration calculated using equation 3.2.9 and using equation 3.2.10.*

The removal of errors due to the relative movement of the targets along the axis parallel to the rod effected angular velocity and acceleration (see equations 3.2.11 to 3.2.17). A comparison of the results for no correction and for corrected data is shown in Figure 4.1.6. This error effects not only the angular velocity and acceleration, but the linear center of mass velocities and accelerations, because they are calculated using angular values.

The results of the inverse dynamic analysis are the calculated forces and moment at the top of the rod. The results for a typical trial are shown in Figure 4.1.7.

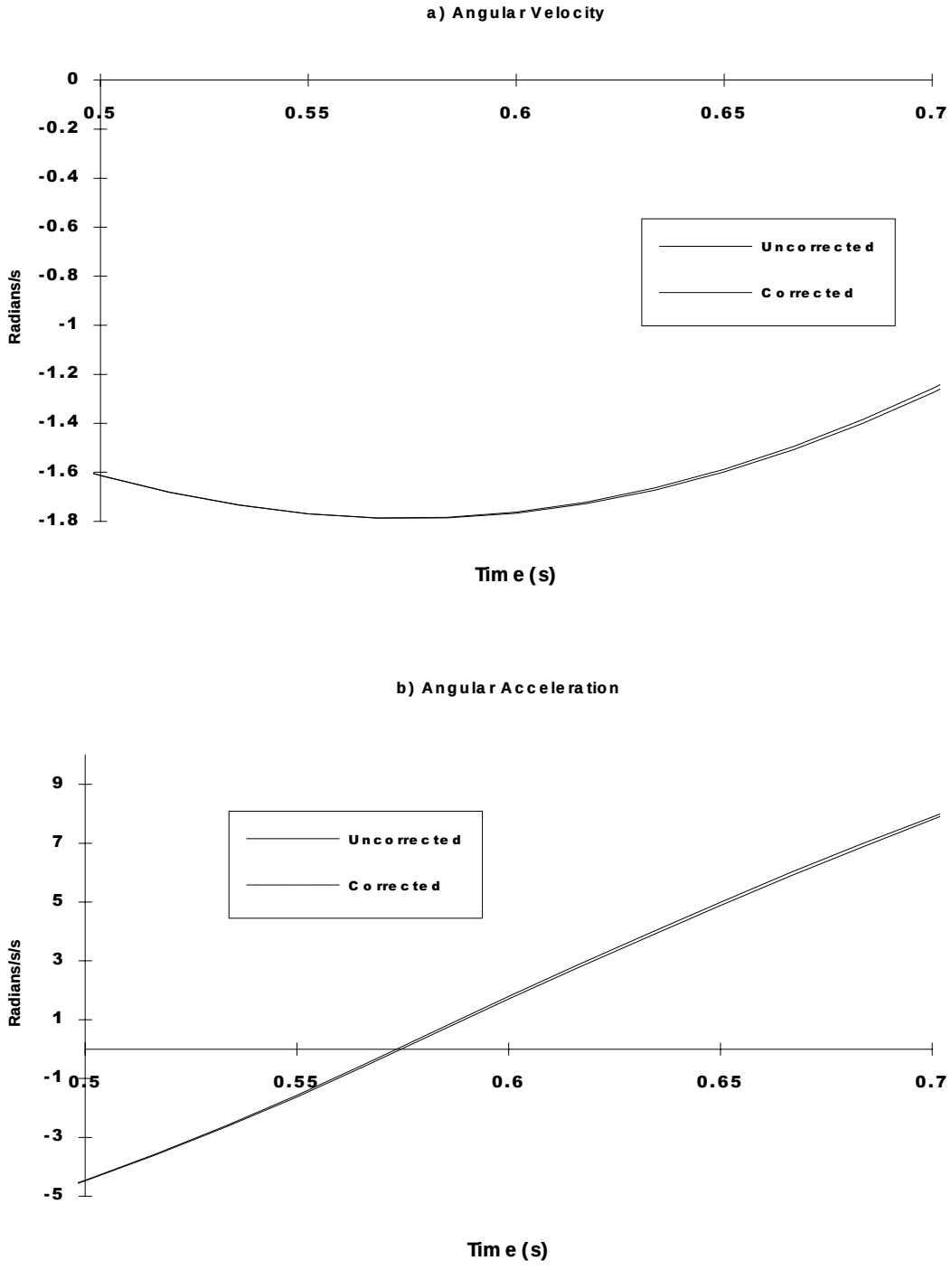

Figure 4.1.6: *Angular derivatives corrected and un-corrected for target motion along the axis of the rod. a) Angular velocity (see equations 3.2.11 to 3.2.13), b) Angular acceleration (see equations 3.2.14 to 3.2.17).*

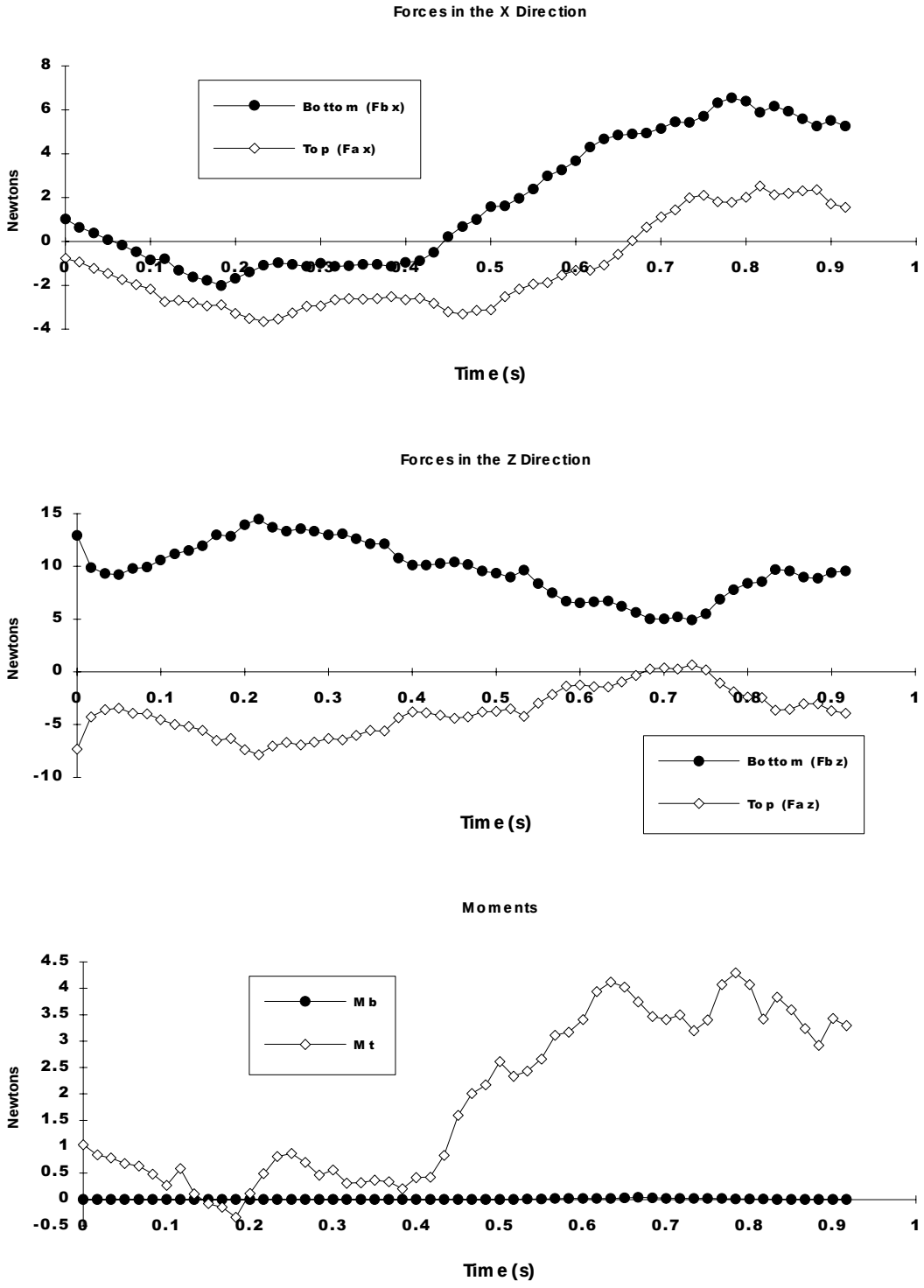

Figure 4.1.7: *Indirect dynamic results. a) X-directed forces. b) Z-directed forces. c) Moments See Figure 3.2.3 for the definition of forces.*

Both Zajac, [Zajac and Gordon 1989], and Meglan, [Meglan 1990] have discussed isolating the relative contributions to acceleration. In the case of the Z coordinate trajectory, the terms of equation 3.2.27 are isolated to show the contributions to the acceleration of the rod in the z direction. This is shown in Figure 4.1.8. The plot shows a considerable difference in the relative magnitudes of the contributing terms and the total Z acceleration, which is their sum. A cause of error in simulation may arise from the magnitudes of the values that are summed to find a net force. If the net force required for motion is relatively small compared to the values used to calculate it, the computer's precision can be critical.

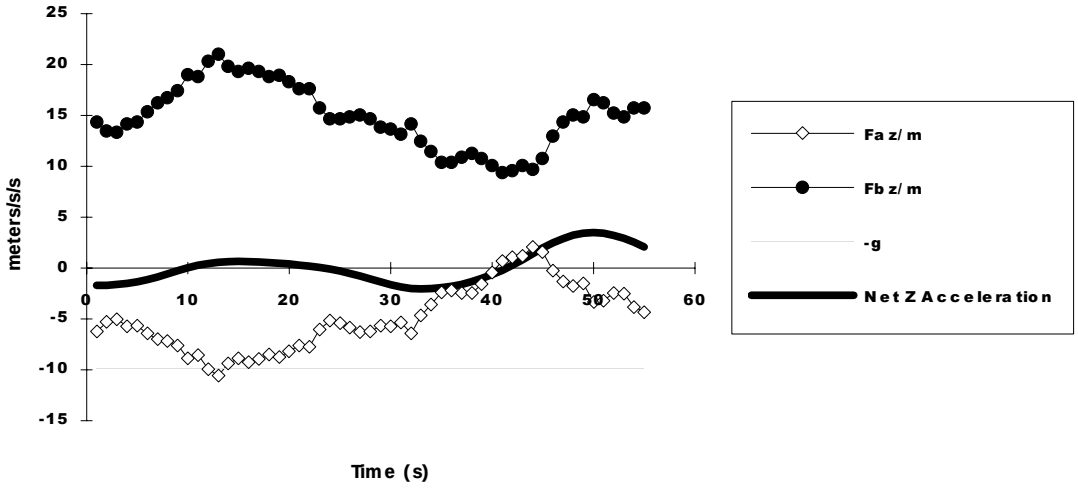

Figure 4.1.8: *The contribution of several different effects to the net acceleration of the rod in the Z direction for a typical trial.*

The results of the dynamic synthesis proved to be very sensitive to the choice of coordinate system in which the forces were specified. Figure 4.1.9 shows the results of Θ for both approaches. The best results were found when the forces were specified in the coordinate system of the rod itself. Particularly sensitive is the angle Θ.

The quality of the integration technique proved to be a critical factor. The use of the Modified Euler Technique is illustrated in Figure 4.1.10 for the z-coordinate trajectory, comparing the effectiveness of a second iteration before continuing to the next time step. The quality continues to improve with further iterations of integration, and this method was applied in the later phases of this work.

Finally, the magnitude of force and motion did not significantly effect the quality of the synthesis. A trial in which the motion was slowed and the forces applied at the top (an increase in vertical force of a factor of approximately 2.5) is presented in Figure 4.1.11.

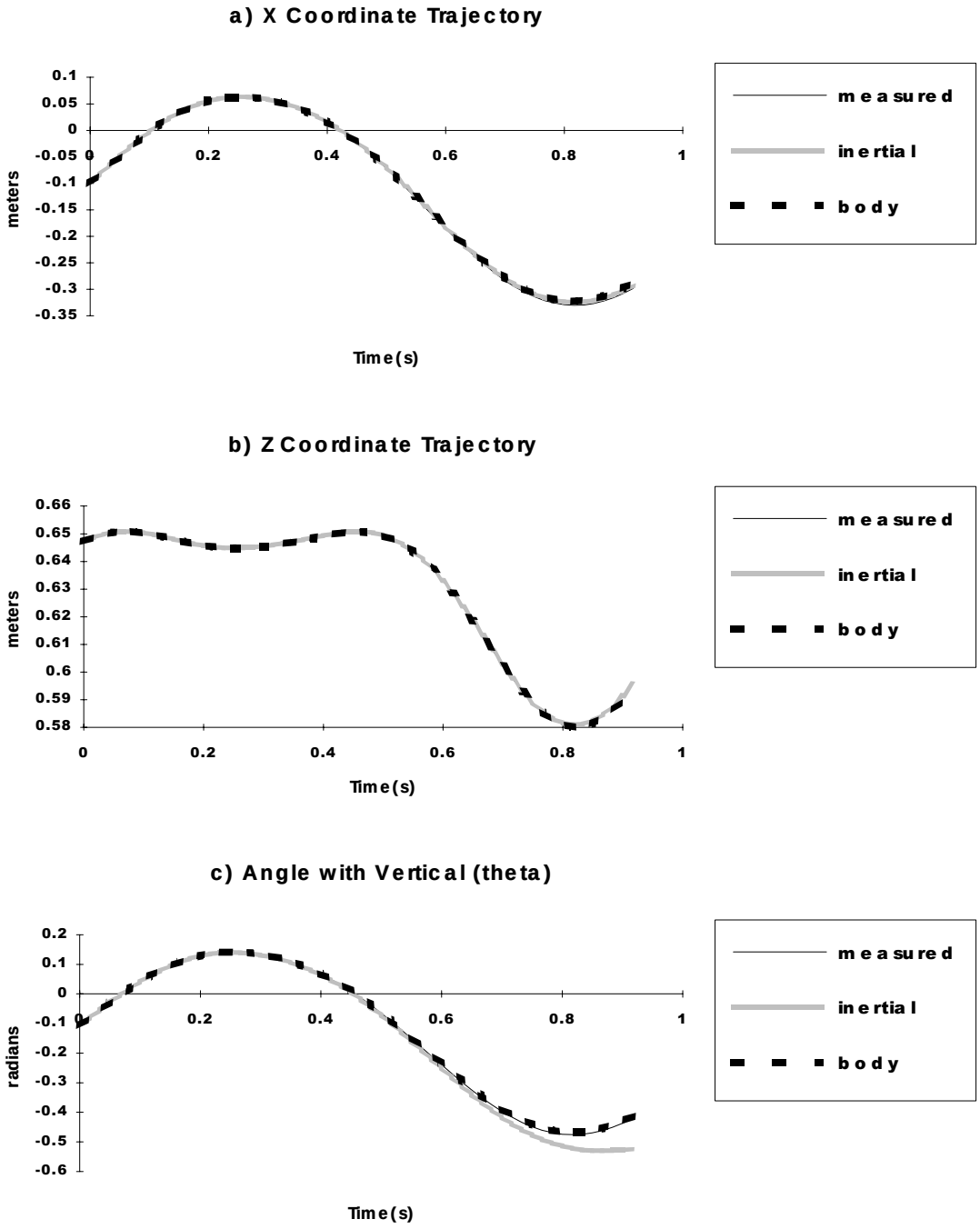

Figure 4.1.9: *Forward dynamics-synthesized trajectories compared with the original measured motion for two mechanical approaches: Forces specified in the inertial reference frame and forces specified in the body-coordinate system embedded in the rod.*

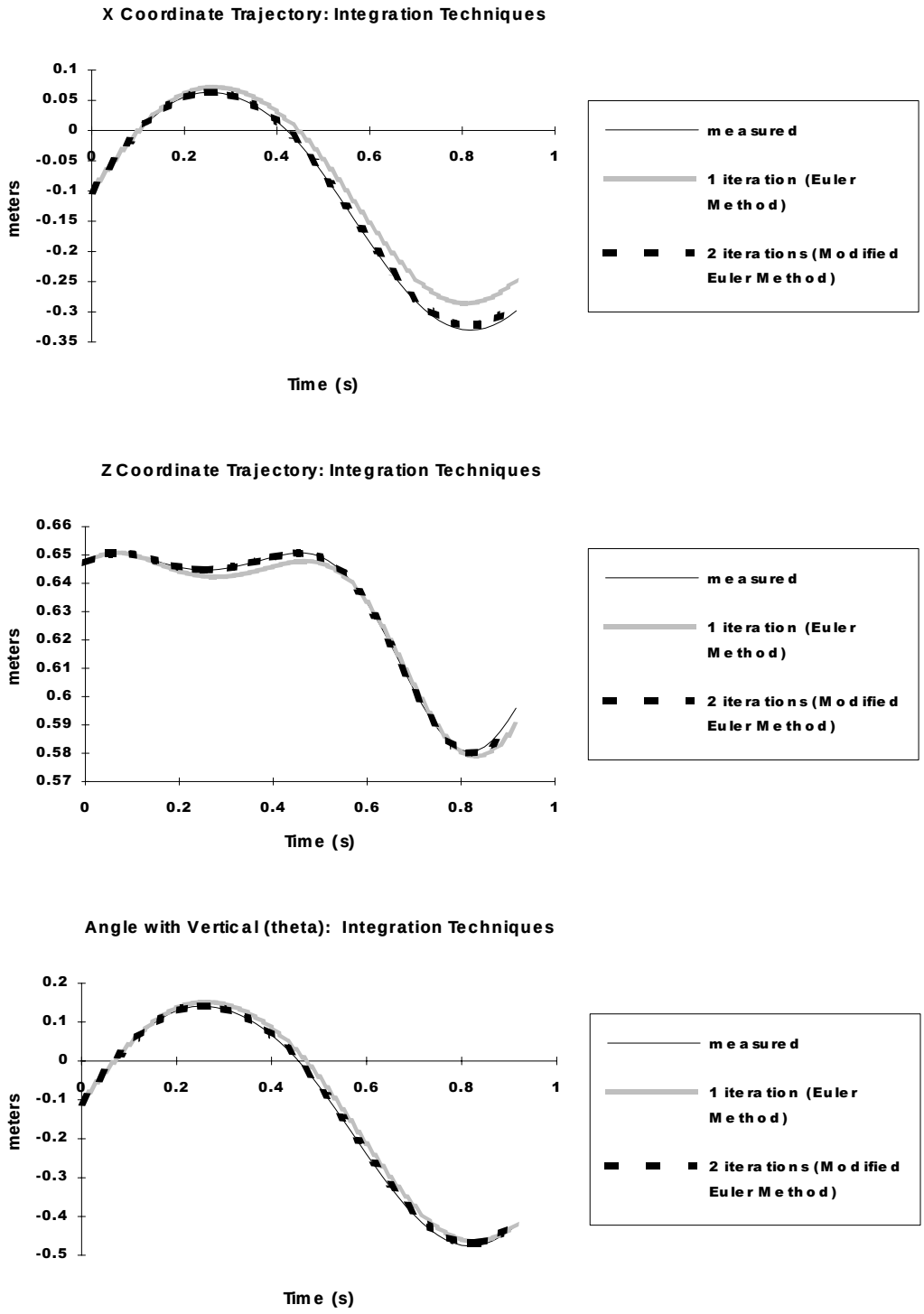

Figure 4.1.10: *Dynamic synthesis results comparing two integration approaches with the original measured values: Single step (Euler) integration and Two step (Modified Euler) integration.*

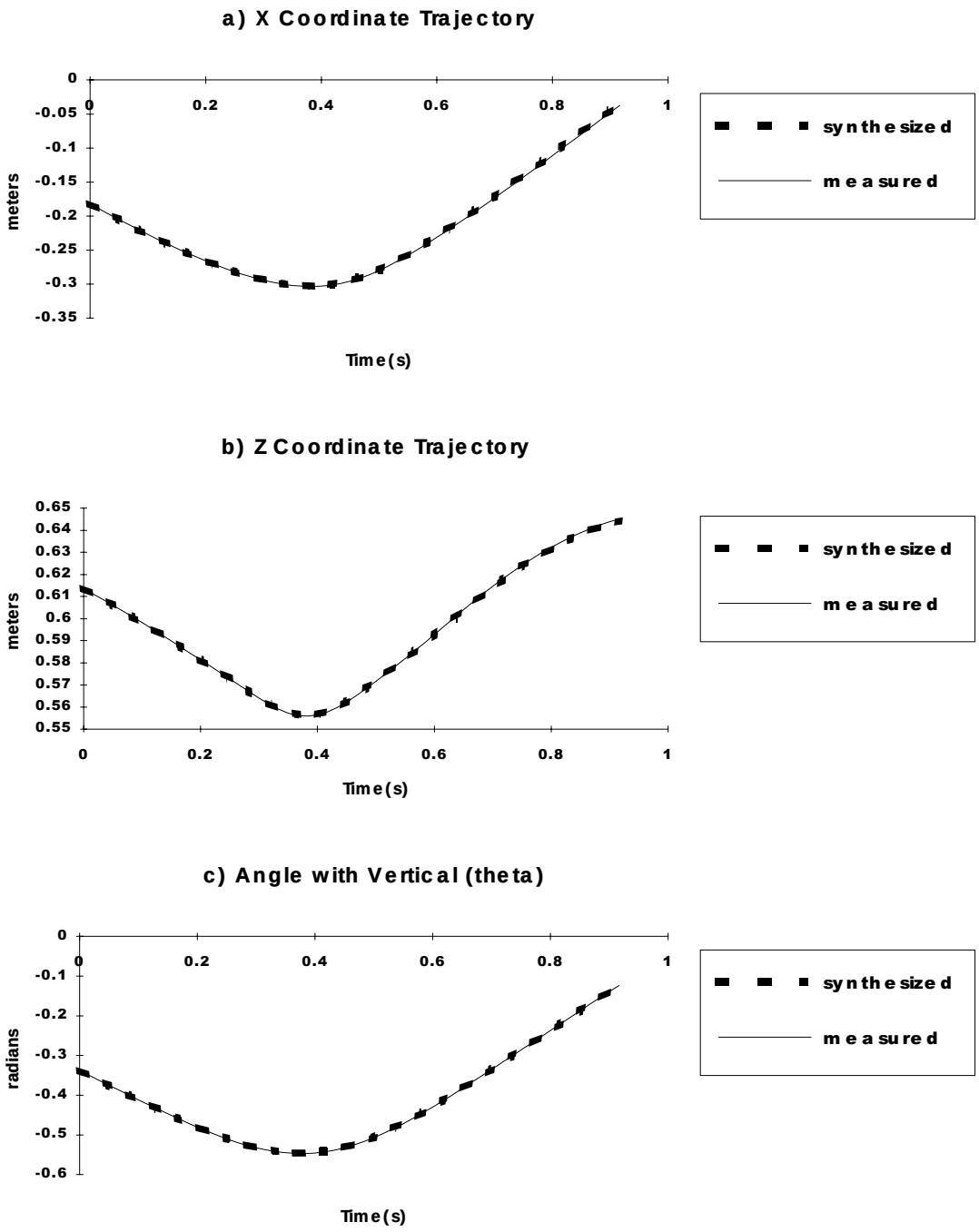

Figure 4.1.11: *Dynamic synthesis results from a trial in which the forces were manually increased. The peak vertical applied force was higher than the trial seen in Figure 4.1.10 by a factor of 2.6.*

4.2 Results and Discussion for Planar Dynamic Analysis of Human Locomotion

The results of the indirect dynamics calculations matched well with the values found in the literature, and are presented in Figure 4.2.1 for a female adult subject walking normally. Note that the joint forces are displayed in the coordinate system of the body segment distal to the joint. (Note the difference of the ankle force patterns compared with the hip and knee. This is due to the fact that the ankle forces are in the foot coordinate system, which is roughly 90 degrees rotated from the leg and the thigh for most of stance phase). This was done to facilitate comparison of the results with the forward dynamics joint forces, which are expressed using this coordinate system convention. In many biomechanical analyses, it may be advantageous to transform the forces at the joints to the proximal segment coordinate system or the inertial coordinate system.

A critical discrepancy between this analysis and an analysis that considers individual muscle forces is that joint reaction forces are severely underestimated. If muscle forces existed between the segments, the joint reactions would be higher. This discrepancy also exists in the forward dynamics problem. However, overall motion should not be effected by the use of concentrated moments at the joints.

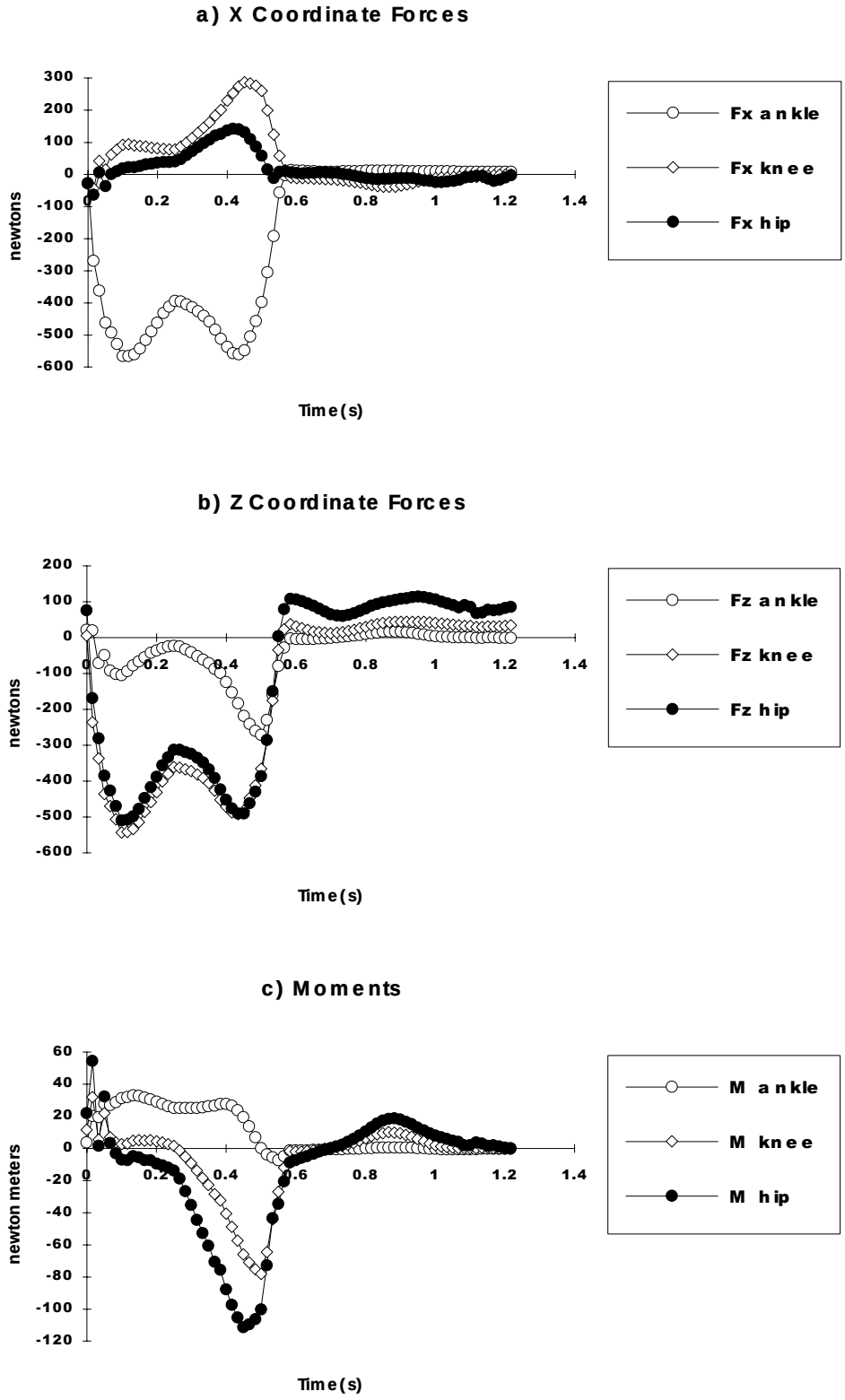

Figure 4.2.1 : *Indirect dynamics results for a female adult subject walking normally. a) ankle b) knee c) hip.*

The model's initial test of allowing it to collapse under its own weight is shown in stick figure form in Figure 4.2.2. The two examples in this figure are the same model with the same initial condition, but subjected to different integration time step sizes (h). Figure 4.2.3b reflects a poor simulation resulting from excessively large h.

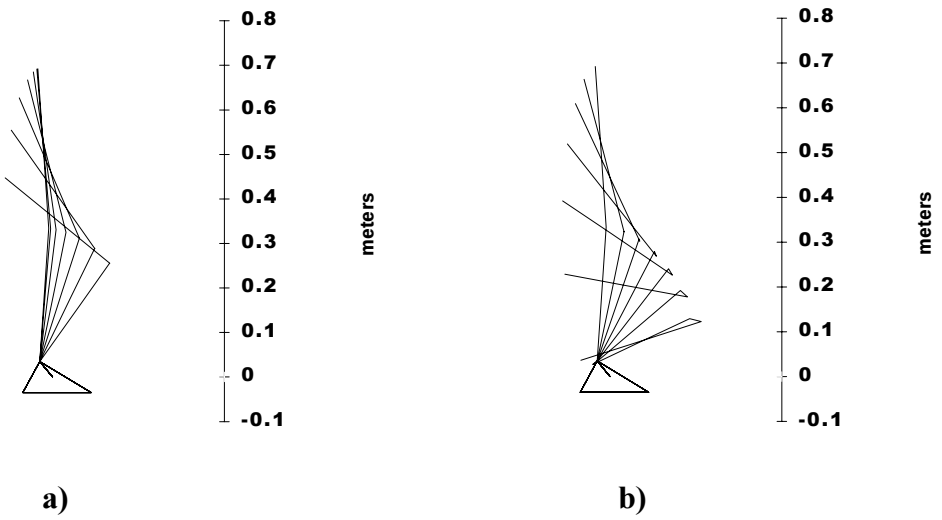

Figure 4.2.2 : *A stick figure representation (0.05 second intervals, end time .3 seconds, using the Modified Euler Method (2 iterations)) of a model being allowed to collapse under its own weight from a standing configuration, for two integration step sizes (h): a) h=.001 sec, b) h=.05sec*

One particular error can be seen by closely inspecting the knee joint in Figure 4.2.2b, where the joint tends to separate. This is a successive violation of the knee constraint due to finite jumps in time. Because the constraint equations for a hinge joint are expressed in terms of accelerations, any changes in angular velocities of the segments during the integration time step cause the independent motion of the segments, and the segments fly apart. A simplified example of this phenomenon can be seen by examining a simple pendulum (Figure 4.2.3). At rest at time zero(Figure 4.2.3a), a concentrated

moment M is applied to the pendulum. Due to the configuration of the pendulum, the moment will cause the angular acceleration of the pendulum and the linear acceleration of the mass to the left. There is no vertical acceleration for the instant calculated, because there is no initial angular velocity which would generate a normal acceleration component. If these accelerations are integrated from time=0 to time=h, we find the constraints violated (Figure 4.2.3b). The joint separation seen in the simulation of the leg is a more complex form of this problem, where instead of there being zero angular velocity for the initial frame, there are many frames where the angular velocity changes from the beginning of the integration time step to the end. These effects can be reduced by changing the integration step size to a much smaller value, as was done in Figure 4.2.2a.

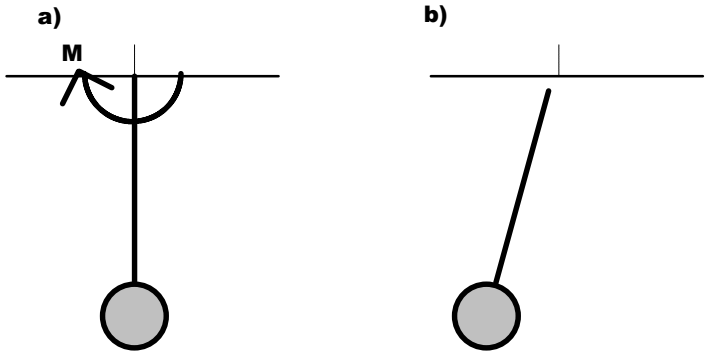

Figure 4.2.3 : *Simple pendulum to demonstrate the constraint violation problem: a) time=0 b) time=h*

The use of more sophisticated techniques for integration of the equations of motion would circumvent this problem. A commonly used method requires the expression of the system of equations in state space form. A linearization procedure is used where a matrix of partial derivatives (the Jacobian) relates infinitesimal changes of the states for a given instant of time

[Phillips and Taylor 1973]. The equations of constraint can then be expressed in terms of the states (position and velocity), and no joint separation would be permitted.

The Modified Euler Method was another approach to minimizing problems due to integration. It calculated an estimate of the next instant's (time=t+h) accelerations, and then averaged these with the current instant's (time=t) accelerations for integration. Thus the accelerations approximate those found at the midpoint of the integration time step. Continuing the iterative process several times was found to greatly improve the dynamic results, and this is illustrated in Figure 4.2.4. A stick figure representation (in Figure 4.2.5) illustrates the overall effect of this on the system. Figure 4.2.5b should also be compared with Figure 4.2.2b, where the only difference in the integration process is the number of iterations. This shows that a great improvement is made when the number of iterations is increased simply from 1 to 2. Certain instants in the simulations required more iterations to converge than others, and the need for more iterations was directly linked to the size of the integration step (h). A safe combination of the two parameters was found to be 10 iterations and step size of .001 seconds for most simulations.

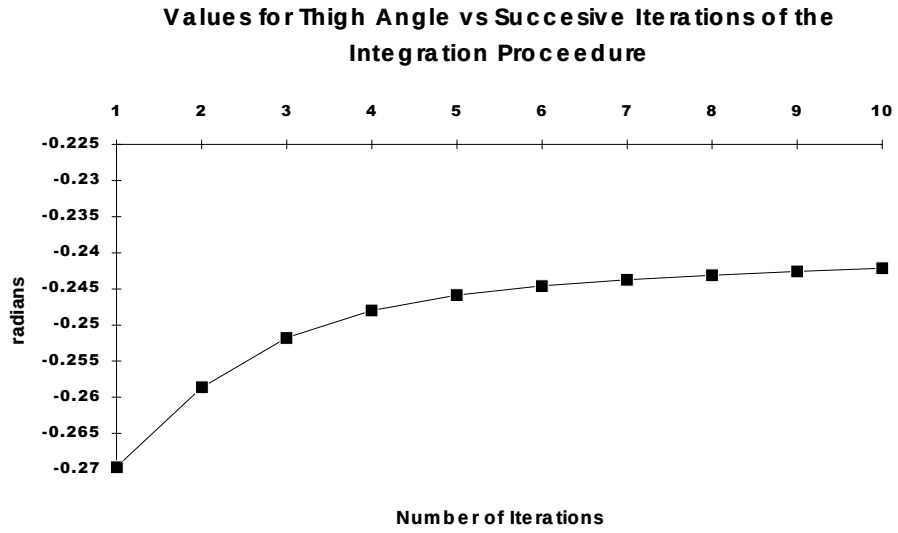

Figure 4.2.4 : *Example of the iterative process of integration and re-evaluation of acceleration. This is the angular position of the thigh for one integration time step, for time=.006 in a) below.*

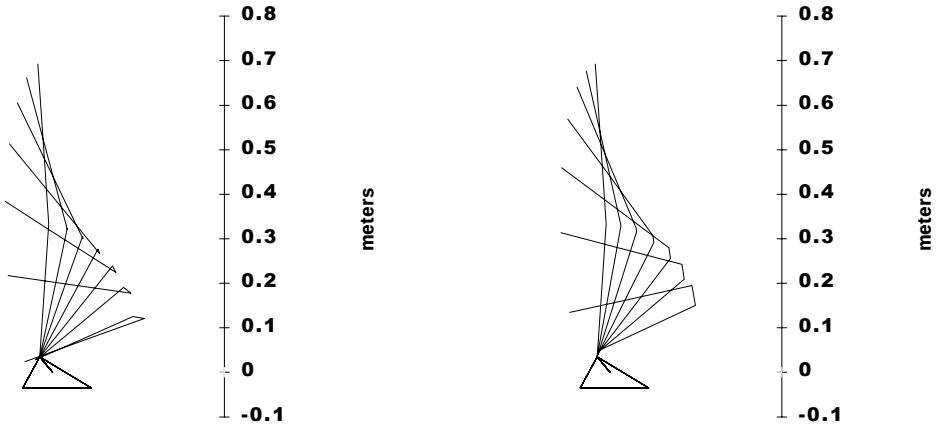

Figure 4.2.5 : *A stick figure representation (0.05 second intervals, end time .3 seconds, h=.05) of a model being allowed to collapse under its own weight from a standing configuration, for two integration strategies: a) 10 iterations, b) 1 iteration.*

It should be mentioned that more sophisticated methods for integration exist. Most involve the interplay between integration step size and the iterative process mentioned above. The process can be made much more efficient and of known accuracy by forcing the integration step size to be dependent on a tolerance value. Using a tolerance criterion, the iterative process is repeated until the difference from one iteration to the next is less a certain value (a convergence criterion). The potential exists for the system to become unstable and not converge for excessively large values of h, thus the integrator must also make the decision, after a certain number of iterations without converging, to start over using a smaller h. This type of approach can be augmented using predictor and corrector extrapolation techniques, [Gear 1971]. These methods greatly facilitate the speed of simulation. A general rule to conducting simulations is that if visibly different results are obtained using a smaller step size or a larger number of iterations, one must continue to decrease the step size and/or increase the number of iterations used until no visible changes occur when you tighten these parameters further.

Initially it was thought that the joint constraints at the knee and ankle could be replaced with what has been referred to as "soft constraints," in which the hinge connection between the segments are replaced by a stiff spring and damper connecting the tips of each segment [Onyshko and Winter 1980]. However, this type of modeling greatly increased the natural frequencies of the system, and such a small integration step size was needed that this approach was considered too time consuming for the amount benefit it offered, [Hatze and Venter 1981]. However, the need for this approach will be more necessary in the future, where more anatomically consistent models will be used. In such models, the soft tissue and articular

surfaces will actually represent a joint, and thus no constraint equations will be used.

When applying this system to gait, the resulting synthesized accelerations were generally larger in magnitude than the original measured values. These deviations varied in time and effected each coordinate differently. The accelerations for the leg and the thigh body segments are shown in Figures 4.2.6 and 4.2.7 for a simulation that resulted in instability. Each deviant acceleration caused others to deviate. The stick figure of this simulation is shown in Figure 4.2.8b, to be compared to the original motion used to generate the indirect dynamics moments that drove the simulation, shown in Figure 4..2.8.a. The simulation was halted after the trajectory appeared to clearly become unstable.

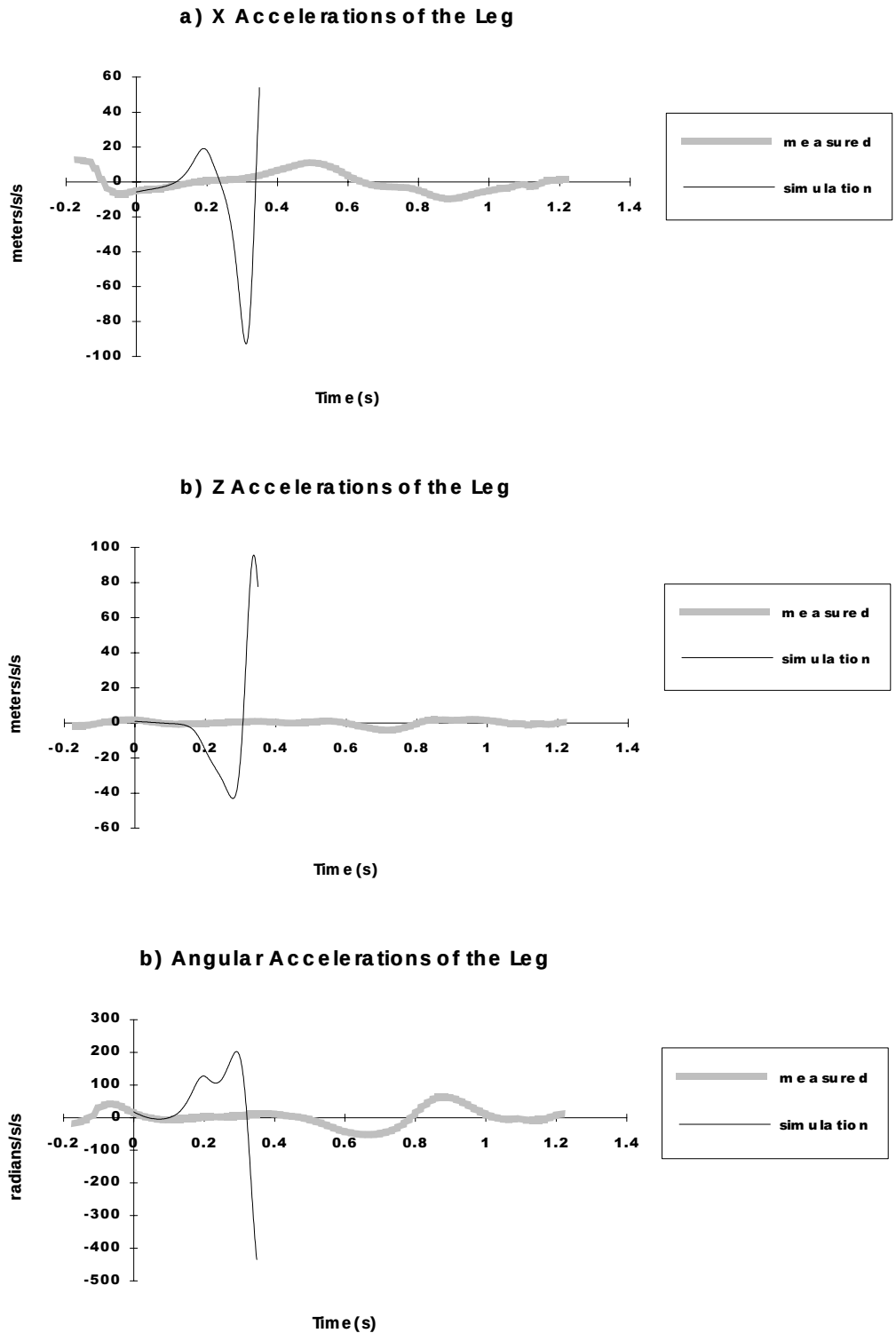

Figure 4.2.6 : *Synthesized accelerations of the leg for an adult walking subject. a) x coordinate b) z coordinate c) theta coordinate.*

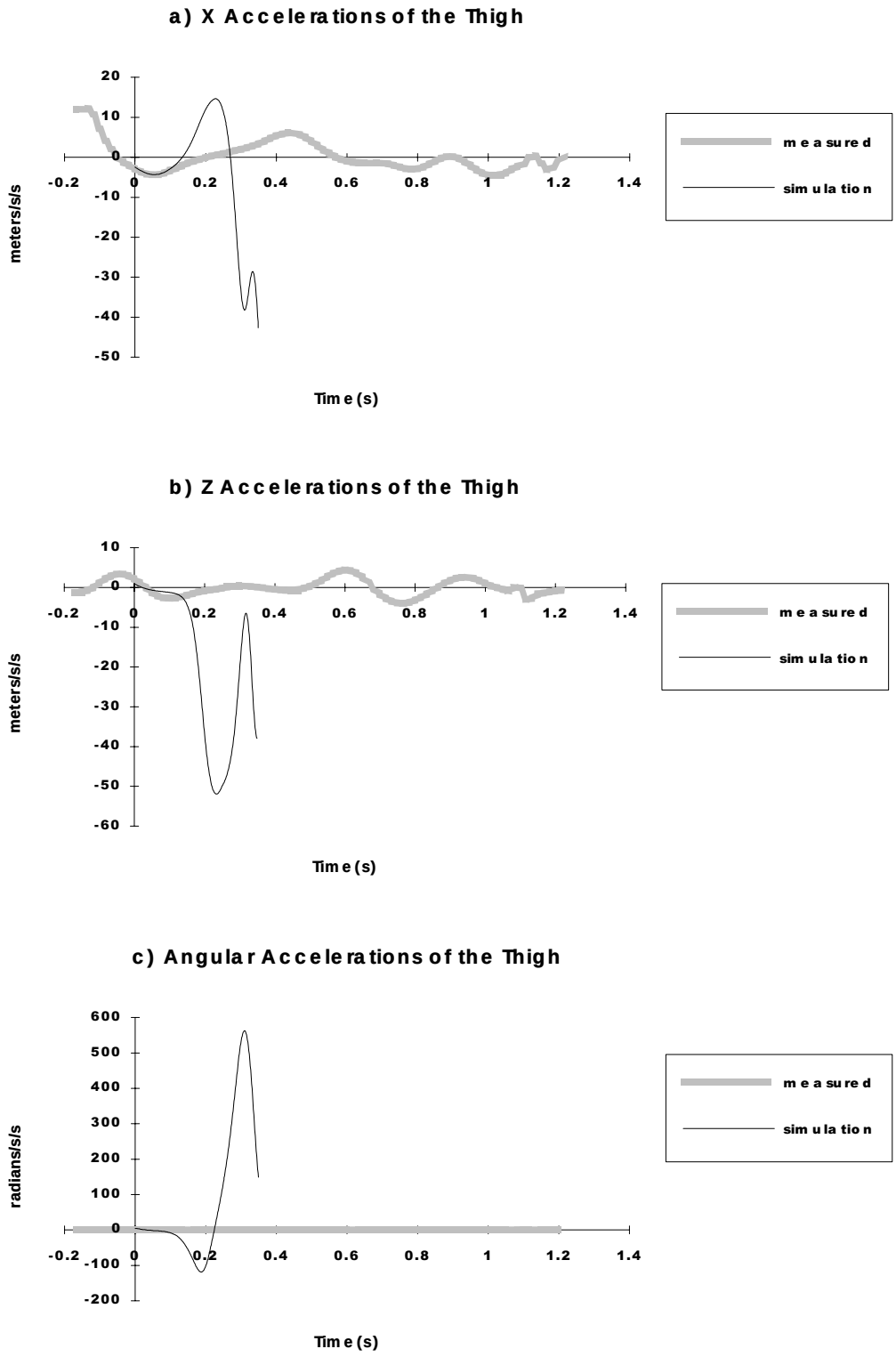

Figure 4.2.7: *Synthesized accelerations of the thigh for an adult walking subject. a) x coordinate b) z coordinate c) theta coordinate.*

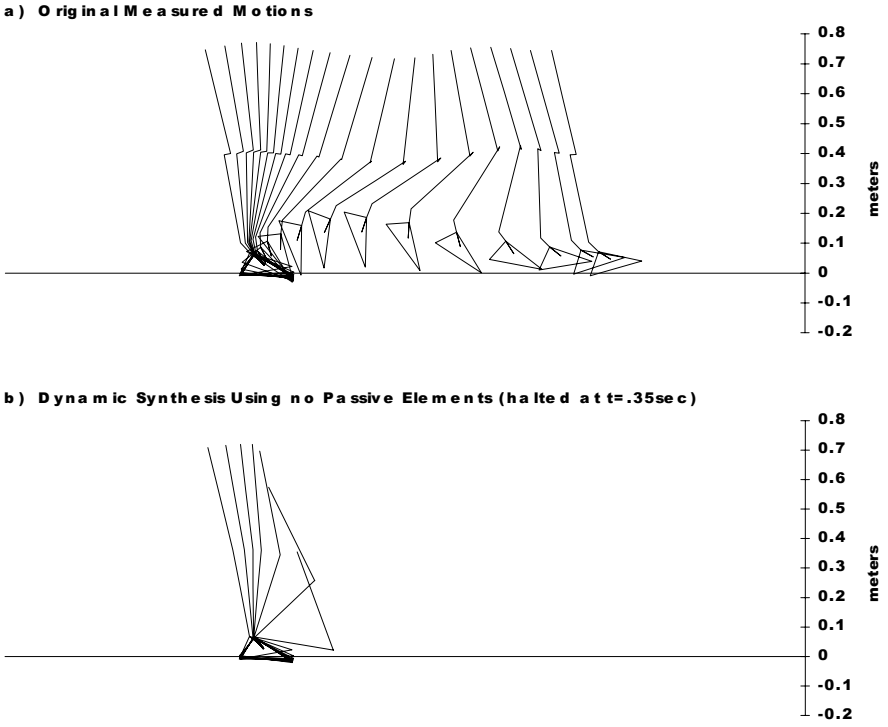

Figure 4.2.8 : *Comparison of initial synthesis results with the measured motions . a) Measured b) Synthesis results, (h=.0005, 15 iterations).*

The addition of passive torsional elements at the joints greatly influenced the quality of the simulation. Figure 4.2.9 shows the results of two combinations of torsional elements. The stability of the system was changed enough to prevent a fall, but increased stiffness produced a "stiff" type of motion, where joints appeared to lack the necessary motion to be realistic. No simulations exactly reflected the original measured motions.

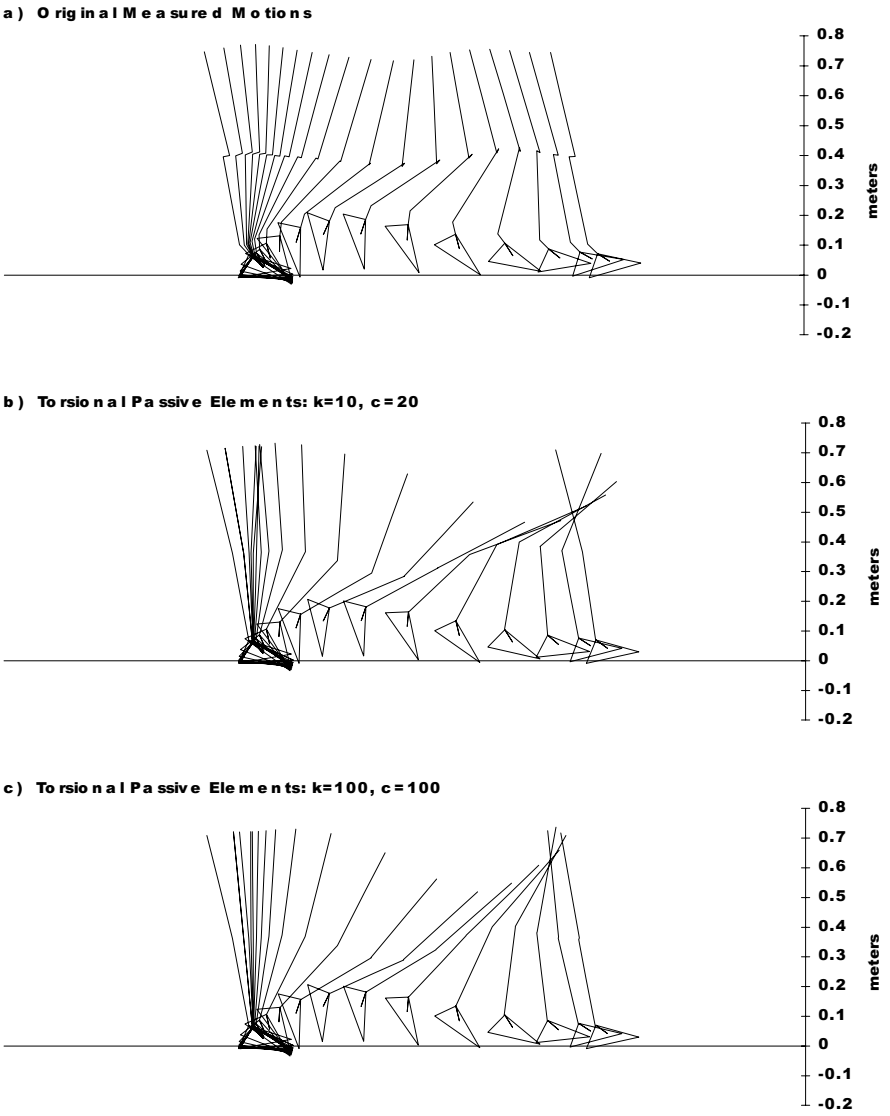

Figure 4.2.9 : *Comparison of synthesis results for varying torsional passive joint elements. a) Measured b) Synthesis results, no passive elements c) Synthesis results, k=10, c=20 d) Synthesis results, k=100, c=100. (h=.0005, 15 iterations).*

The problem with geometric validity mentioned in the methods section is visible in the mesured motion, displayed in Figure 4.2.9a. This illustrates errors in the estimation of limb dimensions (joint positions and centers of mass positions) and in the estimation of segmental principle axes. This results in errors in the indirect dynamic model. The figure shows joint

positions changing throughout the gait cycle. This can be caused by changes in joint center due to non ideal joints as well as errors in geometric estimates.

The mathematical correction to constraint violations (assumption of hinge joints before the indirect problem is calculated) is illustrated in Figure 4.2.10a. Although the graphics for the initial measured motions is more realistic, this approach did little to effect the overall motions of the system (compare Figure 4.2.10b to Figure 4.2.9b).

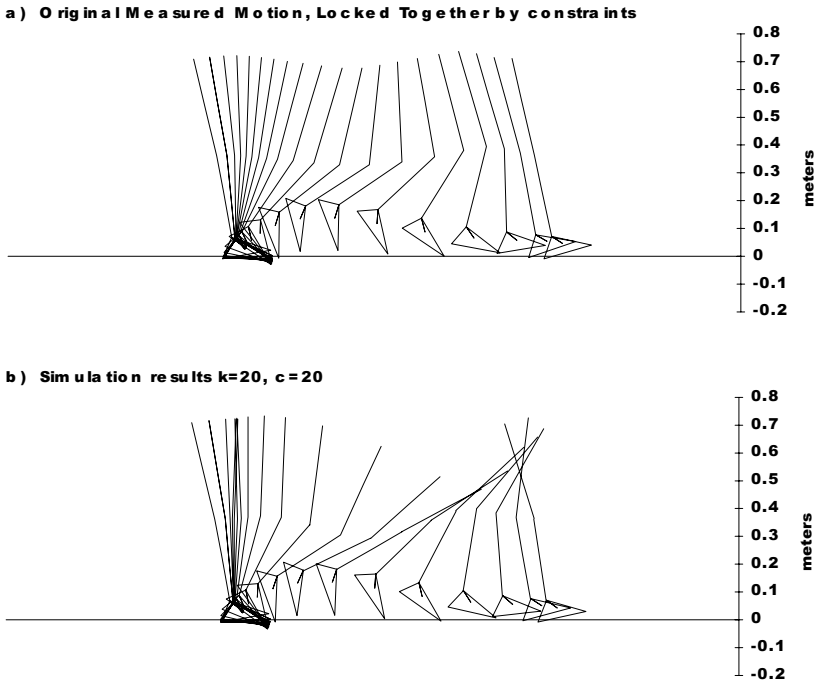

Figure 4.2.10: *Original Motion and simulation results for when the hinge constraints are imposed on the system before the indirect problem. a) motion used for the indirect problem. b) simulation results*

An easily identified problem with these results is the unnatural hyperextension of the knee seen in swing. If one considers the type of passive elements used at the knee, it is clear that a linear torsional spring does not supply anatomical inconsistent constraint forces . Hyperextension

requires the same amount of torque in the model, where this is definitely not the case for the human knee. The involvement of the posterior cruciate ligament, the joint capsular ligaments, the hamstrings, the gastrocnemius, and the articular surface all play a role in the actual dynamics of the knee. As data becomes available, models must employ nonlinear, asymmetrical characteristics that more closely imitate the anatomical structure and function of the joints [Audu and Davy 1985].

The forces from a typical simulation can be seen in Figure 4.2.11a, and the corresponding center of pressure calculated from the results in Figure 4.2.11b. These curves tended to reflect the original measured values well. Data showed increasing deviation from the original measured values as the simulation progressed, due to successive errors in the dynamics. The decrease in the maximum acceleration and propulsion, and the slow progression forward of the COP may all be related.

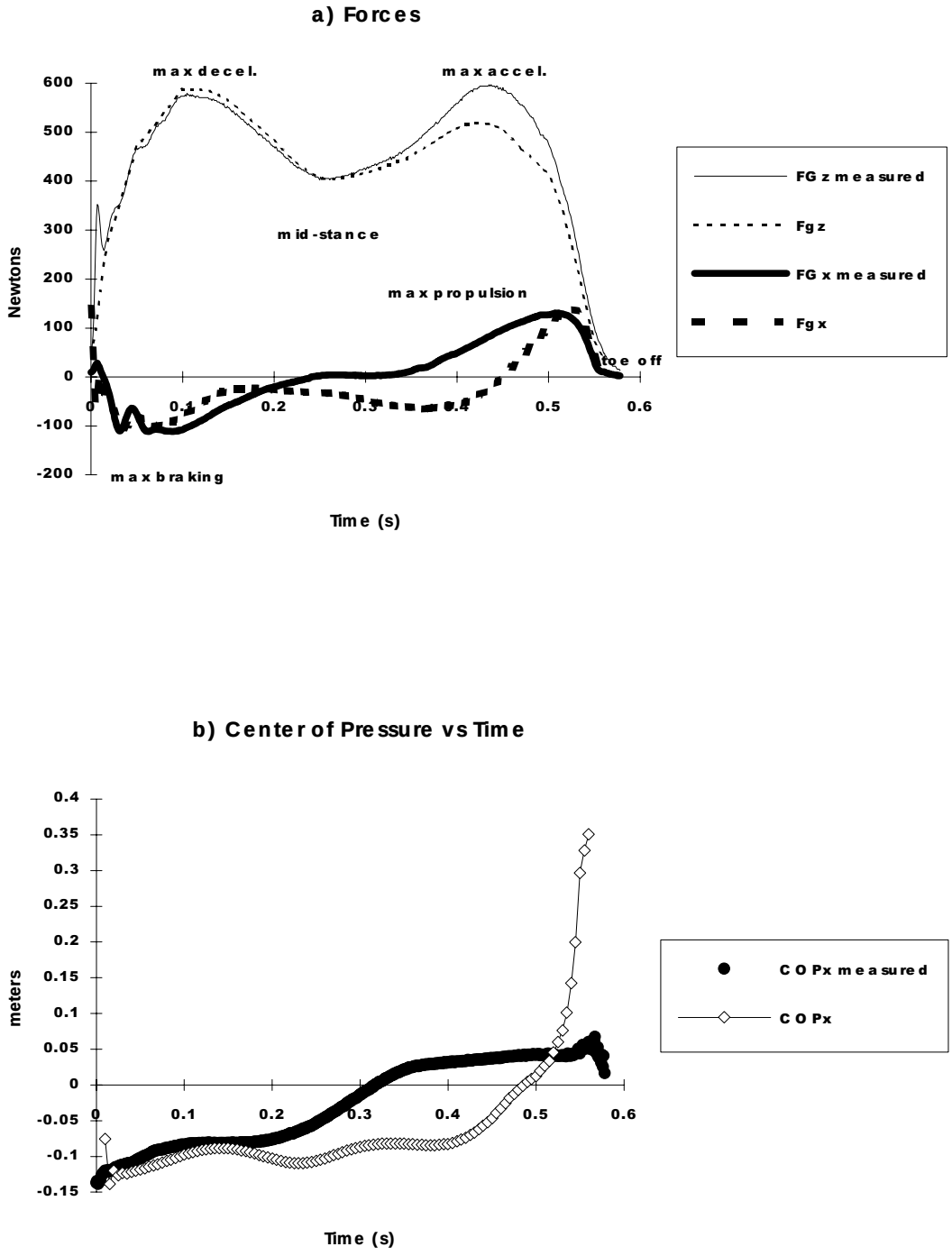

Figure 4.2.11: *Ground Applied Force (GAF) parameters in the inertial coordinate system for a simulation compared with original measured values from the force plate. a) Forces b) center of pressure (COP).*

A shortcoming of the modeling approach used was that ground applied forces (GAF) acting on the plantar surface of the foot were not forced to be zero after the foot left the floor. As a result, any deviation from the original measured motion caused slight forces to exist during swing phase. Subsequently, the allowance of these forces could cause the deviant motion (seen in Figure 4.2.10b, during swing) because forces and moment in the system could be transferred to GRF 's at the foot instead of causing motion. An example of this is that if the forces and moments at the hip were simply transferred through the system to the foot during swing phase thus failing to cause the necessary flexion of the knee. Therefore, this model loses its accuracy during swing, and predictive analyses must be conducted with great care. The solution to this problem would be to reformulate the system of equations at the point of toe off, and begin a new initial value problem that does not consider GRF's possible at the foot. This type of approach has been attempted in other studies with variable success [Onyshko and Winter 1980].

The moments were further inspected by isolating the individual contributions to the moments on each segment. Figure 4.2.12 shows the contribution of the active and passive elements on the motions of each of the segments. The passive elements appeared to play a large role in the moment amplitudes. Such a large role may suggest that the collective contribution of ligaments, tendons, aponeuroses, skin, muscle, and articular cartilage may contribute heavily to the stability of gait. This phenomenon is mentioned in the literature [Mansour and Audu 1986], where the collective passive moment caused by all tissues in the leg tended to be roughly the same magnitude as the moments seen in gait. The relative magnitude of the passive and active force contributions are about the same in magnitude, while the moments generated by inertial effects were comparatively small.

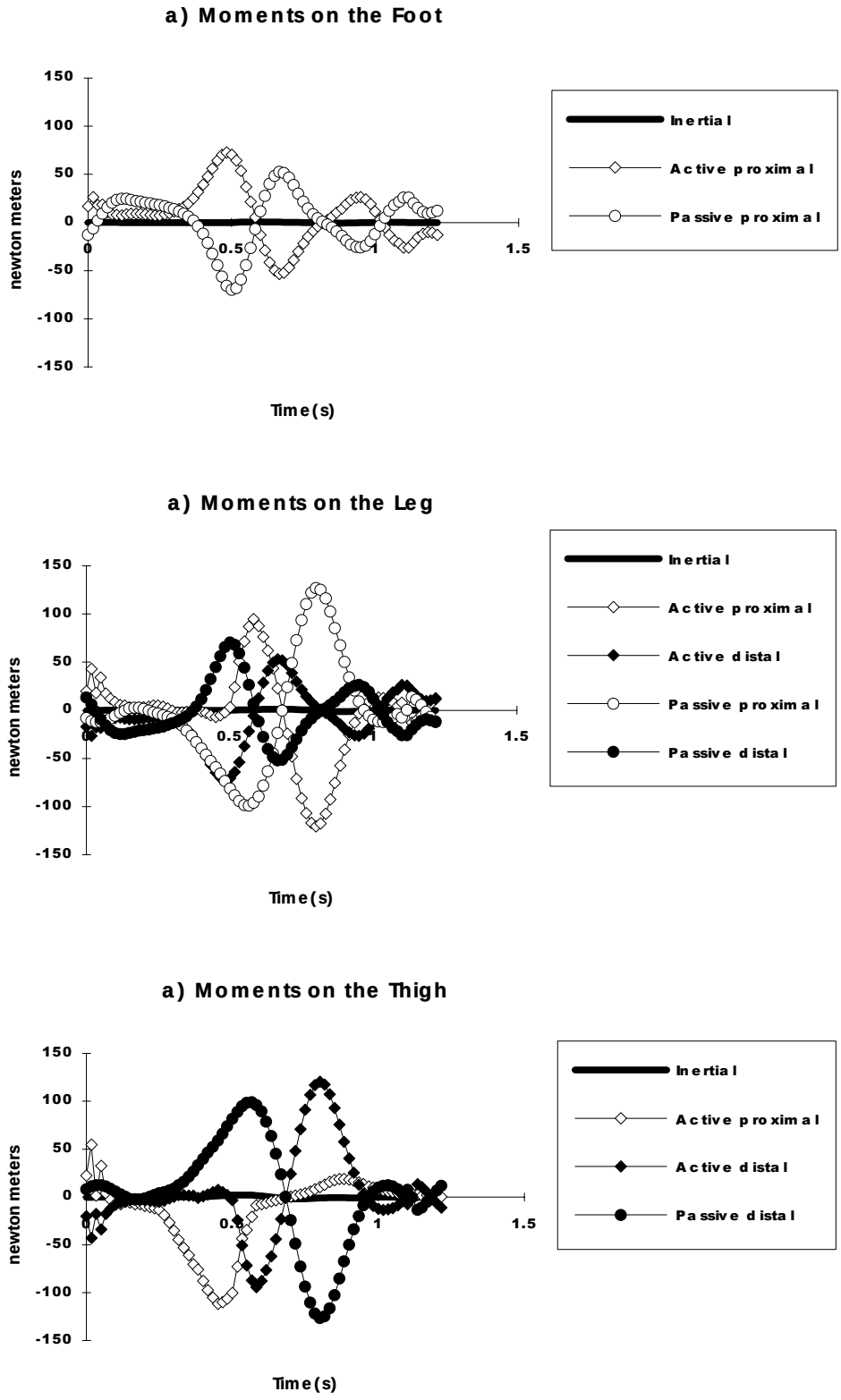

Figure 4.2.12 : *The contribution of each factor to the moments on the segments. a) foot b) shank c) thigh.*

The question still exists, "why is this system inherently unstable?" An inverted pendulum (Figure 4.2.13) can be manipulated by a known moment using a known time history *M(t)* calculated in an inverse dynamic analysis, but any deviation in the rotation causes an unexpected increase (or decrease) in the gravitational contribution to the net moment. The result is a rotation too far (or not far enough) in the intended direction. This is yet another deviation, which leads to yet another increase (or decrease) in the gravitational contribution to the net moment, and the process continues. The result is an eventual collapse of the pendulum. Changes in the direction and magnitude of M(t) can coincidentally reduce the errors described above temporarily, but an eventual collapse is certain. The best one can hope for is for the system to follow an intended trajectory, and any deviation from it will most likely precipitate a fall. Unfortunately, even the best integration packages provide only estimates, and even a infinitesimal deviation in the motions can eventually result in a fall. Also, digital computers use values that are truncated to a finite number of decimal places, thus we can only approach perfection, and not attain it.

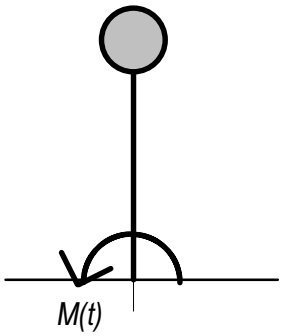

Figure 4.2.13 : *An inverted pendulum driven by a manipulating moment M(t).*

One cause of instability is that the system has no "restoring" characteristics that may correct a deviant motion (unless the pendulum is swinging in the region below ground, in which case the gravity becomes a restoring force). The addition of passive elements to the system can supply restoring forces.

One can think of the leg model as three inverted pendulums balancing on top of each other. With this in mind, it is understandable why the system tends to collapse when simulated. In the case of the slender rod, using body-based forces meant the forces did not change their direction with respect to the rod if the rotations of the rod deviated from the original motion. However, if inertial-based forces were used, the motion eventually deviated. In the case of the three body segments, the direction of the forces at each joint is independent of the coordinate systems of the joints and depend solely on the dynamics of the system. Thus a deviation in the motion of any segment will change joint forces, and therefore change the motions of all other segments [Zajac and Gordon 1989].

It was shown that joint torsional spring dampers provided enough restoring capacity for stable gait. However, deviations in the motion are well noted, and other approaches to passive elements need to be addressed to improve motion [Audu and Davy 1985]. An argument can be made that although the passive forces restore stability, they do not completely restore the motion so that it is identical to measured motion. It has been suggested [Van Den Bogert, Schamhardt, et al. 1989] that a simple first order linear feedback can be used to restore the motion towards the intended state trajectory. Control appears to hold great promise for predictive dynamic modeling, because it is neurologically relevant (we all are assisted by our visual, vestibular, and propreoceptive feedback control systems [Hemami

and Stokes 1983]) . This approch also bypasses many of the problems encountered in this work, such as the foot striking the ground slightly before or after it should. These methods must be explored in the future.

Stability can also be explored from a control dynamics standpoint. A system which has a segment moving near one of its natural frequencies may cause attenuation of velocities. In the future it may be important to perform a linear dynamic analysis on the system at the critical instants of the simulations. The natural frequencies for the model at these times can be estimated and compared with+ the observed motions to see if any attenuation is likely. Passive elements (springs) greatly increase the natural frequencies of the system, and thus may sufficiently remove the danger of the system's motion ever approaching a hazardous frequency (in other words, move the natural frequencies out of the way). However, this approach should be taken once anatomical elements are included in the model in order to study realistic effects on stability.

Clearly, the forward dynamic modeling of the neuromusculoskeletal system is a complex task. Stability of motion is an issue that is believed by the author to not be avoided without employing control strategies and considering all relevant anatomical passive and active elements. Many researchers have succeeded in producing movement when employing control schemes and considering the mechanical contributions of muscle, tendon, cartilage, and ligament.

5. SUMMARY AND CONCLUSIONS

This thesis investigated the use of inverse dynamic analysis results (forces and moments) to model the synthesis of motion. It was hoped that if the original motions were obtained, then the synthesis could be repeated with certain parameters varied in order to simulate the outcome of a surgical intervention, a rehabilitation strategy, or an orthotic device. Such a tool could have great clinical utility by preventing risky or costly ventures.

Initially a model of the human muskuloskeletal system was developed using a commercial software package, ADAMS, by Mechanical Dynamics, Inc., Ann Arbor, Michigan. A planar model was developed using this package, in which measured gait analysis laboratory data was used to drive an inverse dynamic simulation. The moment time history of one knee joint was then used to drive a forward dynamics simulation. This model walked for the duration of a gait cycle only with heuristically determined joint torsional springdampers, but did not match the original kinematic patterns.

An additional module of the ADAMS system, Android, was used to generate a full body, three dimensional model of a human subject. Moment time histories were calculated, and then used to drive forward dynamic syntheses. Due to inaccuracies in the model's geometry, late and early strikes of the foot to the floor led to precipitating errors that eventually led to a fall. Other errors due to numerical instability, lack of anatomically consistent model structures, and dynamic coupling could be identified, but not isolated

As a result, simpler models were developed to better understand the underlying complexity of forward dynamic modeling of human motion.

The goals were to develop models that were sufficiently complex to use in predictive analyses yet sufficiently simple to allow the underlying process to be understood and manipulated. Two planar models were developed: a single-segment rod contacting the floor and manipulated in space, and a three-segment model of the foot, leg and thigh moving through a normative gait cycle.

As the rod was manipulated, the motions and ground forces were measured using gait analysis laboratory aparati. The motions and ground forces were used in a indirect model to calculate the moment and force time histories at the manipulating end. These moment and force time histories were used to drive a dynamic synthesis of motion for the rod. It was found that smoothing the motion target trajectories before differentiating gave the best results, particularly in acceleration calculations. Force time histories that were established in the coordinate system of the rod (and then converted back to the inertial coordinate system in the equations of motion) resulted in stable simulations. In contrast, force time histories that were established in the inertial coordinate system resulted in instability. Integration technique accuracy proved to be critical to the stability of the simulations.

Similar to the rod, the motions and ground forces of the leg were measured, and were used in an indirect model to calculate the moment and force time histories at each of the three joints (the ankle, knee, and hip). The moment time histories were used to drive a dynamic simulation of the leg in locomotion. The model was found to be extremely sensitive to integration technique parameters. Additionally, passive joint torsional springdampers were necessary to achieve stable gait patterns. No gait simulation reflected

the original measured motions. The contributions of these passive elements necessary for stable gait were calculated. It was discovered that the motion-producing moments due to the passive elements was large relative to the dynamic coupling and gravitational effects. This suggested that the inherent causes of instability must be overwhelmed by the restoring and damping passive forces. However, the forces the passive elements produced were not anatomically realistic, nor did the moment patterns change to compensate for deviations from the intended motions (i.e., active muscle control). Therefore, any deviations from the desired motions resulted in more deviations, until a fall occurred.

Future predictive modeling will require more sophisticated, non-linear relations for passive joint elements. Additionally, it will be necessary to apply control theory principles to supply the necessary forces that damp and restore motion towards a desired trajectory. Both of these approaches will require extensive knowledge of human anatomy and physiology in order to remain true to actual human motor control of locomotion.

APPENDIX A:
A SYSTEM OF EQUATIONS FOR DYNAMIC SYNTHESIS

The equations for the solution of the forward dynamic problem discussed in Section 3.3.4 can be put in to matrix form for solution ($A\underline{x} = \underline{B}$), and are presented on the following page. The first 9 equations are the equations of motion (three equations for each segment). Equations 10 through 13 are equations of constraint. Equations 14 through 16 are the joint moment drivers, 17 and 18 are the hip force drivers. Equations 19 through 21 are the motion drivers of the foot. The nomenclature is as follows:

- Subscripts f, l, and t denote the foot, leg , and thigh segments respectively.
- Subscripts G, A, K, and H denote points where forces act. Specifically, the ground, ankle, knee, and hip, respectively.
- The degrees of freedom of the system are x,z, and Θ for each of the three segments. The subscripts denote which segment.
- F denotes force and M denotes moment.
- m denotes segment mass and I denotes the polar moment of inertia about the center of mass.
- R denotes the joint position vector, with subscripts indicating the segment to which it belongs. The component directions,

indicated by subscripts x and z, are in the segmental coordinate system.

- Functions specifying the force and motion drivers for the system (from the indirect dynamics problem) are specified as functions of time as $f_q(t)$, where q denotes which quantity (i.e. $f_{MA}(t)$ is the function from the indirect dynamics calculations that supplies the moment at the ankle).

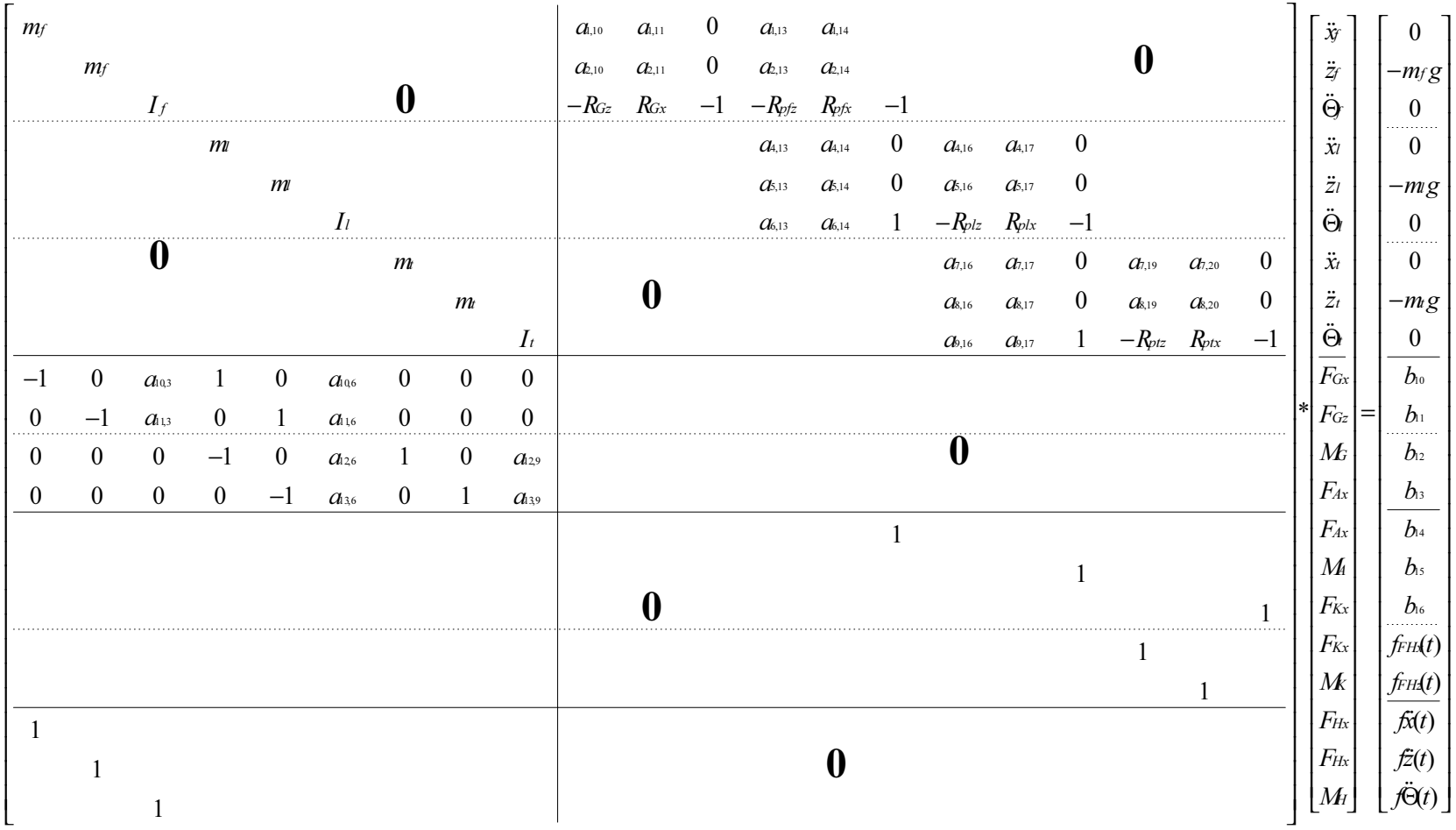

Figure A.1: The matrix form of the 21 Equations for the forward dynamics problem

The $\tilde{\mathbf{A}}$ matrix elements are specified in detail as follows:

$a_{1,10} = -\cos \Theta_f$
$a_{1,11} = -\sin \Theta_f$
$a_{1,13} = -\cos \Theta_f$
$a_{1,14} = -\sin \Theta_f$

$a_{2,10} = \sin \Theta_f$
$a_{2,11} = -\cos \Theta_f$
$a_{2,13} = \sin\Theta_f$
$a_{2,14} = -\cos \Theta_f$

$a_{4,13} = \cos \Theta_f$
$a_{4,14} = \sin \Theta_f$
$a_{4,16} = -\cos \Theta_l$
$a_{4,17} = -\sin \Theta_l$

$a_{5,13} = -\sin \Theta_f$
$a_{5,14} = \cos \Theta_f$
$a_{5,16} = \sin\Theta_l$
$a_{5,17} = -\cos \Theta_l$

$a_{6,13} = -R_{dlx}\sin(\Theta_l - \Theta_f)+R_{dlz}\cos(\Theta_l - \Theta_f)$
$a_{6,14} = -R_{dlx}\cos(\Theta_l - \Theta_f)-R_{dlz}\sin(\Theta_l - \Theta_f)$

$a_{7,16} = \cos \Theta_l$
$a_{7,17} = \sin \Theta_l$
$a_{7,19} = -\cos \Theta_t$
$a_{7,20} = -\sin \Theta_t$

$a_{8,16} = -\sin \Theta_l$
$a_{8,17} = \cos \Theta_l$
$a_{8,19} = \sin\Theta_t$
$a_{8,20} = -\cos \Theta_t$

$a_{9,16} = -R_{dtx}\sin(\Theta_t - \Theta_l)+R_{dtz}\cos(\Theta_t - \Theta_l)$
$a_{9,17} = -R_{dtx}\cos(\Theta_t - \Theta_l)-R_{dtz}\sin(\Theta_t - \Theta_l)$

$a_{10,3} = R_{pfx}\sin\Theta_f - R_{dfz}\cos\Theta_f$
$a_{10,6} = -R_{plx}\sin\Theta_l + R_{dlz}\cos\Theta_l$

$a_{11,3} = R_{pfx}\cos\Theta_f + R_{dfz}\sin\Theta_f$
$a_{11,6} = -R_{plx}\cos\Theta_l - R_{dlz}\sin\Theta_l$

$a_{12,6} = R_{plx}\sin\Theta_l - R_{dlz}\cos\Theta_l$
$a_{12,9} = -R_{ptx}\sin\Theta_t + R_{dtz}\cos\Theta_t$

$a_{13,6} = R_{plx}\cos\Theta_l + R_{dlz}\sin\Theta_l$
$a_{13,9} = -R_{ptx}\cos\Theta_t - R_{dlz}\sin\Theta_t$

and the **B** vector elements are specified in detail as follows:

$b_{10} = -R_{pfx}\dot{\Theta}_f^2\cos\Theta_f - R_{pfz}\dot{\Theta}_f^2\sin\Theta_f + R_{dlx}\dot{\Theta}_l^2\cos\Theta_l + R_{dlz}\dot{\Theta}_l^2\sin\Theta_l$
$b_{11} = R_{pfx}\dot{\Theta}_f^2\sin\Theta_f - R_{pfz}\dot{\Theta}_f^2\cos\Theta_f - R_{dlx}\dot{\Theta}_l^2\sin\Theta_l + R_{dlz}\dot{\Theta}_l^2\cos\Theta_l$
$b_{12} = -R_{plx}\dot{\Theta}_l^2\cos\Theta_l - R_{plz}\dot{\Theta}_l^2\sin\Theta_l + R_{dtx}\dot{\Theta}_t^2\cos\Theta_t + R_{dtz}\dot{\Theta}_t^2\sin\Theta_t$
$b_{13} = R_{plx}\dot{\Theta}_l^2\sin\Theta_l - R_{plz}\dot{\Theta}_l^2\cos\Theta_l - R_{dtx}\dot{\Theta}_t^2\sin\Theta_t + R_{dtz}\dot{\Theta}_t^2\cos\Theta_t$
$b_{14} = f_{MA}(t) + (M_A)_{passive}$
$b_{15} = f_{MK}(t) + (M_K)_{passive}$
$b_{16} = f_{MH}(t)$

where $(M_A)_{passive}$ and $(M_K)_{passive}$ are defined using equations 3.3.1 and 3.3.2.

APPENDIX B:
THE BEL DATA LINK PROGRAM (BLINK)

Introduction

The Biomechanics Evaluation Laboratory (BEL) Data Link program, (BLINK), was developed to link the motion and force data, perform gait analysis data reduction, and output kinematics and kinetic data in a format that is readable by other programs. Of particular interest are the output procedures that accommodate the Mechanical Dynamics Inc. ADAM/Android software file formats for the dynamic analysis and simulation of human motion. Blink provides initial conditions, as well as function definitions for force, position and angular time-histories of human motion.

The original goal of BLINK was to provide a link for analysis of human motion using ADAMS/Android. Previously, ADAMS/Android software sufficiently enabled the user to correctly generate a model of any subject, but the development of BLINK allowed the automatic generation of driving functions for the model from gait analysis laboratory data. These functions are written as Android-formatted data files for motions, forces, and initial conditions .

This allows the user to prepare and simulate a subject-specific model of gait in a matter of minutes.

Description of Program

BLINK is a program (written in C) that reduces and generates kinematic and kinetic data. Blink generates full body three dimensional kinematic and kinetic data files in an interactive and user-friendly procedure. It also creates two critical files necessary to completely specify motions and forces measured for ADAMS/Android: the __**.prp** (property) file and the ___**.pst** (posture or initial configuration) file.

Construction is organized into modular groups of functions and subprograms to accomplish each task. These structures are outlined as follows in the order in which they are executed:

- **Force Plate Data Reduction.** The three moment and three force channels from the force plate are converted to a mechanical wrench and a center of pressure (COP) for each instant of time.

- **Kinematic Data Reduction.** Several targeting protocols are available for 3-dimensional analysis. The target trajectories determined by the motion analysis system are used to establish local coordinate systems (LCS) for each body segment Not all target coordinate systems are perfectly aligned with the principle coordinate system of the body segment, so a function is provided to establish the coordinate transformation between target and principle coordinate systems based on "standing file" data and/or extraneous mesurements. The relative 3-dimensional angles of rotation between each body segment are calculated using the

Cardan (or Bryant)-type Eulerian angles of rotation [Goldstien 1981]. A library of other Eulerian-type angular calculations (yaw pitch roll, ZXZ, etc.) are also available for analysis. The trajectory and orientation of the pelvis is also calculated relative to the lab (inertial) coordinate system. Also calculated are the derivatives of the target trajectories, angular velocity and angular acceleration of each segment, and trajectories of the centers of mass.

- **Synchronization of Force and Motion.** Data is shifted so that time zero is heel contact, and is re-sampled at 60 Hz. (for ADAMS/Android files, data is re-sampled at 30 Hz) . Also, the COP is transformed to the coordinate system of the foot and imaged in a footprint.

- **Kinetics calculations.** Joint moments are calculated using the force and motion data.

- **ADAMS/Android Output Files**. The __**.prp** and ___**.pst** files are generated in an ADAMS/Android format.

The resulting files contain kinematic and kinetic information which can be used in whole or in parts with an android model. For example, the all joint degrees of freedom can be specified kinematically except for knee flexion, which may be driven by a moment time-history obtained in an indirect dynamics analysis (from ADAMS or from an external system.). ADAMS/Android integrates all choices of inputs with a human model, and poses the particular dynamics analysis problem to be solved in ADAMS.

LIST OF REFERENCECES

1. Amirouche, F. M. L., S. K. Ider, J. Trimble, "Analytical Method for the Analysis and Simulation of Human Locomotion," *Journal of Biomechanical Engineering*, Vol. 112, pp. 379-386, 1990.

2. Audu, M. L., D. T. Davy, "The Influence of Muscle Model Complexity in Musculoskeletal Motion Modeling," *Journal of Biomechanical Engineering*, Vol.107, pp. 147-149, 1985.

3. Bandera, C., D. Minen,G. Manzilli, "Human Walking Dynamic Model Using ADAMS -- An Approach to Biomechanics of the Knee Under Dynamic Loads," Mechanical Dynamics, Inc., Ann Arbor, MI, 1990.

4. Braune, W., O. Fischer, *On the Center of Gravity of the Human Body,* Translated by P. G. Maquet and R. Furlong, Springer-Verlag, New York, 1985.

5. Bresler, B, J. P. Frankel, "The Forces and Moments in the Leg During Level Walking," *Transactions of the American Society of Mechanical Engineers*, pp. 27-36, 1950.

6. Chace, M. A. , "Modeling of Dynamic Mechanical Systems," *CAD/CAM Robotics and Automation Institute and International Conference*, Tucson (MDI #31), 1985.

7. Chandler, R. F., C. E. Clauser, J. T. McConville, H. M. Reynolds, J. W. Young, "Investigation of Inertial Properties of the Human Body," US Department of Transportation, Report #DOT HS-801 430, Washington D.C., 1975.

8. Chao, E. Y. S., "Justification of Triaxial Goniometer for the Measurement of Joint Rotation," *Journal of Biomechanics*, Vol. 13, pp. 989-1006, 1980.

9. Chow, C. K., D. H. Jacobson, "Studies in Human Locomotion via Optimal Programming," *Mathematical Biosciences*, Vol. 10, pp. 239-306, 1971.

10. Chow, C. K., D. H. Jacobson, "Further Studies in Human Locomotion: Postural Stability and Control," *Mathematical Biosciences*, Vol. 15, pp. 93-108, 1972.

11. Clauser, C. E., J. T. McConville, J. T., J. W. Young, "Weight, Volume and Center of Mass of Segments of the Human Body," AMRL Technical Report, Wright patterson Air Force Base, Ohio, 1969.

12. Crownenshield R., M. H. Pope, R. J. Johnson, "An Analytical Model of the Knee," *Journal of Biomechanics*, Vol. 9, pp. 397-405, 1976.

13. Delp, S. L., "Applications of Computer Graphics in Motion Analysis," *Seventh East Coast Clinical Gait Conference*, Richmond VA, 1991.

14. Delp, S. L., E. E. Bleck, F. E. Zajac, G. Bollini, "Biomechanical Analysis of the Chiari Pelvic Osteotomy: Preserving Hip Adductor Strength," *Clinical Orthopaedics and Realated Research*, No. 254, pp. 189-198, 1990.

15. Delp, S. L., J. P. Loan, M. G. Hoy, F. E., F.E. Zajac, "An Interactive Graphics-Based Model of the Lower Extremity to Study Orthopaedic Surgical Proceedures," *IEEE Transactions on Biomedical Engineering*, Vol. 37, pp. 757-767, 1990.

16. Delp, S. L., M. Maloney, "Effects of Hip Joint Center on the Moment-Generating Capacity of the Muscles," *Journal of Biomechanics*, Vol 26, pp. 485-499, 1993.

17. Dempster, W. T., "Space Requirements of the Seated Operator," WADC Technical Report 55-159, Wright patterson Air Force Base, Ohio, 1955.

18. Elftman, H., "Forces and Energy Changes in the Leg During Walking," *American Journal of Physiology*, Vol. 25, pp. 339-356, 1939.

19. Gage, J. R., *Gait Analysis in Cerebral Palsy*, Mac Keith Press, London, 1991.

20. Gear, C. W., *Numerical Initial Value Problems in Ordinary Differential Equations*, Prentice-Hall, Englewood Cliffs, 1971.

21. Goldstien, H., *Classical Mechanics*, Addison-Wesley Publishing Co., Reading Mass, 2nd. ed., 1981.

22. Green, J. I., G. T. Yamaguchi, J. K. DeWitt, "The Effects of Bilateral Assymmetry on a Model of the Counter Movement Jump," *Second North American Congress of Biomechanics*, Chicago, pp. 543-544, 1992.

23. Greenwood, D. T., *Principles of Dynamics*, Prentice Hall, Inc., Englewood Cliffs, New Jersey, 1988.

24. Grood, E. S., W.J. Suntay, "A Joint Coordinate System for the Clinical Description of Three-Dimensional Motions: Application to the Knee," *Journal of Biomechanical Engineering*, Vol. 105, pp. 136-144, 1983.

25. Hardt, D. E., R. W. Mann, "TECHNICAL NOTE: A Five Body -- Three Dimensional Dynamic Analysis of Walking," *Journal of Biomechanics*, Vol. 13, pp. 455-457, 1980.

26. Hatze, H., "A Complete Set of Control Equations for the Human Musculo-Skeletal System," *Journal of Biomechanics*, Vol. 10, pp. 799-805, 1977.

27. Hatze, H.,"A Comprehensive Model for Human Motion Simulation and its Application to the Take Off Phase of the Long Jump," *Journal of Biomechanics,* vol. 14, pp. 135-142, 1981.

28. Hatze, H., " The Complete Optimizataion of Human Motion," *Mathematical Biosciences*, Vol. 28, pp. 99-135, 1986.

29. Hatze, H., "Quantitative Analysis, Synthesis, and Optimization of Human Motion," *Human Movement Science*, Vol. 3, pp. 5-25, 1984.

30. Hatze, H., A. Venter, "Practical Activation and Retention of Locomototion Constraints in Neuromusculoskeletal Control System Models," *Journal of Biomechanics*, vol. 14, pp. 873-877, 1981.

31. Haug, E. J., "Computer Aided Kinematics and Dynamics of Mechanical Systems -- Volume 1: Basic Methods," Allyn and Bacon, Needham Heights, MA., 1989.

32. Hemami, H., B. T. Stokes, "A qualitative Discussion of Mechanisms of Feedback and Feedforward Control of Locomotion," *IEEE Transactions on Biomedical Engineering*, Vol. 30, pp. 681-689, 1983.

33. Hemami, H. R., Y.-F. Zheng, "Initiation of Walk and Tiptoe of a Planar Nine-Link Biped," *Mathematical Biosciences,* Vol. 61, pp. 163-189, 1982.

34. Hill, A. V., "The Heat Shortening and the Dynamic Constants of Muscle," *Proc. R. Soc. B.*, Vol. 126, pp. 136-195, 1938.

35. Hill, A. V., "Chemical Change and Mechanical Response in Stimulated Muscle," *Proc. R. Soc. B.*, Vol. 141, pp. 314-320, 1953.

36. Hof, A. L., "TECHNICAL NOTE: An Explicit Expression for the Moment in Multibody Systems," *Journal of Biomechanics*, Vol. 25, pp. 1209-1211, 1992.

37. Hoy, M. G., F. E. Zajac, M. E. Gordon, "A Musculoskeletal Model of the Human Lower Extremity: The Effect of Mucle, Tendon, and Moment Arm on the Moment-Angle Relationship of Musculotendon Actuators at the Hip, Knee, and Ankle," *Journal of Biomechanics*, Vol. 23, 1990.

38. Hurmuzlu, Y., "The Effect of Stance Ankle Torques on the Nonlinear Stability of a Two Degree of Freedom, Three Element Bipedal Locomotion System," *Modeling and Control Issues in Biomechanical Systems, ASME Winter Annual Meeting*, Chicago, pp. 73-88, 1988.

39. Hurmuzlu, Y., G. D. Moskowitz, "Bipedal Locomotion Stabilized by Impact Switching: I. Two- and Three-Dimensional, Three Element Models," *Dynam. Stabil. Sys.*, Vol. 2, pp. 73-96, 1987a.

40. Hurmuzlu, Y., G. D. Moskowitz, "Bipedal Locomotion Stabilized by Impact Switching: II. Structural Stability Analysis of Four-Element Bipedal Locomotion Model," *Dynam. Stabil. Sys.*, Vol. 2, pp. 97-112, 1987b.

41. Ishac, M. G., David A. Winter, "Internal Validity of Link-Segment Models of Gait Analysis," *Sixth East Coast Clinical Gait Conference*, East Lansing, MI, Michigan State University, pp. 75-78, 1990.

42. Jensen, R. K., "Body Segment Mass, Radius and Radius of Gyration Proportions of Children," *Journal of Biomechanics,* pp. 359-368, 1986.

43. Kadaba, M. P., Ramakrishnan, M. E. Wooten, J Gainey, G. Gordon, and G. V. B. Cochran,. "Repeatability of Kinematic, Kinetic, and Electromyographic Data in Normal Adult Gait," *Journal of Orthopaedic Research*, Vol. 7, pp-849-860, 1989.

44. Kane, T. R., D. A. Levinson, "The Use of Kane's Dynamical Equations in Robotics," *The International Journal of Robotics Resarch*, Vol. 2, pp. 3-21, 1983.

45. Kepple, T, "Status Report for NIH-ADAMS/Android Project," Personal Communication, 1992.

46. Koopman, H. F. J. M., H. J. Grootenboer, H. J. de Jongh, "Mechanical Model to Simmulate and Predict Human Walking Patterns," *XII International Congress of Biomechanics*, Los Angeles, CA USA, 342, 1989

47. Lew, W. D., J. L. Lewis, "Technique for calculating in-vivo Ligament Lengths with application to the Human Knee Joint," *Journal of Biomechanics,* Vol. 11, pp. 365-377, 1978.

48. Loch, D. A., Z. Luo, J. L.Lewis, N. J. Stewart, "A Theoretical Model of the Knee and ACL: Theory and Experimental Verification," *Journal of Biomechanics*, Vol. 25, pp. 81-90, 1982.

49. Mann, R. W., "Computer aided Surgery," *Proc. of the 8th Annual Conference of the Rehabilitation Engineering Society of North America (RESNA)*, pp. 160-162, 1985.

50. Mansour, J. M., J. M. Periera, "Quantitative Functional Anatomy of the Lower Limb with Application to Human Gait," *Journal of Biomechanics*, Vol. 20 , pp. 51-58, 1987.

51. Mansour, J. M., M. L. Audu, "Passive Elastic Moment at the Knee and its Influence on Human Gait," *Journal of Biomechanics*, Vol. 19, pp. 369-373, 1986.

52. McConville, J. T., T.D. Churchill, I. Kaleps, C. E. Clauser, J. Cuzzi, "Anthopometric Measurement of Body and Body Segment Moments of Inertia," AFAMRL Techical Report, Wright patterson Air Force Base, Ohio, 1980.

53. Meglan, D. A., "Enhanced Analysis of Human Locomotion," PhD. Dissertation, Ohio State University, 1991.

54. Meglan, D. A., N. Berme, "A 3D Passive Mechanical Model of the Human Foot for Use in Locomotion Synthesis," *Second North American Congress of Biomechanics*, Chicago, pp. 351-352, 1992.

55. Moeinzadeh, M. H., A. E. Engin, "Dynamic Modeling of the Human Knee Joint," *Computational Methods in Bioengineering, ASME Winter Annual Meeting*, Chicago, pp. 145-156, 1988.

56. Onyshko, S., D. A. Winter, "A Mathematical Model for the Dyanmics of the Human Locomotion," *Journal of Biomechanics*, Vol. 13, pp. 361-368, 1980.

57. Orin, D. E., R. B. McGhee, M. Vukobratovic, G. Hartoch, "Kinematic and Kinetic Analysis of Open-Chain Linkages Utilzing Newton-Euler Methods," *Mathematical Biosciences*, Vol. 43, pp. 107-130, 1979.

58. Orlandea, N., "Node-Analgous, Sparsity-Oriented Methods for Simulation of Mechanical Dynamic Systems," PhD. Dissertation, University of Michigan, 1973.

59. Ounpu, S., "Joint Kinetic Patterns and Interpretation in Pathalogical Gait," *Seventh East Coast Clinical Gait Conference*, Richmond, VA, 1991.

60. Ounpuu, S., J. R. Gage, R. B. Davis, "Three Dimensional Lower Extremity Joint Kinetics in Normal Pediatric Gait," *Journal of Pediatric Orthopaedics*, Vol. 11, pp. 341-349, 1991.

61. Pandy, M. G., F.E. Zajac, M. G. Hoy, E.L. Topp, S. Tashman, P. J. Stevenson, E. Sim, W. S. Levine, "Sub-Optimal Control of a Maximum Height, Countermovenment Jump," *Modeling and Control Issues in Biomechanical Systems, Proceedings of the ASME Winter Annual Meeting* , Chicago, pp. 27-44, 1988.

62. Pandy, M. G., N Berme, "Model for the Understanding of the Ankle and Knee During Double Support," *Modeling and Control Issues in Biomechanical Systems, ASME Winter Annual Meeting*, Chicago, pp. 89-102, 1988a.

63. Pandy, M. G., N. Berme, "A Numerical Method for Simulating the Dynamics of Human Walking," *Journal of Biomechanics,* Vol. 21, pp. 1043-1051, 1988b.

64. Pandy, M. G., N. Berme, "Synthesis of Human Walking: A Planar model for Single Support," *Journal of Biomechanics*, Vol. 21, pp. 1053-1060, 1988c.

65. Pandy, M. G., N. Berme, "Quantitative Assesment of Gait Determinants During Single Stance Via a Three-Dimensional Model -- Part I. Normal Gait," *Journal of Biomechanics,* Vol. 22, pp. 717-724, 1989a.

66. Pandy, M. G., N. Berme, "Quantitative Assesment of Gait Determinants During Single Stance Via a Three-Dimensional Model -- Part II. Normal Gait," *Journal of Biomechanics*, Vol. 22, pp. 725-733, 1989b.

67. Perry, J., "Anatomy and Biomechanics of the Hindfoot," *Clinical Orthopedics and Related Research,* Vol. 177, pp. 9-15, 1983.

68. Phillips, G. M. , P. J. Taylor, *Theory and Applications of Numerical Analysis*, Academic Press, New York, 1973.

69. Ramakrishnan, H. K., G. Masiello, M. P. Kadaba, "On the Estimation of the Three Dimensional Joint Moments in Gait," *ASME Biomechanics Symposium,* AMD-Vol.120, pp.333-339, 1991
.

70. Ramakrishnan, H. K., M. P. Kadaba, "On the Estimation of the Three Dimensional Joint Moments in Gait," *Journal of Biomechanics*, Vol. 24, pp.969-977, 1991.

71. Ringwelski, D. A., S. L. Delp, N. C. Carroll, "'Knee Flexion Moment Arms of the Rectus Femoris After Tendon Transfer," *Second North American Congress of Biomechanics*, Chicago, pp. 91-92, 1992.

72. Rosenthal, D. E., M. A. Sherman, "High Performance Multibody Simulations via Symbolic Equation Manipulation and Kane's Method," *Journal of Astro. Science*, Vol. 34, pp. 223-239, 1986.

73. Schacter, D. B., L. A. Levinson, "Interactive Computerized Symbolic Dynamics for the Dynamicist," *Proceedings of the American Control Conference*, Atlanta, GA., pp. 177-188, 1988.

74. Scott, S. H., D. A. Winter, "Talocural and Talocalcaneal Joint Kinematics and Kinetics During the Stance Phase of Walking," *Journal of Biomechanics*, Vol. 24, pp. 743-752, 1991.

75. Seirig, A., R. J. Arvikar, "The Prediction of Muscular Load Sharing and Joint Forces in the Lower Extremities Durring Walking," *Journal of Biomechanics*, Vol. 8, pp. 89-102, 1975.

76. Siegler, S., R. Seliktar, "Simmulation of Human Gait with the Aid of a Simple Mechanical Model," *Journal of Biomechanics*, Vol. 15, pp. 415-425, 1982.

77. Soutas-Little, R. W., "Center of Pressure Plots for Clinical Uses," Biomechanics of normal and Prosthetic Gait, *ASME Winter Annual Meeting*, Boston, pp. 69-75, 1987.

78. Soutas-Little, R. W., "Suggested Marker Location and Analysis of Lower Extremity Movement," *Sixth East Coast Clinical Gait Conference,* East Lansing, MI, Michigan State University, pp. 66-69, 1990.

79. Speers, R., S. Delp, C. Moore, "Length of Hamstrings in Crouch Gait," *Eighth East Coast Clinical Gait Conference,* Rochester, MN., pp. 5-6, 1993.

80. Townsend, M. A., A. Seireg, "The Synthesis of Bipedal Locomotion," *Journal of Biomechanics*, Vol. 5, pp. 71-83, 1972.

81. Townsend, M. A., A. Seireg, "Effect of Model Complexity and Gait Criteria on the Synthesis of Bipedal Locomotion," IEEE Transactions on Biomedical Engineering, Vol. BME-20, pp. 433-444, 1973.

82. Tsai, C.S., J. M. Mansour, "Swing Phase Simmulation Design of Above Knee Prostheses," *Journal of Biomechanical Engineering*, Vol. 108, pp. 65-72, 1986.

83. Valiant, G.A. (ed.), *Transmission and Attenuation of Heelstrike Accelerations*, Human Kinetics Books, Champaign, IL., 1990.

84. Van Den Bogert, A. J., H. C. Schamhardt, A. Crowe, "Simulation of Quadrepedal Locomotion Using a Rigid Body Model," *Journal of Biomechanics*, Vol. 22, pp. 33-41, 1989.

85. Verstraete, M. C., A method For Computing the Three Dimensional Forces and Moments in the Lower Limb During Locomotion, PhD. Dissertation, Michigan State University, 1988.

86. Verstraete, M. C., R. W. Soutas-Little, "A Method for Computing the Three-Dimensional Angular Velocity and Acceleration of a Body Segment From Three Dimensional Position Data," *Journal of Biomechanical Engineering*, Vol. 112, pp. 114-118, 1990.

87. Walton, J. S., "Close Range Cine-Photogrammetry: A generalized Technique for Quantifying Gross Human Motion," PhD. Dissertation, The Penn State University, 1981.

88. Wells, R. P., "The Projection of Ground Reaction Force as a Predictor of Internal Joint Moments," *Bulletin of Prosthetic Research,* Vol. 18, pp. 15-19, 1981.

89. Winter, D. A., "Kinematic and Kinetic patterns in Human Gait: Variability and Compensating Effects," *Human Movement Science*, Vol. 3, pp51-76, 1984.

90. Winter, D. A., *Biomechanics and Motor Control of Human Movement*, John Wiley and Sons, Inc., New York, 1990.

91. Wismans, J., F. Veldpaus, J. Jannsen, "A Three Dimensional Mathematical Model of the Knee Joint," *Journal of Biomechanics*, Vol. 13, pp. 677-686, 1980.

92. Wylie, C. R., L. C. Barret, *Advanced Engineering Mathematics*, MgGraw-Hill, New York, 1982.

93 Yamaguchi, G. T., F. E. Zajac, "Sensitivity of Simulated Human Gait to Neuromuscular Control Patterns," *XII International Congress of Biomechanics*, Los Angeles, CA USA, 166, 1989a.

94 Yamaguchi, G. T., F. E. Zajac, "A Planar Model of the Knee Joint to Characterize the Knee Extensor Mechanism," *Journal of Biomechanics*, Vol. 22, pp. 1-10, 1989b.

95. Yamaguchi, G. T., F. E. Zajac, "Restoring Unassisted Natural Gait to Paraplegics Via Fuctional Neuromuscular Stimulation: A computer Simmulation Study," *IEEE Transactions on Biomedical Engineering*, Vol. 37, pp. 886-902, 1990.

96. Yamaguchi, G. T., J. I. Green, D. W. Moran, "Development of a Subject-Specific, Dynamic Model of Pathological Gait," Second North American Congress of Biomechanics, Chicago, pp. 399-400, 1992.

97. Yeadon, M. R., "Simmulation of Aerial Movement -- I. The Determination of Orientation Angles From Film Data," *Journal of Biomechanics*, Vol. 23, pp. 59-66, 1990a.

98. Yeadon, M. R., "Simmulation of Aerial Movement -- II. A Mathematical Inertia Model of the Human Body," *Journal of Biomechanics*, Vol. 23, pp. 67-74, 1990b.

99. Yeadon, M. R., "Simmulation of Aerial Movement -- III. The Determination of the Angualr Momentum of the Human Body," *Journal of Biomechanics*,, Vol. 23, pp. 75-83, 1990c.

100. Yeadon, M. R., "Simmulation of Aerial Movement -- IV. A Computer Simulation Model," *Journal of Biomechanics*, Vol. 23, pp. 85-89, 1990.

101. Young, J. W., R. F. Chandler, C. C. Snow, K. M. Robinette, G. F. Zehner, M. S. Loftberg, "Anthopometric and Mass Distribution of the Adult Female," FAA-AM Techical Report, FAA Civil Aeromedical Institute, Oklahoma, 1983.

102. Yoon, Y.S., J. M. Mansour, "The Passive Elastic Moment at the Hip," *Journal of Biomechanics,* Vol. 15, pp. 905-910, 1982.

103. Zajac, F. E., M. E. Gordon, "Determining Muscle's Force and Action in Multi-Articular Movement," *Exercise and Sport Science Reviews*, Vol. 17, pp. 187-230, 1989.